PB193417

STUDY OF CONTINUOUS FLOW COMBUSTION SYSTEMS FOR EXTERNAL COMBUSTION VEHICLE POWERPLANTS

FOR

THE DIVISION OF MOTOR VEHICLES
RESEARCH AND DEVELOPMENT

THE Marquardt COMPANY
VAN NUYS, CALIFORNIA

Reproduced by the
CLEARINGHOUSE
for Federal Scientific & Technical
Information Springfield Va. 22151

THE Marquardt CORPORATION VAN NUYS, CALIFORNIA

NATIONAL AIR POLLUTION CONTROL ADMINISTRATION
DEPARTMENT OF HEALTH EDUCATION AND WELFARE

FINAL REPORT UNDER CONTRACT CPA 22-69-128

JUNE 1970

STUDY OF CONTINUOUS FLOW COMBUSTION SYSTEMS FOR EXTERNAL COMBUSTION VEHICLE POWERPLANTS

FOR

THE DIVISION OF MOTOR VEHICLES
RESEARCH AND DEVELOPMENT

C. V. BURKLAND
W. B. LEE
G. BAHN
R. CARLSON

TABLE OF CONTENTS

SECTION	TITLE	PAGE
I.	INTRODUCTION	1
II.	SUMMARY AND CONCLUSIONS	4
III.	RECOMMENDATIONS	8
IV.	ANALYSIS	9
	A. Low Emission Combustion	9
	1. Introduction	9
	2. Fuel Preparation	10
	3. Burning as a Chemical Process	12
	B. Kinetic Results	12
V.	EXPERIMENTAL EQUIPMENT	15
	A. Combustion Apparatus	15
	1. Air Supply	15
	2. Fuel Supply	16
	3. Ignitor	18
	4. Combustor	19
	5. Heat Exchanger	19
	B. Fuel Injectors	20
	C. Instrumentation	21
	1. Instrument List	22
	2. Flow Measurement	23
	a. Air Supply	23
	b. Fuel Supply	24
	c. Cooling Water	24
	3. Temperature	24
	D. Gas Analysis Instrumentation	26
	E. Component Checkout	28
	F. Operating Procedures	30
VI.	TEST RESULTS	32
	A. Description of Test Conditions	32

Table of Contents (Continued)

Section Title Page

B. Gas Emission 32
  1. Prevaporized, premixed Fuel 34
  2. SUE Burner Configuration 35
  3. Pressure atomized Liquid Fuel 35
  4. Methane Fuel 36
C. Particulate Emissions 36
  1. Particle Collection and Analysis 36
  2. Sampling System 37
  3. Data Collection and Counting Technique 38
  4. Data Evaluation 41
D. Heat Exchanger Interface 46

VII. DESIGN CRITERIA 50
  A. Experimental Results 50
    1. Steady State Emission Criteria 50
      a. Temperature 50
      b. Residence Time 50
      c. Injector Characteristics 51
      d. Turbulent Mixing 51
      e. Air Addition 51
      f. Quenching 52
      g. Burning Characteristics 52
    2. Other Emission Criteria 52
      a. Fuel Modulation 53
      b. Startup and Shutdown 53
    3. Summary of Design Criteria 54

VIII. REFERENCES 57

APPENDICES

A. Combustion Generated Air Pollutants
B. Fuel Selection
C. Test Fuels Specifications
D. Data Summary
E. Data Analysis

LIST OF ILLUSTRATIONS

FIGURE	TITLE	PAGE
1	Continuous Flow Combustion System for External Combustion Engine	59
2	Values From the Steady-State Solution for Hydrocarbon Combustion	60
3	Analytical Model	61
4	Instantaneous Temperature of Recirculating Hydrocarbon/Air Flames	62
5	Performance of Primary Combustion Zone	63
6	Afterburner Calculations, Diluent Air at 2700°R	64
7	Afterburning Calculations, Diluent Air at 2456°R	65
8	Combustion Test Rig Schematic	66
9	Air Supply Schematic	67
10	Fuel Supply Schematic	68
11	Combustor and Igniter Schematic	69
12	Burner Assembly - External Combustor	70
13	Combustor Assembly	71
14	Combustor Control Area	72
15	Fuel Manifold (SUE Burner Configuration)	73
16	Gas Analysis Instrumentation Schematic	74
17	Ideal Gas Temperature Rise	75
18	Typical Pressure Data	76
19	Typical Wall Temperature Data	77
20	Effect of Overall Equivalence Ratio Vaporized Premixed Injection	78
21	Variation of Emissions with Heat Release Vaporized Premixed Injection, $\phi_p = 0.8$	79

List of Illustrations (Continued)

Figure	Title	Page
22	Variation of Emissions with Heat Release Vaporized Premixed Injection, $\phi_p = 1.0$	80
23	Variation of Emissions with Heat Release Vaporized Premixed Injection, $\phi_p = 1.2$	81
24	Effect of Overall Equivalence Ratio SUE Burner Configuration	82
25	Effect of Primary Equivalence Ratio SUE Burner Configuration	83
26	Variation of Emissions with Heat Release SUE Burner Configuration, $\phi_p = 1.0$	84
27	Variation of Emissions with Heat Release SUE Burner Configuration, $\phi_p = 1.2$	85
28	Effect of Primary Equivalence Ratio Liquid Injection	86
29	Effect of Overall Equivalence Ratio Liquid Injection	87
30	Variation of Emissions with Heat Release Liquid Injection, Kerosene	88
31	Variation of Emissions with Heat Release Liquid Injection, TMH	89
32	Effect of Overall Equivalence Ratio Methane Fuel	90
33	Variation of Emissions with Heat Release Methane Fuel	91
34	Particle Collection Schematic	92
35	Particle Collection System	93
36	Particulate Sample - External Combustor Run 11, Condition 3	94
37	Particulate Sample - External Combustor Run 14, Condition 8	95
38	Particulate Sample - External Combustor Run 14, Condition 8	96

List of Illustrations (Continued)

Figure	Title	Page
39	Particulate Sample - External Combustor Run 14, Condition 8	97
40	Particulate Sample - External Combustor Run 19, Condition 1	98
41	Particulate Sample - External Combustor Run 19, Condition 1	99
42	Particulate Sample - Internal Combustion Engine	100
43	Particulate Sample - Internal Combustion Engine	101
44	Typical Gas Temperature Data	102
45	Measured Fuel Injector Flow Characteristics	103
B-1	Distillation Curves - Hydrocarbon Fuels	B-3
E-1	Summary of Heat Exchanger Performance	E-15
E-2	Equivalence Ratio Based on Carbon Dioxide	E-16
E-3	Conversion Factor to Account for Water Vapor in Exhaust Gases	E-17
E-4	Conversion of Gas Emission Data to Unit Mass of Fuel: TMH	E-18
E-5	Conversion of Gas Emission Data to Unit Mass of Fuel: Kerosene	E-19
E-6	Conversion of Gas Emission Data to Unit Mass of Fuel: Methane	E-20

LIST OF TABLES

TABLE	TITLE	PAGE
I	Test Variables	4
II	Mass Emission Comparison	5
III	Test Summary	33
IV	Summary of Particulate Data	42
V	Typical Particulate Data	45
VI	Heat Exchanger Characteristics	48
VII	Rankine Engine Boiler Characteristics	49
VIII	Recommended Design Criteria for Low Emission Burners	55

I. INTRODUCTION

This report presents the results of a study of continuous flow combustion systems for external combustion vehicle powerplants conducted by The Marquardt Company for the Division of Motor Vehicles, Research and Development, National Air Pollution Control Administration. Analytical and experimental investigations were carried out in the period June 18, 1969 to June 18, 1970. The particle sampling and analysis reported herein were performed by personnel of the UCLA School of Engineering under the direction of Professor A. F. Bush.

The Motor Vehicles Division is conducting a program to develop external combustion, Rankine Cycle engine technology. The external combustion engine is intended for eventual use in a passenger-type automobile that would have a level of air pollutant emission from the exhaust that is significantly lower than present internal combustion engines. The external combustion Rankine engine requires a combustion system that provides a modulated source of thermal energy.

In a continuous flow combustion system (shown schematically in Figure 1), a fuel such as kerosene is burned at ambient pressure with air supplied from a blower. The high temperature combustion products are directed through a vapor generator (boiler), giving up heat, and are then exhausted to the atmosphere. In the external combustion engine cycle the vapor from the boiler is expanded in a reciprocating engine or turbine to produce shaft power, condensed and returned to the boiler as a liquid.

The purpose of the study was to develop design criteria for the combustor of such a continuous flow combustion system that had very low emission of air pollutants. The air pollutants of interest were carbon monoxide, unburned hydrocarbons, oxides of nitrogen and particulate matter. In addition to low emissions, it was desired that the combustion system have a high heat release per unit volume and be capable of being modulated over a range of heat releases corresponding to engine power settings from idle to full throttle.

The specific objectives of the study were to analytically and experimentally examine the external combustor variables that were considered to have a major effect on emissions of air pollutants. These included fuel type, fuel preparation prior to injection, fuel-air ratios, fuel-air mixing, combustor staging and residence time of the gases in the combustor.

The nomenclature used commonly throughout this report is listed below. Other symbols and abbreviations are defined in the text as they occur.

Gas Properties

ϕ - Equivalence ratio = $\frac{\text{Fuel-Air Ratio}}{\text{Stoichiometric Fuel-Air Ratio}}$

ϕ_P - Primary equivalence ratio-occurring in initial or primary burning zone

ϕ_O - Overall equivalence ratio-occurring after secondary air addition and afterburning

CH - Total hydrocarbons in parts per million of gas volume

CO - Carbon monoxide in parts per million of gas volume

CO_2 - Carbon dioxide in volume percent

NO_x - Oxides of nitrogen in parts per million of gas volume

NO - Nitric oxide in parts per million of gas volume (constituting the majority of the nitrogen oxide compounds in the combustion gas)

P - Pressure

ΔP - Pressure loss

T - Temperature

t - Time

Fuels

CH_4 - Methane

JET A - Aviation turbine fuel, kerosene

TMH - 2,2,5-trimethylhexane

Burner Configuration

IL_1 - Pressure atomizing fuel injection (high fuel pressure)

IL_2 - Pressure atomizing fuel injection (low fuel pressure)

IV_1 - Vaporizing, premixed fuel injection

IV_2 - SUE burner configuration using multiple slot nozzles

II. SUMMARY AND CONCLUSIONS

Chemical kinetic studies were employed to better understand how and at what rate air pollutants are formed in an external combustion process. With this background, an experimental combustion test rig employing a recirculating step, staged burner was built. Tests were conducted with various liquid and vaporized liquid fuel injectors using aviation turbine fuel (Jet A) and 2,2,5-trimethylhexane. A wide range of fuel-air ratios were examined by individually controlling primary and secondary air flow rates. Fuel flows were varied from a maximum corresponding to a heat release of 500,000 BTU/hr to 1/30 of this value. Two runs were also made using gaseous methane fuel. The range of test variables is presented in Table I below.

TABLE I
TEST VARIABLES

FUELS:	Kerosene, 2,2,5-trimethylhexane, methane
INJECTOR CONFIGURATIONS:	Pressure atomizing, vaporizing, vaporizing premixed
FUEL FLOWS:	0.15 to 4.5 gallons per hour
AIR FLOWS:	3.4 to 103 standard cubic feet per minute
FUEL EQUIVALENCE RATIO:	
PRIMARY:	ϕ_P = 0.53 to 1.59
OVERALL:	ϕ_O = 0.40 to 0.84
NUMBER OF TEST CONDITIONS:	140
CUMULATIVE COMBUSTION TIME:	22 hours

The tests demonstrated that gaseous and particulate emissions less than those established as the 1980 Federal Research goals can be achieved simultaneously in a high heat release, low pressure drop, burner configuration. The emission data measured at steady state conditions is compared to current and future emission goals for automobiles below.

TABLE II

MASS EMISSION COMPARISON

Grams/Gallon of Fuel

Air Pollutant	1970 (1) Federal Standards	California (1) "Low Emission Vehicle"	1980 (1) Research Goals	Continuous Flow (2) Combustion System Data
CO	230	110	47.0	5.6
CH	22	5	3.0	0.2 (as hexane)
NO_x	None	7.5	4.0	3.1 (as NO)
Particulates	None	None	0.3	0.04 (as carbon)

(1) Assuming 10 miles/gallon average fuel consumption

(2) Measured at steady state conditions, averaged over 3:1 turndown

The major conclusions from the tests regarding low emission burner design criteria are:

Air Addition

It was shown by analysis and experiments that a fuel rich reaction followed by air introduction and afterburning produce the minimum NO. It was possible to burn at a higher temperature and avoid a rise in NO formation by staging the air addition such as to produce a deficiency of oxygen in the high temperature primary burning zone. Introduction of the secondary air produced a fairly rapid completion of burning with the CO reaching equilibrium values.

Temperature

The temperature of the reaction, both in the primary and secondary burning zones, has a major effect on the formation and destruction of the air pollutants. Rich burning(primary fuel equivalence ratio, $\emptyset_P = 1.2$), followed by air addition to bring the overall fuel equivalence ratio between $\emptyset_O = 0.6$ and $\emptyset_O = 0.8$ gave the optimum results. Gas temperatures in this range of fuel-air ratios are also desirable to maximize the thermal efficiency of the vapor generator and keep the air pumping requirement to a minimum. From the analysis, a slight preheat of the inlet air appears desirable to minimize unburned hydrocarbons and more readily oxidize the carbon monoxide.

Residence Time

Residence time requirements are extremely important and it was shown there is a distinct trade-off in the afterburner between minimizing NO formation and increasing CO oxidation. The kinetic calculations also indicated that the primary zone in the experimental test rig could be reduced, as the reaction was calculated to be complete in considerably less than the full length. The afterburner section was shown to have two conflicting requirements: (1) with less time allowed for afterburning, the NO emissions showed a sharp drop, (2) however, with less time available, the oxidation of the CO to CO_2 could not be completed. This was confirmed by the experimental results where NO emissions continued to drop with higher flows through the combustor, whereas the CO stayed about the same up to a point where the time was insufficient to complete the oxidation step and the values climbed sharply.

Injector Characteristics

The method of fuel injection and fuel preparation prior to injection had a significant effect on the steady state emissions. The use of vaporized fuel produced lower emissions at higher heat release rates. The injection of liquid kerosene or TMH through pressure atomizing nozzles produced low emissions up through one-half of design flow. The time required for vaporization of the fuel droplet was apparently of sufficient magnitude to significantly reduce the time available for the complete burning of the fuel. Carbureting fuel injection where the vaporized fuel and air were premixed produced the best results.

Mixing

The burner used in the tests produced a strong recirculation zone that aided significantly in gas phase mixing. The inlet velocities and velocities through the primary zone and in the afterburner were sufficiently high to produce turbulent flow conditions. The secondary air inlet was sized to produce vigorous mixing boundaries. The completeness of burning is enhanced by strong mixing of the fuel and air that avoids pockets of over-rich or over-lean mixtures. This is especially important where the fuel is not premixed with the air. In the SUE burner configuration, the injection of the fuel in the corner of the step at right angles to the high velocity air jet provided the best possible mixing.

Quenching

Quenching can occur: (1) locally from cold walls, (2) from heat extractions from the gases and (3) by introduction of cold air. To prevent quenching and creation of unburned fuel, the walls of the burner were always operated hot (500°F and higher). Heat transfer away from the gas was limited to radiation to a water cooled outer chamber and by convection to the slow moving secondary air. For a typical run at 100 percent design loads, the heat transferred away from the burner was less than 10 percent. This produced a reduction in the actual gas temperature by approximately 150°F. Downstream air addition was very helpful in completing the combustion reactions, but the amount and method of introduction are critical with respect to freezing the CO composition by quenching.

Fuels

Very little differences in emission characteristics were noted between a commercial grade of kerosene and a pure hydrocarbon, 2,2,5-trimethylhexane having comparable molecular weights. Combustion tests made with methane and computer runs using pyrolized fuel fragments strongly indicate that hydrocarbon fuel blended with lighter fractions than kerosene types could have significantly lower emissions (including oxides of nitrogen) if used in an external combustion engine.

Transients

Starting and stopping emission transients were very low with the closely coupled fuel system and low thermal mass burner used in the experiments. More significant were the large changes in emissions observed at off-design fuel-air ratios that occurred in moving from one heat release condition to the next. A control system for the combustion system having rapid response and maintaining narrow fuel-air limits is needed.

III. RECOMMENDATIONS

It is recommended that further development work for low emission, external combustion systems be directed towards the following goals:

1. Design, fabricate, and test a prototype burner based on the experimental design criteria that uses kerosene and has the full range of required transient response.
2. Develop an advanced control system for continuous flow combustion systems having wide fuel modulation limits, narrow fuel-air limits and rapid transient response.
3. Establish the significance of low emissions (especially NO_x) associated with lighter fuel fractions and evaluate the logistics (availability, costs, etc.) of lighter fuels.

IV. ANALYSIS

A. Low Emission Combustion

1. Introduction

The combustion process under consideration here is the constant-pressure process operating at steady-state conditions. This process has certain basic characteristics whether applied to oil burners, jet engines, or the external combustion system for automotive propulsion. Perhaps the most outstanding characteristics is the maximum temperature, for this bounds the combustion environment to which the fuel is subjected and thus largely dictates details of burning. Another very important characteristic is the sequence of physical and chemical steps involved in the process of burning. The efficient burning of a liquid hydrocarbon fuel commences with control of the processes of injection, atomization, dispersion, and vaporization of the fuel. With the creation of a combustible mixture in air, a flame may be established in a number of ways: (1) by continuing auto-ignition; (2) by recirculating ignition via hot gases from fuel already burned; (3) by continuous operation of an ignition source, such as a pilot flame. The second of these is the customary one for combustion in continuous flow, utilizing one or more flameholding elements. At very low air flow velocities, such as those induced by natural convection, the fuel injector itself may effectively serve as the flameholder.

A flame stabilized by a flameholder may operate with a homogeneous gaseous mixture, conditioned by complete prior vaporization of liquid fuel droplets, or with a dispersion in the air of suitably small droplets essentially unvaporized, or with combined vapor/liquid fuel conditions as the combustible mixture reaches the flameholder; this will depend upon such parameters as temperature, time, and fuel volatility. At temperatures of the order of flame temperatures, large hydrocarbon molecules crack to smaller fragments via free radical chain mechanisms before they burn. The oxidation steps also involve free radical mechanisms as the smaller fragments, whether themselves stable molecules or free radicals, are converted to H_2O and CO_2. The participation of H_2O fragments in a multiplicity of shuffling reactions is extremely important to the ready progress of combustion.

Depending upon the initial conditions of pressure, temperature, and fuel-air ratio, the final equilibrium products of combustion will reflect partial completion of reaction versus partial dissociation. In the context of pollutants, the only equilibrium dissociation products of consequence are CO and NO. As an intermediate in the combustion process, CO cannot be avoided as it is ordained by equilibrium considerations. However with excess air, the CO can be oxidized to CO_2 and the concentration reduced to very low values. On the other hand, the creation of NO, as an adverse circumstance, involves kinetics considerations apart from the direct combustion process, and its final concentration need not necessarily be as equilibrium would dictate.

Unburned hydrocarbons are primarily attributable to imperfect fuel distribution, since the equilibrium limits for wide ranges of stoichiometry are only H_2O and CO_2 versus H_2 and CO. Particulate carbon arises from too rich a flame, with fuel cracking and reforming at too high a temperature, for too long a time, before exposure to oxygen. More complete discussion of specific combustion-generated air pollutants of interest in this program is presented in Appendix A.

2. Fuel Preparation

The injection of the fuel and subsequent mixing is critical to the process of complete combustion. For good burning, liquid fuels must be broken up into small droplets (atomized) or changed to the gas phase (vaporized). Atomization can be accomplished by forcing the fuel through a small orifice under pressure such as done in conventional oil burners, by air atomizing nozzles, by ultrasonics, etc. The injector design will dictate the penetration of the fuel jet into the air stream, and the characteristics of the spray that is created with respect to both spray pattern and droplet size distribution. The spray formation from the liquid jet depends upon the interplay between surface, viscous, and inertial forces. Ultimately a minimum attainable droplet size is imposed by a practical minimum size of fuel jet, whether this be a "solid" jet, a hollow cone, or something else in cross section, because droplet size is some direct function of jet size. In practical terms, the minimum attainable mean droplet size is of the order of 20 microns, although with strong inertial forces of the jet and the air stream, somewhat smaller sizes are possible.

After injection of the fuel and formation of a spray, droplet vaporization and mixing become important. Vaporization prior to entering the flame region is not necessarily essential, because small enough droplets can burn sufficiently rapidly to sustain a flame even if there is no advance release of vapor to feed the flame region. However, the requisite droplet size for such operation is evidently appreciably less than 20 microns, and thus considerable vaporization ahead of the flame region ought to be anticipated and provided for in a practical system. This requirement is similar to that for volatilization of gasoline in a carburetor in an internal combustion engine.

Relative to vaporization of hydrocarbons, the influence of relative velocity between droplets and air stream may not be significant, because small droplets are soon accelerated to the air stream velocity. An influence of the close proximity of adjacent droplets in a cloud exists, but this normally relates to a burning cloud with significant radiation and/or to a cloud of large droplets with significant natural convection currents. Aside from these factors, either vaporization alone or the vaporization-with burning of a droplet is described by a simple law, as follows: $\lambda = d\,(D^2)/dt$.

The value of the vaporization constant, λ, is defined by the operating conditions, but not by the droplet size. When the environmental temperature is very high relative to the droplet boiling temperature, the boiling condition is essentially established and the rate of heat transfer is controlling; i.e., the value of λ is dictated only by heat transfer considerations. When the environmental temperature is low relative to the droplet boiling temperature, the diffusivity of the fuel vapor away from the droplet surface is controlling upon λ. High speed computer programs designed to solve the droplet vaporization problem exist. These differ in the interative steps required for solution. The faster program employs as the independent variable the degree of depression of the droplet surface temperature below the boiling temperature. The dependent variables solved for are requisite gas temperature and initial vaporization rate (zero vapor component in the atmosphere). The other program employs as the independent variable the system enthalpy. It iterates first to define the compatible gas temperature and droplet surface temperature and then proceeds to compute the complete progress of vaporization. The principal output of this program is the time to achieve complete vaporization, with intermediate rates and temperatures as auxiliary information.

The proper distribution of fuel is important for several reasons. First of all, with really gross maldistribution it may be impossible to maintain a flame at a flameholder. Flameholder operating limits of fuel-air ratio correspond to restrictions of the simple flammability limits of the fuel under consideration. The restrictions are imposed by factors of limited time for reaction, heat loss, etc. Clearly, the fuel distribution must be compatible with the operating limits of a flameholder. Beyond this, too lean a flame locally may lead to quenching, and thus to unburned hydrocarbons, and too rich a flame may lead to pyrolysis, and thus to particulate carbon. Therefore, it is important that no "pockets" either too rich or too lean persist through the flame region. Finally, nonuniform fuel distribution preserved through the combustion process likely will result in performance losses.

The fuel distribution is continuous-flow combustion system is partly dependent upon the initial spray pattern created at injection. However, it is largely dependent upon the natural, turbulent flow of the air stream as a statistical mixing process. The application of fuel distribution correlations for such flow has been exploited to enhance both flame stabilization and combustion efficiency. In conjunction with judicious location of fuel injection elements, assurance can be provided of not only near-stoichiometric burning of the fuel (for optimum combustion) but also nearly uniform composition of the exhaust products.

3. Burning as a Chemical Process

Analysis of the chemical kinetics of hydrocarbon combustion has been performed and a representative result from homogeneous mixture calculations for the external combustion program is shown in Figure 2. Note first the temperature history for the case considered. The fuel feed is pyrolyzed to fragments in approximately 10^{-5} second, and this mildly endothermic process causes a slight temperature decrease over this period. Oxidative recovery to the assigned starting temperature occurs at 2-½ x 10^{-5} second; i.e., just the recovery takes 1-½ times as long as the pyrolysis. Appreciable oxidation and heat release take very much longer, and the histories of concentrations of H_2O, CO_2, and O_2 verify this on the figure, changing noticeably only at the longer times.

It is important that the situation represented by the figure is a homogeneous one. Under these conditions, where competitive secondary degradation of the fuel to particulate carbon was allowed for, this did not eventuate, and the pyrolysis fragments proceeded simply to burn. On the other hand, if a substantial period of time at high temperature were afforded to the fuel in the absence of oxygen, secondary pyrolysis steps to produce particulate carbon could be expected, and such has indeed been calculated for conditions without oxygen present. There thus is a requirement for rapid vaporization of any fuel droplets and rapid admixture of the vapors out into the surrounding air. The ease or rapidity of access to the requisite air for combustion is dependent upon the droplet size because the effective boundary layer thickness of fuel vapor around the droplet is proportional to the size. Thus, it is important in forestalling secondary pyrolysis to work with small droplet sizes (if not vaporized fuel).

The reaction of primary pyrolysis fragments, such as CH_3, CH_4, C_2H_2, etc. to the ultimate products, CO_2 and H_2O, takes place one discrete chemical step at a time, and these integrate by multiple parallel paths to a developed temperature-time profile. Possible limits to completion of reaction are: (1) equilibrium limits of CO concentration, as noted earlier; (2) relatively slow scavenging of last traces of intermediates, especially at near-stoichiometric conditions where the O_2 concentration also falls to a trace level as reaction nears completion; and (3) off-design local concentrations.

B. Kinetic Results

A sample calculation has been made to correspond to one of the program data points where the primary burning zone operated at a fuel equivalence ratio of 1.24 and the secondary burning zone operated at an overall fuel equivalence ratio of 0.65, see Figure 3. First of all, the equilibrium products and flame temperature were computed with $\phi_P = 1.24$, to represent recirculating products within the primary burning zone. Various proportions of fresh combustible mixture and of the recirculating products were then taken as inputs for separate kinetics calculations, and with these it was established that, regardless of the proportions (but considering that the primary zone was not overloaded so as to affect recirculation adversely), the residence time in the primary burning zone was more than adequate to prepare the fuel very well for the secondary reaction zone. Indeed, after only 1 millisecond the preparation appeared to be quite favorable, and one of the mixtures produced after 1 millisecond was employed in a subsequent kinetic calculation of afterburning.

The performance of the primary zone was assessed in a number of ways. Figure 4 shows temperature-time profiles for three different proportions of fresh mixture and recirculating products. In each case reaction, as measured by temperature, is indicated to be substantially complete in 1 millisecond. Figure 5 shows further results for one of the three mixtures, giving concentrations of O_2, CO, C_2H_2 and total unreacted hydrocarbons in 10^6 moles/mole of total gas (ppm). The disappearance of O_2 is closely tied to temperature increase, and is essentially complete after 1½ milliseconds. The concentration of CO at first decreases while oxygen is plentiful, and then increases again as oxygen deficiency is felt and the reaction $H_2 + CO_2 \rightarrow H_2O + CO$ proceeds. The summation of all mole fractions of unburned hydrocarbons initially builds up from an assigned value of 8230 ppm for C_8H_{18} fuel to a maximum about four times as great; this is the result of pyrolysis, and very grossly might be represented by conversion of C_8H_{18} to $2\ C_2H_6 + C_2H_4 + C_2H_2$. With further time allowed, two ensuing processes are exemplified: (1) further pyrolysis leading to a peak somewhat later in C_2H_2 concentration, and (2) further oxidation leading to lower total hydrocarbons. The relative thermal stability of acetylene is demonstrated by its indicated persistence. These various concentration profiles indicate that a residence time of 1-3 milliseconds, after recirculation mixing, would be appropriate for a homogeneous primary zone with vaporized fuel.

In addition to the simple evidence of these figures, the rate of disappearance of C_2H_2 was compared for the primary with the secondary combustion zone (otherwise discussed below). Thus it was ascertained that the fractional rate of disappearance of C_2H_2 at a given concentration level, was very much slower in the primary. This comparison tended to substantiate the decision already made, to initiate the afterburning kinetics calculations with the mixture produced after 1 millisecond in the primary zone. All in all, from a reaction standpoint the primary combustor thus could be shortened markedly. However, in actually shortening it, careful attention would need to be paid to the prevailing aerodynamics, since the record of reaction time needs to be based upon the effective completion of recirculation and allowance for pyrolysis and burning to commence at this point.

For the first of the two secondary zone calculations, the initial temperature was taken as 2700°R to represent the condition of more gradual addition of secondary air to the effluent from the primary burning zone. Abrupt and total mixing of the secondary air would have reduced the temperature to a somewhat lower level at the outset, but this would not have been representative of the true kinetic situation at the outset of afterburning. On the other hand, the assigned temperature of 2700°R could be achieved overall within the burning cycle by regenerative heating of the secondary air. Figure 6 presents results of the afterburning calculation, and the point of the discussion immediately preceding is an explanation of a final indicated temperature on the figure somewhat higher than the equilibrium flame temperature for $\emptyset_0 = 0.65$ if calculated without any regenerative heating of the secondary airflow.

Shown on Figure 6 are the profiles of temperature, CO concentration, NO concentration, and concentration of unburned hydrocarbons. Burning is essentially complete after about 20 milliseconds, the CO concentration attaining near identity with the equilibrium value (for the prevailing temperature) at this time. At the temperature level achieved, where the concentration of atomic oxygen has stabilized, the production of NO proceeds in a steady fashion (with false appearance of acceleration on a semilog plot) because of the reaction chain represented by

$$\begin{tikzcd} O & + N_2 = & N \arrow[d] & + NO & \\ & & N + O_2 = & O + NO \arrow[ulll] & \end{tikzcd}$$

Another secondary calculation was performed, starting this time with a temperature of 2456°R so as to correspond with no regenerative heating of the secondary air. Results are presented on Figure 7. Unburned hydrocarbons endured as traces a little longer than previously, but again the test of effective completeness of combustion was the decrease of CO concentration nearly to an equilibrium value, and again about 20 milliseconds was indicated to be sufficient for this, with a CO level of about 200 ppm resulting. (The equilibrium value for the point in question, obtained by continuing the kinetics calculation until equilibrium was finally achieved, was 119 ppm.) By ending the reaction at about 3300°R, rather than at about 3500°R according to Figure 6, the rate of production of NO was decreased by a factor of about ten, and the resulting (homogeneous kinetics) value of NO was negligible. This indicates that NO observed in practice can be attributed to temperature nonuniformities, keeping in mind that NO, once formed, is quite stable.

Figure 7 implies a desirability to shorten the afterburning time consistent with attainment of nearly the equilibrium concentration of CO, which itself is a function of fuel equivalence ratio (and regenerative heating, if any). This would lead to the most compact hardware and to minimal production of NO. It is in the area of predicting suitable design modifications which will inherently foreshorten allowable reaction times that future kinetics calculations can be helpful, especially as off-design operation is taken into account.

V. EXPERIMENTAL EQUIPMENT

A. Combustion Apparatus

The combustion apparatus consisted of five (5) component sections. These were: (1) air supply, (2) fuel supply, (3) igniter, (4) combustor and (5) heat exchanger. A block diagram layout of the arrangement is shown in Figure 8. Each of these sections is described below:

1. Air Supply

A schematic of the air supply system is shown in Figure 9. Facility air, at a supply pressure of approximately 95 psig, was used as air source to the combustor. Choked venturi were used to measure air flows. This permitted an accurately measured flow of air to be delivered independent of minor pressure fluctuations in the combustor.

The facility air was regulated to a suitable pressure (usually 80 psig) by an air actuated loader. The air then entered a swirl tank where entrained water droplets were separated by inertial action. This was followed by a bank of two large drying tubes in parallel, to complete the water removal operation. It should be noted that it was neither necessary nor desirable to obtain complete drying of the air, but rather to remove entrained water droplets and to insure that the relative humidity was sufficiently low to avoid condensation in the venturi inlet. It was also of interest at times to know the approximate humidity of the air entering the combustor. Accordingly, a bleed line was tapped off the air flow downstream of the main air venturi. Flow through this line passed over two exposed tip chromel/alumel thermocouples. A moistened wick was placed around the second of these. The two, therefore, provided a wet and dry bulb temperature measurement of the supply air. A rotameter in this bleed line was used to verify that the air velocity over the wet bulb was approximately 1.25 lbm/ft^2 sec, which provides an unbiased estimate of wet bulb temperature. Standard humidity charts were then used to determine the percentage humidity of the air supplied to the combustor. This bleed flow was activated only during the period of wet bulb measurement.

Tests of the air supply humidity control system at maximum air flow of 0.138 lb/sec were performed. These tests demonstrated a reading of 50 percent humidity after 2 hours 20 minutes flow of saturated air through the same bed of desiccant.

The air flow was divided, as desired, between primary air (venturi A) and secondary air (venturi B) by means of valves V_{1a} and V_{1b}. Readings of P^o_{1a} and P^o_{1b} determined the corresponding mass flow rates. Valve V_{2b} was provided for use in certain low flow rate applications.

Pressure adjustment to that of the combustor occurred in the diverging section of each venturi. The pressure of the primary air stream (referenced to ambient) was read by manometer in inches of mercury upstream of the combustor. The pressure of the primary air was also referenced against the secondary air, and against the combustor exit pressure, in two other manometers. The latter two manometers were read in inches of water.

2. Fuel Supply

Three hydrocarbon fuels were tested in this program as designated below:

Fuel	Grade	Purity	Source
2,2,5-Trimethylhexane	Tech.	95 mole %	Phillips Petroleum Co.
Kerosene (Jet A Turbine Fuel)	Aeroshell Turbine Fuel 640	ASTM D1555	Shell Development Co.
Methane	Tech.	97 mole %	Air Products Co.

The 2,2,5-trimethylhexane was used as a "base" fuel in that its properties (particularly the boiling point) are clearly defined, and it is representative of the molecular class of fuels of prime interest to this program.

Aeroshell Turbine Fuel 640 is representative of kerosenes, and was used in pressurized atomizing nozzle tests.

Methane was used as a comparative fuel in some tests. Specifications for each of these fuels are given in Appendix C. All these fuels were tested as received from the supplier.

For the liquid fuels, a nitrogen pressurized fuel system was used. This system had the capability of delivering the hydrocarbon fuel at design flow rate at all conditions ranging from ambient liquid to vapor with 50°F superheat. The system could deliver the fuel at pressures of ambient to 1000 psig.

A schematic of the fuel supply system is shown in Figure 10. The fuel reservoir was a stainless steel tank of 15 gallon capacity, rated at 1000 psig. The hydrocarbon fuel within this tank was pressurized from a cylinder of commercial grade nitrogen.

The fuel system was designed to deliver fuel in accordance with two design modes. One calls for the introduction of the fuel into the combustor in the form of a superheated vapor at low pressure. The other involves injecting the fuel, as ambient temperature liquid, through a high pressure atomizing nozzle into the combustor. In accordance with the latter mode, all components were rated at 1000 psi at ambient temperature. For the former mode, a 1.6 KW heater, plus a 785 Watt auxiliary heater, was capable of delivering 2,2,5-trimethylhexane at 50°F superheat to the combustor at design flow rate. The system could also deliver the fuel at various intermediate states between the above two cases.

Fuel flow rate was determined by a turbine meter, whose output was read from a digital readout device. The output of the turbine meter was calibrated directly in terms of fuel flow rate by collecting a measured mass of fuel for a measured time, over the flow range of interest.

For tests with methane, the gas cylinder was plumbed in downstream of the heating element. A precision rotameter was used to measure methane flow rate, corrected for the existing gas pressure at the rotameter.

A key feature of the fuel supply system was the three-way solenoid valve. In the absence of electrical power, the valve was in the bypass mode in which no fuel entered the combustor, but was rather diverted into the collection vessel. A water-cooled coil of copper tubing was provided in the bypass line. This served to condense the superheated fuel vapor (when operating in this mode) before routing it to the collection vessel.

The solenoid valve was energized by a circuit which included a photo-conductive cell. This latter device is described in further detail subsequently, but in essence it de-energized the solenoid valve in the absence of flame in the combustor. The solenoid valve could not be energized to the burner mode unless an override button was depressed on the ignition switch box. It would not remain energized unless combustion was occurring. Thus, in the event of loss of flame, fuel flow was automatically diverted from the burner into the bypass mode.

It was necessary that this valve function properly under all operating conditions including the use of hot hydrocarbon vapors, in excess of 350°F. An existing low temperature valve was reworked. This rework involved: (a) changing the seat material to Viton A, (b) enlarging the bypass and discharge ports, and (c) providing external cooling of the solenoid coil while not significantly reducing the temperature of the hot hydrocarbon vapor passing through the valve. This valve had a low closure pressure rating (≈ 60 psi). With some of the liquid pressure spray nozzles, however, operating pressures of 400 psi or higher were used. For these tests, the modified valve was replaced with a conventional, small-port solenoid rated for these pressures. With the use of liquids, the smaller port size was not a problem. The seat material of this valve was also replaced by Viton A.

3. Igniter

Initial igniter component testing was performed with catalytic igniters. Although promising, these tests indicated that a basic problem of igniter durability remained. Accordingly, attention was directed to the use of a high voltage spark igniter.

The high voltage electrical components from a commercial oil burner were modified for use. This was done by building a housing shown schematically in Figure 11, which supported the high voltage (10,000 volt) transformer, and also served as a plenum into which the primary air supply to the burner was directed. Specifically adapted high voltage electrodes were prepared. These electrodes passed through the inlet section of the two-inch diameter connecting tubing, six inches long, between the primary air plenum and the combustor. The fuel inlet line was brought in at the upstream end of this connecting line. Depending on the mode of operation, either a vapor injector (0.10-inch diameter converging nozzle) or a liquid pressure spray nozzle was installed. These different nozzles were installed and removed through the downstream opening of the igniter tube, without having to disturb the high voltage electrodes. The latter extended the full length of the tube. For use in the vapor injection mode, the nozzle throat was located approximately 4 inches upstream of the arc, permitting mixing of the fuel to occur prior to reaching the spark. For the liquid injection mode, the spray nozzle was positioned so that the top of its spray pattern just intercepted the spark. These conditions were verified experimentally during the preliminary component tests. Once the desired injector-igniter geometry had been established, injector-support fittings were prepared which permitted different spray nozzles to be inserted, without having to readjust the electrodes. The downstream face of the connector tube was flange-mounted to the combustor.

The photoconductive cell was mounted directly under the transformer and was positioned so that it would "see" axially down the length of the combustor. The cell was a cadmium sulfide device, Honeywell C554A. It was designed for use with a commercial, oil fired burner. It was found necessary to shunt the photo-conductive cell with a 4 KΩ resistor in order to obtain satisfactory operation of the device over all the combustion conditions encountered during the program. The output of the photoconductive cell controlled the position of the 3-way fuel solenoid valve, as described in the preceding section.

Electric current to the high voltage primary coil was controlled by a separate 110 V switch. A primary current of 2.2 amps was required to maintain the high voltage arc; an ac ammeter in the primary line was used to verify, during a combustion test, that the arc was operating properly.

4. Combustor

A detail of the combustor is shown in Figure 12 and a photograph in Figure 13. The combustor inlet was bolted to the igniter section exit flange. The combustor consisted of an outer water cooled jacket surrounding the replaceable inner burner can.

The burner chamber was 5 inches in outside diameter and 36 inches long with a double wall for water cooling. Secondary air was introduced as desired into the chamber through the tube on the upstream end. A small baffle was used downstream of the tube inlet to help distribute the secondary air around the periphery of the chamber. The replaceable burner cans consisted of a variable length hot wall section, an afterburner section for the introduction of secondary air, and a volume downstream that could be operated with either a hot or a cold wall.

The burner can used in all the tests of this report was of 321 stainless. The combustor wall was 0.028-inch, the wall thickness of the conical afterburner section was 0.032.

The combustor has eight taps for measuring burner wall temperature; four taps were in use on each run.

Temperature of the hot gases at the combustor exit was indicated by a Pt/Pt-10% Rh thermocouple (encased in a Pt-6% Rh sheath), which passed through the front flange of the transition section. The latter section reduced the flow area to the 2-inch diameter of the heat exchanger. The transition section and part of the heat exchanger are shown in Figure 13. This transition section was cooled by means of an outer water jacket. It was formed into a relatively close 180° bend, which was AN coupled to the first heat exchanger section. The combustor inner wall thermocouples can also be seen in the photograph of Figure 13.

5. Heat Exchanger

The function of the heat exchanger in the experiment was to cool the gases leaving the combustor to $400\text{-}500^\circ F$ or less, simulating actual exhaust conditions. A sampling line to the gas analysis instruments was provided at this point. Additional gas taps at intermediate positions in the heat exchanger were provided for possible future use. A single tube heat exchanger, emphasizing low cost and facility of instrumentation, was selected.

A generalized analysis was performed relating the basic factors (L, D, t, and ΔP) for conditions of developing a given temperature drop for a fixed mass flow rate. Here L = heat exchanger length, D = heat exchanger tube I.D., t = residence time and ΔP = pressure drop. The residence time increases approximately as $D^{2.8}$ and length as $D^{0.8}$, while ΔP changes as $D^{-4.2}$. Based on a series of heat transfer calculations, it was decided to construct the exchanger of 2-inch O.D. stainless steel tubing, 0.016-inch wall. The required length was 33 ft, with a calculated ΔP of about 1.5 psi, and a total residence time of about 130 milliseconds. The gas temperature was reduced to below 2500°F for all conditions (essentially freezing the reaction) in less than 5 milliseconds. These design calculations were based on the maximum design flows. A comparison of the design calculations with subsequent experimental data is given in Appendix E.

The different heat exchanger sections are shown in the photographs of Figures 13 and 14. The first 13 ft of heat exchanger length was cooled by ½-inch copper tubing, close coiled, through which cooling water flowed. The last 20 ft of exchanger length was placed in a water cooled trough. There were four separate cooling water flows to the heat exchanger and combustor. The individual water flow rates and exit temperatures were measured, permitting a determination of the amount of heat transferred and thus establishing a heat balance. Heat balance data are given in Appendix E. Gas temperature measurements were taken at four positions along the heat exchanger length.

B. Fuel Nozzles

Three different configurations of nozzles were tested in this program. The first was a converging nozzle for vapor injection. The throat diameter was 0.10 inches. This nozzle was mounted along the centerline of the ignitor tube as shown in Figure 11. There was a 4 inch mixing length downstream of the nozzle throat, prior to the combustor inlet.

Appendix E presents calculations describing flow conditions in the nozzle and ignitor section, based on experimental measurements during a combustion test.

A second nozzle, also for vapor fuels, was a multiple slot nozzle. In this arrangement, fuel vapor entered a ring-shaped manifold surrounding the ignitor tube. Leaving this manifold were six ¼ inch O.D. tubes, spaced symmetrically around the exterior of and parallel to the ignitor tube. These tubes passed through the ignitor tube exit flange via Swagelok bulkhead fittings. Each tube projected about 1/8 inch beyond the inner flange face. A detail of this nozzle is shown in Figure 15. The end of each tube was sealed, with the fuel exiting through a slot nozzle. The slots were arranged so that the fuel vapor of each tube was directed toward the centerline of the combustor. The gap in the ring manifold was required to permit mounting on the existing ignitor tube without rework of previously attached fittings. This nozzle configuration installed in the step burner constituted the Marquardt patented Sudden Expansion or SUE Burner.

The third type of nozzle was a pressure atomizing spray nozzle, for liquid fuels. The nozzles were procured from Spraying System Co. Two nozzles of this type were tested, bearing the designations "¼ LND SS 1", and "¼ LND SS 1.5". The difference between the two lies in the pressure-flow rate relationship. The '1.5' nozzle required about 330 psi to deliver full flow rate of 2,2,5-trimethylhexane, while the '1' nozzle required 550 psi to deliver the same fuel at 88% fuel flow. The orifice diameter was 0.020 inches for both nozzles. The pressure-flow rate characteristics of each nozzle were measured using 2,2,5-trimethylhexane, over the full range of flow rates to be tested, or up to a maximum of 550 psi, depending on the nozzle. The spray angle of each nozzle is listed by the manufacturer as 70-72° for fully developed spray. Each nozzle projects a hollow cone spray pattern.

These different injectors are designated as follows in the remainder of this report:

Vapor nozzles:	
0.10"converging nozzle	I_{V_1}
6-tube slot nozzle	I_{V_2}
Liquid nozzles:	
¼ LND SS 1 (higher pressure)	I_{L_1}
¼ LND SS 1.5 (lower pressure)	I_{L_2}

All three internal nozzles were installed and removed from the downstream opening of the ignitor tube. It was not necessary to remove the latter or the high voltage electrodes during these operations.

C. Instrumentation

This section profides a listing of the instrumentation used (exclusive of gas analysis instruments), followed by a discussion of details of the test instrumentation.

1. Instrumentation List

Measurement	Type of Instrument	Range or type of Read Out
Flow Rates		
Primary air to combustor Secondary air to combustor	Venturi	Venturis of following throat diameters were used 0.074" 0.115 0.1695 0.170 0.235 0.250 0.296 0.330
Fuel flow to combustor	1. turbine meter with digital readout	5-27 lb/hr
	2. Cox precision rotameter (for methane)	3.5×10^{-4} - 0.060 lb/sec (std air)
	3. Matheson rotometer 603	1/10 and 1/30 scale tests
Pressures		
Primary air venturi total	Bourdon gage	0-100 psig
Primary air venturi static	Bourdon gage	0-100
Secondary air venturi total	Boundon gage	0-100
Secondary air venturi static	Boudron gage	0-200
Primary air	Manometer	0-12 in. Hg gage
Differential pressure, primary vs. secondary air	Manometer	0-90 cm H_2O
Differential pressure, pri. air vs. combustor exit gas	Manometer	0-12 in. H_2O
Fuel tank	Bourdon gage	0-600 psig
Fuel heat exchanger exit	Bourdon gage	0-60 psig
	Bourdon gage	0-600 psig
Fuel nozzle inlet	Bourdon gage	0-100 psig
	Bourdon gage	0-600 psig

Temperature

Combustor exit gases	Pt/Pt - 10% Rh	Potentiometer plus 0-20 mv penchart
Heat exchanger 1	Pt/Pt - 10% Rh	Potentiometer plus 0-20 mv print chart
Heat exchanger 2	Pt/Pt - 10% Rh	0-20 mv print chart
Heat exchanger 3	chromel/alumel	Potentiometer plus 0-20 mv print chart
Combustor wall 1	Pt/Pt - 10% Rh	Potentiometer plus 0-20 mv print chart
Combustor wall 2	Pt/Pt - 10% Rh	Potentiometer plus 0-20 mv pen chart
Combustor wall 3	Pt/Pt - 10% Rh	Potentiometer plus 0-20 mv print chart
Combustor wall 4	Pt/Pt - 10% Rh	Potentiometer plus 0-20 mv print chart
Fuel heat exchanger exit	chromel/alumel	Potentiometer plus 0-20 mv print chart
Fuel heater element	chromel/alumel	Potentiometer plus 0-20 mv print chart
Cooling water 1	chromel/alumel	Potentiometer plus 0-20 mv print chart
Cooling water 2	chromel/alumel	Potentiometer plus 0-20 mv print chart
Cooling water 3	chromel/alumel	Potentiometer plus 0-20 mv print chart
Cooling water 4	chromel/alumel	Potentiometer plus 0-20 mv print chart
Cooling water 5	chromel/alumel	Potentiometer plus 0-20 mv print chart
Air supply, dry bulb	chromel/alumel	Potentiometer
Air supply, wet bulb	chromel/alumel	Potentiometer

2. Flow Measurement

a. Air Supply

Except for one condition at 1/30 scale, all air rates to the combustor were measured by the use of venturis operating in the choked condition, or very close to this condition. Eight different venturis were used during the program. Each of these venturis was calibrated with air, using a Cox Precision Rotameter as standard. The latter had been calibrated by an outside laboratory 3 months prior to initiation of this program. The calibrations were performed under conditions of choked flow through each venturi. It was found that for 6 of these venturis the measured flow rate during calibration agreed within 3% with the theoretical equation for choked flow. Accordingly, for these venturis the theoretical flow equation was used in subsequent tests. For the other two venturis, a flow equation based on the measured flow during the calibration was used in subsequent tests.

In each flow measurement the venturi inlet (total) and throat (static) pressures were measured, and the pressure ratio computed and logged with the data. This was to verify that the nozzle was in fact operating in the choked state at each test condition. Under certain conditions, and particularly with the 0.1695 inch venturi, the nozzle was operating slightly unchoked (total/static ratio approximately 1.7 - 1.8). Whenever this occurred, the flow rate was corrected by introducing the flow coefficient for a subsonic nozzle. This correction factor was never less than about 0.985 and was usually greater than 0.99. The main effect of this condition was that the instantaneous flow rate through the nozzle was not independent of pressure fluctuations within the burner. This factor also turned out to be not significant, as pressure fluctuations within the burner were usually less than 0.1 inch of Hg, and were considerably less than this at the desired operating conditions.

b. Fuel Supply

For operation with either 2,2,5-trimethylhexane or kerosene, fuel flow was measured by a turbine meter (Cox Flowmeter Model LF 6-100) with digital readout (Anadex Model CF-604R). The output of the latter was calibrated directly in terms of mass flow rate of each fuel by collecting a measured amount of fuel over a measured time interval at steady state conditions. This procedure was repeated at several points to determine a calibration curve for each fluid from ¼ to full scale flow rate.

For fuel flow rates less than this, a Matheson No. 603 Rotameter was calibrated (by the same procedure) over a range of flow rates from 1/100 to 1/10 scale.

When methane was used as fuel, flow rate was measured by the same rotameter used to calibrate the air venturis. Correction was applied for the pressure existing at the rotameter at each condition.

c. Cooling Water

A rotameter was installed in each of the four cooling water lines. These were not calibrated, as high accuracy was not needed in this case.

3. Temperature

Combustion temperature was indicated by a Pt/Pt - 10% Rh exposed tip thermocouple (all test thermocouples used on this apparatus had exposed tips). The tip of this thermocouple was approximately at the combustor centerline, passing radially in through the inlet flange of the transition section (which was bolted directly to the combustor outlet). The sheath of this thermocouple was of Pt - 6% Rh, to withstand the extreme conditions to which it was subjected. The sheath O.D. was 0.020 inches. The output of this thermocouple was displayed on the dual pen recorder in view of the operator, and (as with all but one of the test thermocouples) could also be read out simultaneously on a potentiometer. This provided a rapid and sensitive indication to the operator of such phenomena as ignition, shutdown, combustion instability, and transitioning from one condition to another. It was recognized that a simple exposed tip thermocouple would be prone to radiation errors at the combustion gas temperatures. Installation of a thermocouple assembly with radiation shields, would have compromised the design of the combustor-heat exchanger interface.

The magnitude of the radiation error involved in the combustor thermocouple is analyzed in Appendix E.

The combustor had 8 locations for wall temperature measurement. Location 1 was 3½ inches from the face of the combustor inlet flange; there was 4 inch spacing between all of the taps. The last, location 8, was 4 inches upstream of the face of the combustor exit flange. During this program, 4 wall thermocouples (all Pt/Pt - 10% Rh) were in use. These were in locations 1, 2, 5 and 8. Locations 1 and 2 were utilized since they covered the region of the combustor at which possible hot spots were anticipated. Location 5 corresponds to the region where secondary air was entering the combustor; and thus would detect excessive temperature which might be associated with the onset of afterburning. Location 8 was in the "dead air" region of the conical portion of the afterburner can, where there was little or no net flow of secondary air past the burner wall.

The output of wall thermocouple No. 2 (location 2) was displayed on the second pen of the dual pen recorder. Thus the operator could always detect any undesirable increase in wall temperature promptly, and take corrective action.

Each of these wall thermocouples was installed connected to an ohmmeter to verify that the tip was in contact with the wall. This condition was rechecked at various times throughout the program.

Presentation of typical wall temperature data is given in Section VI-A. No excessively high wall temperatures were measured at any time during this program. There was no burnout, and post run inspection revealed no point of significant damage or deterioration of the wall.

The transition section made a 180° bend, whence it was connected to the first section of heat exchanger tubing. This was a 5 foot section. A Pt/Pt - 10% Rh thermocouple ($T_{H.E.\ 1}$) was installed at the end of this section. This was followed by a second straight section of heat exchanger tubing 8 feet long. A second Pt/Pt - 10% Rh thermocouple ($T_{H.E.\ 2}$) was installed at the end of this section. From here the heat exchanger entered a trough through which cooling water flowed. The tubing made a 10 foot pass, close 180° bend, then another 10 foot straight section, at which point it left the trough, ending the heat exchanger section. A chromel/alumel thermocouple ($T_{H.E.\ 3}$) recorded this heat exchanger exit flow.

Five cooling water flows were measured, as follows:

$T_{c.w.1}$	Exit of the combustor cooling water. This stream was then routed back into the jacketed transition section.
$T_{c.w.2}$	Exit of the transition section.
$T_{c.w.3}$	Exit of first (5 foot) section of Cu coil-wrapped heat exchanger.
$T_{c.w.4}$	Exit of the second (8 foot) section of Cu coil-wrapped heat exchanger.
$T_{c.w.5}$	Exit of the cooling water trough.

The location of the remaining thermocouples was covered in the section on fuel and air supply systems.

Each thermocouple was connected to thermocouple extension wire, and routed to the 16-channel print chart recorder, potentiometer, or dual pen recorder, as appropriate. The print chart recorder and potentiometer were located in the adjacent room.

D. Gas Analysis Instrumentation

Gas analyses were performed by the four instruments shown below:

CONTINUOUS FLOW GAS ANALYZERS

GAS	TYPE	RANGES
Carbon Dioxide	Infrared Beckman Model IR-315A	0-15%
Carbon Monoxide	Infrared Beckman Model IR-315A	0-1000 PPM 0-5000 PPM

Continuous Flow Gas Analyzers (Continued)

GAS	TYPE	RANGES
Nitric Oxide	Infrared Beckman Model IR-315A	0-200 PPM 0-2000 PPM
Total Hydrocarbons	Flame Ionization Beckman Model 109A	0-5 PPM 0-15,000 PPM (8 ranges)

These instruments were set up in accordance with the schematic shown in Figure 16. Water vapor in the exhaust gas was removed in the prefilter and in the ice bath. Thus the mole fraction water vapor content in the gases to the instruments was equal to the vapor pressure of water at 0°C divided by 1 atmosphere. This small amount of water vapor does not have measurable influence on the NDIR analysis for CO and CO_2, and on the hydrocarbon analyzer. It could have interfered with the NO analyzer, however. Two drying agents were, therefore, placed in the line leading to the NO analyzer. The first was "Aquasorb", a trademark for a P_2O_5-based desiccant. This material was recommended by the instrument manufacturer. The second drying tube contained Linde Molecular Sieve Type 3A, 1/16 inch pellets.

The Aquasorb was removed (and replaced with a glass tube) from the line in Run 15, Condition 5, and in Run 17, Conditions 2 and 3. The molecular sieve was left in the system. The meter reading was about 2 units lower with the Aquasorb removed, corresponding to a decrease in apparent NO reading of about 3 PPM.

This change is relatively small, and in the direction of a lower reading, indicating that the use of the Aquasorb in conjunction with the molecular sieve did not in any way result in an erroneously low reading of NO.

Upon receipt of these instruments, an electronics check was performed on each, in accordance with supplier recommendations. Each instrument was calibrated daily when in use, by means of calibration gases procured from Matheson Company. The concentrations of these calibration gases are:

CO	405 ppm, balance N_2
NO	113 ppm, balance N_2
CO_2	10.95 vol. %, balance N_2
CH	435 ppm propane (1305 ppm C), balance N_2 26 ppm n-hexane, balance N_2 (156 ppm C)

It should be noted that the hydrocarbon analyzer is calibrated at Marquardt in terms of ppm carbon, and the data of this report are given in the same units.

Calibration data of each instrument were logged for each day of use; this permits prompt detection of any loss in sensitivity (or other possible instrument malfunction). Appropriate adjustments or replacements can then be made, to assure that the instrument remains within satisfactory operating limits.

In accordance with Beckman recommendations, the hydrocarbon analyzer was calibrated using the 435 ppm propane (1305 ppm C), and then a reading taken with the second gas (26 ppm n-hexane). In each case, the reading obtained was 160 ppm C, in close agreement with value of 156 ppm, based on the concentration determined by the supplier.

After standardization and calibration, the 3-way selector valve of Figure 16 was turned to the N_2 purge position. Just prior to starting an ignition, the valve was turned to the sample position, which brought gas from the probe in the heat exchanger tube through each instrument. The flow rate through each instrument was checked and adjusted as necessary to equal the value used during the calibration. Each instrument then analyzed continuously and automatically for its specific component. The only attention necessary was to switch from one scale to another, depending on the concentration of the gas being sampled.

The instruments were left in the "sample" mode during startup, transition, and shutdown.

Initially the sample probe in the heat exchanger exit consisted of a static pressure-type tap. After combustion test 8, a total pressure type of probe (of ¼-inch tubing) was used. This change did not have an effect on the gas analysis data as determined by comparing the data measured at the same combustion conditions with the tap and with the probe.

E. Component Checkout

Component tests were performed as necessary during installation and fabrication of the combustor assembly subsystems. The purpose of these tests was to assure that each subsystem was operating properly before uniting them into the final assembly.

Air Supply System - Twelve tests were performed for the following purposes:

(a) Determine operating limits of facility air supply.

(b) Calibration of venturis and pressure gages.

(c) Operational checkout of various plumbing fixtures and control valves.

(d) Quantitative checkout of water removal equipment of the facility air, and of the humidity measurement installation.

Fuel Supply System - Fifteen tests were conducted on the following items:

(a) Operational checkout of fuel heater performance at full scale flow rate.

(b) Operational checkout of vapor injection.

(c) Calibration of pressure vs. flow rate relationship for liquid injectors.

(d) Operational checkout of 3-way fuel control valve under different fuel conditions.

Igniter System - Initial testing was done with noble metal catalytic igniters, with and without external heating of the igniter element. Nine tests of this type were performed in which the igniter device was coupled with the fully operational air and supply systems. These tests all involved actual ignition of the fuel, and combustion for a brief time, over a wide range of conditions. These tests produced promising results, but the resulting igniter devices were not sufficiently rugged for the intended purpose.

A high voltage arc igniter had meanwhile been assembled, and two tests under operating conditions verified that this device should perform satisfactorily over the full range of test conditions.

Preliminary Combustion Tests - The preceding subsystems were combined, in their operating configuration, with a breadboard, uncooled test combustor. This arrangement was used for final checkout of the system prior to the main combustion tests. Ignitions were obtained over a wide range of conditions, and final modifications were made to the configuration of the high voltage electrodes. Seven tests of this sort were performed, up to full scale flow rate. Combustion was limited to a maximum of about 60 seconds in these tests.

A final checkout combustion test was then performed with entire apparatus, including heat exchanger, assembled. The main phase of combustion testing was then initiated.

F. Operating Procedure

A set of test conditions was selected for each run, based on the independent variables of fuel flow rate, overall and primary equivalence ratios. The tests were run in terms of varying heat release rates. Full scale heat release for the present program was selected as 500,000 BTU/hr. The flow rate of each fuel was controlled, based on its heat of combustion, to provide a heat release rate equal to (nominally) 1/4, 1/2, 3/4 and 100 percent of the full scale heat release rate. Some tests were run at 1/10 and 1/30 heat release scale, to observe operation at these low flow conditions.

The required primary and secondary air flows were calculated, and a selection made of the proper venturi to use for each condition. The sequence of operating conditions was always selected to require the minimum number of changes in the air venturis.

In the case of a run using superheated vapor, fuel flow was established at the desired operating value. The fuel heater was turned on in steps to bring the fuel up to the desired superheated conditions in about 20 minutes. During this period, all of the fuel flowed into the bypass mode, through the condenser and into the collection vessel.

When the fuel was up to condition, both air flows were brought up to operating values. The gas analysis instrumentation was connected to "sample" mode, and a final check made of the overall test setup. The high voltage transformer was then activated, and the primary current observed to see if it corresponded to normal arc conditions. The 4 KΩ shunt resistor to the photoconductive cell was shorted out by a switch, and the photocell override button was depressed. The fuel solenoid was then switched to the burner mode, introducing fuel into the line leading to the fuel nozzle contained in the igniter section. It should be noted that this valve would not divert the fuel into the burner unless the override button was depressed. Immediately after activating the solenoid valve, however, the override button could be released without shutting off fuel flow (provided that the shunt resistor was shorted out). Depending on the flow conditions, the fuel was often introduced into the fuel nozzle in short spurts, since the initial process was necessarily, accompanied by some condensation of the fuel as the insulated plumbing downstream of the fuel solenoid valve became heated. This was continued until the combustor thermocouple readout on the pen recorder showed a response. This meant the system was ready to sustain combustion. The fuel valve was left in the burner mode, and as soon as it was verified that continuous combustion was occurring, the short on the photocell shunt resistor was switched off. This brought the photocell back into the circuit. If, at any subsequent time, loss of flame occurred, the photocell circuit would, as previously describied, shut off fuel flow to the burner.

At this time the operator was able to leave the ignition control switch box, and examine all instruments for proper functioning. It was then merely a matter of making minor adjustments to fuel and air flow rates, and perhaps fuel heater setting, to bring the combustor up to the first condition. Normally, at this time the igniter arc was shut off. Only for conditions involving operation in "fringe" combustion conditions would it be left on.

After verifying that conditions were at steady state, readings were taken of all pressure gages, manometers, and other appropriate control settings. This was followed immediately by reading and recording the output of each gas analysis instrument.

Conditions were then changed to the next set of desired values. If this involved a change in air settings only, combustion occurred continuously during the transition. If a change in venturis was involved, or a change in heat release rate (fuel flow), the combustor was shut down simply by turning off the fuel solenoid valve switch. When the new venturis and/or the new fuel flow had been established, the startup procedure described above was repeated.

Runs with injection of liquid fuels, or with methane, were basically very similar. The main difference was the elimination of the fuel conditioning time required in the superheated vapor tests.

The duration of actual cumulative combustion was generally in the range of 1 to 2 hours for each test.

VI. TEST RESULTS

A. Description of Test Conditions

The schedule of runs is given in Table III. A total of 19 runs were made with various fuels, fuel injectors and fuel preparation over a wide range of equivalence ratios and heat release rates. The complete set of raw data is compiled in Appendix D.

The majority of the data is plotted versus fuel equivalence ratio or fraction of fuel flow referenced to a design point of 500,000 BTU/hr. The fuel equivalence ratio is defined as the actual fuel-to-air ratio divided by the stoichiometric fuel-to-air ratio for the particular fuel under consideration. The relationship between fuel equivalence ratio, air-to-fuel ratio, and temperature for a typical kerosene-type, hydrocarbon fuel with a heating value of 18,600 BTU/lbm is shown in Figure 17. Samples of the gas temperatures measured by thermocouples at the burner exit are shown in this figure. The deviation from the ideal are due to two effects: (1) a heat loss from the burner can to the water cooled chamber walls, and (2) thermocouple errors. These are discussed in Appendix E where a heat balance over the complete system is presented. A typical temperature drop due to heat loss at full design flow was 150°F.

The burner always operated just slightly above atmospheric pressure as shown by the plotted data in Figure 18. The burner pressure loss was the order of 5 inches of water or less, whereas the majority of the pressure drop was taken through the heat exchanger.

The walls of the inner can were cooled by radiation to the outer chamber and by forced convection to the secondary air flow. Typical wall temperatures are presented in Figure 19. Although stoichiometric burning with gas temperatures higher than 3500°F occurred in the primary combustion zone, the cooling was more than adequate to keep the temperature well within the range of conventional materials.

B. Gas Emissions

The gas emission data plotted in the following curves is in two forms: (1) carbon monoxide (CO), nitric oxide (NO) and hydrocarbons (as carbon) in parts per million of gas passing through the instruments and (2) the same parts per million corrected to stoichiometric conditions ($\phi_0 = 1.0$). Whenever the second condition is used it is noted on the figure. A correction that has not been included is that correcting the measurements to account for the total volume of the exhaust gas. This correction is discussed in Appendix E and is necessary as the instrument sampling system is such that the water vapor in the gas is removed prior to analysis. Thus the emission data will be lower when calculated in terms of the total exhaust products. A typical correction factor is 0.89 for $\phi_0 = 0.8$ for kerosene fuel from the graph in Appendix E.

TABLE III

TEST SUMMARY

Run No.	Injector Configuration	Fuel	Equivalence Ratio ϕ_P	Equivalence Ratio ϕ_O	Heat Release (Ratio to Design Load)	No. of Points	Purpose
1	Vaporizing, Premix, I_{V_1}	TMH	0.6-1.25	0.6-0.8	1/2	10	Effect of ϕ
2	Vaporizing, Premix, I_{V_1}	TMH	0.8	0.6-0.8	1/4, 1/2, 3/4	5	Effect of Load
3	Vaporizing, Premix, I_{V_1}	CH_4	0.8	0.6-0.8	1/4, 1/2	4	Effect of Fuel
4	Atomizing, I_{L_1}	TMH	0.4-0.8	0.4-0.8	1/4, 1/2, 3/4	10	Effect of Injection
5	Atomizing, I_{L_1}	Jet A	0.6-1.0	0.6-0.8	1/2	11	Effect of ϕ
6	Atomizing, I_{L_1}	Jet A	0.8-0.9	0.5-0.6	1/2, 3/4	6	Effect of Load
7	SUE, I_{V_2}	CH_4	0.4-0.8	0.4-0.8	1/4, 1/2	7	Effect of Injection
8	SUE, I_{V_2}	TMH	0.4-0.8	0.4-0.8	1/4, 1/2	12	Effect of Fuel
9	Vaporizing, Premix, I_{V_1}	TMH	0.80	0.6-0.8	1/2, 3/4	6	Compare to Run 8
10	Vaporizing, Premix, I_{V_1}	TMH	0.85	0.78	1	1	Design Maximum
11	Vaporizing, Premix, I_{V_1}	TMH	0.80	0.6-0.8	1/10, 1/30	4	Minimum Flow (Particles)
12	SUE, I_{V_2}	TMH	0.80	0.6-0.8	1/10, 1/30	Discontinued-Faulty Ignitor	
13	SUE, I_{V_2}	TMH	0.80-1.20	0.6-0.8	1/2	6	Reduced NO
14	SUE, I_{V_2}	TMH	1.0-1.2	0.6-0.8	1/4, 1/2, 3/4	12	Effect of Load (Particles)
15	SUE, I_{V_2}	TMH	0.8-1.2	0.6-0.8	1/10	6	Low Flow
16	SUE, I_{V_2}	TMH	0.8-1.2	0.6-0.8	1/30	6	Minimum Flow
17	SUE, I_{V_2}	TMH	1.2-1.6	0.6	1/2	4	Rich Primary
18	Vaporizing, Premix, I_{V_1}	TMH	1.0-1.2	0.6-0.8	1/4, 1/2, 3/4, 1.0	14	Reduced NO (Particles)
19	Atomizing, I_{L_2}	Jet A	0.6-1.0	0.6-0.8	1/4, 1/2, 3/4, 1.0	13	Effect of Fuel Pressure (Particles)

To convert the data to a mass basis, a set of graphs has been prepared and is also presented in the appendix. Thus the data as given in Figures 20 to 33 can be simply converted to milligrams of pollutants per pound of fuel burned by applying the appropriate multiplying factor given in Figures E-5 to E-7 of Appendix E.

The overall fuel equivalence ratios used in the data plots are those calculated from the carbon dioxide measurements (see Appendix E). Discrepancies that occur between these measurements and those calculated from the fuel and air mass flow measurements are also discussed in Appendix E.

1. Prevaporized, Premixed Fuel

The emission results for the basic case where the fuel is vaporized and mixed with the air prior to ignition are given in Figures 20 to 23.

The pronounced effect on NO of burning with a minimum or deficiency of oxygen is shown in Figure 20. Very low levels of CO and CH are present with all primary equivalence ratios at ½ fuel flow.

The effect of different simulated load conditions are shown in Figures 21 to 23. Going to richer primary mixture ratios causes a general decrease in NO (accented at higher flows) but a more difficult problem to keep CO emissions down at the higher fuel flows. In the analysis (Section IV-B), it was shown that little or no NO is formed in the primary zone, but large amounts of CO are created. At the higher flows, the residence time is apparently decreased below that required to oxidize the majority of the CO to CO_2. With less air addition ($\phi_0 = 0.8$), the flow velocities are less (increasing the time) and the temperature is higher (increasing the oxidation rate constant) and the CO rise occurs at a higher heat release than for $\phi_0 = 0.6$. The reason for the rise in NO at 3/4 fuel flow is not evident. The data results taken together with the analysis point to several possible directions for further improvements in simultaneously reducing CO and NO. These would be:

(a) An increase in the afterburner length with a corresponding reduction in the primary zone.

(b) Increase in regenerative heating of the secondary air to speed up the oxidation reaction.

(c) Operation at an overall equivalence ratio greater than 0.8.

2. SUE Burner Configuration

In the SUE burner configuration, the vaporized fuel is injected in a fan from slot nozzles to intersect the incoming air at right angles. Both liquid and gaseous fuel can be used with these nozzles, however, the slot size becomes extremely small for liquid fuels for the size of burner under consideration here. The fuel fan is broken up by the high velocity jet of air from the small diameter inlet duct and the recirculating zone in the step stabilizes the flame. The initial fuel-air mixture is generally quite rich regardless of the overall mixture ratio by reason of the fuel-air mixing. The air in the central core mixes with the annular burning zone as it proceeds downstream. Thus the mixing process itself gives a degree of staging.

As shown in Figure 24, burning richer in the primary zone did make a significant difference in NO formation. The effect of primary equivalence ratio is shown more clearly in Figure 25. It appeared that an upper limit of $\phi_P = 1.2$ was optimum with regard to keeping NO, CO and CH low simultaneously.

The emission data is plotted versus fuel flow for $\phi_P = 1.0$ and 1.2 in Figures 26 and 27. Data was not obtained at the maximum fuel flow point due to a facility limitation on the fuel pressure. The same type of variation in NO as occurred in the premixing fuel injection results is apparent in the $\phi_P = 1.0$ runs. In general, the SUE burner configuration gave lower CO readings but higher NO readings than the premixed fuel system. It also appeared from the $\phi_P = 1.2$ case that the CO rise occurred at a lower fuel flow.

3. Pressure Atomized Liquid Fuel

The gas emission data taken with pressure atomizing fuel nozzles spraying directly into the burner are presented in Figure 28 to 31. As discussed in the preceding section, two atomizing nozzles were employed, differing by the swirl insert that developed the hollow cone spray and by the pressure required to deliver rated flow. The "low" pressure nozzle delivered ½ the design fuel flow at a pressure of 85 psig, whereas the high pressure nozzle required 160 psig for the same flow.

As shown in Figure 28, the maximum primary equivalence ratio useable was significantly smaller than that for the vapor injectors. CO levels rose sharply above $\phi_P = 1.0$ and smoke was visible in the exhaust. It appears that a $\phi_P = 0.8 - 0.9$ was optimum for the atomizing injectors. At ½ design flow, a $\phi_P = 0.87$ run showed quite low levels of emissions for overall equivalence ratios between $\phi_O = 0.65$ and 0.75 (Figure 29).

The effect of heat release is shown in Figure 30 for a primary equivalence ratio, $\phi_p = 0.8$ and an overall equivalence ratio of $\phi_O = 0.6$. The emissions of CO and CH rise sharply at 3/4 design flow and also are higher at the 1/4 flow point - at least for the low pressure nozzle where the ΔP is only 25 psig for this fuel flow. The higher pressure nozzle shows better CO and CH characteristics at ½ flow and could be expected to be better at ¼ flow.

The characteristics of the same nozzle with liquid TMH fuel is shown in Figure 31. The available kerosene data at corresponding equivalence ratios are also shown for comparison. The TMH exhibits the same characteristics as the kerosene and the actual data are very close to the same values. Note that with the higher pressure nozzle, the CO and CH data at ¼ fuel flow remains low.

4. Methane Fuel

A series of runs were made with methane to make a comparison with a lighter gaseous fuel. Prior analysis (see Appendix B) had indicated that lighter fuel fractions could burn in an external combustion process with a lower yield of NO as well as CO and CH. This was confirmed by the data shown in Figures 32 and 33. The lowest readings of CO and CH were recorded during these runs. In addition, NO (corrected to stoichiometric) at the corresponding ϕ_p and ϕ_O at ½ scale was reduced from the value of 136 PPM for TMH to 89 PPM for CH_4 or a reduction of 35%. Facility limitations prevented data being taken at full fuel flow.

C. Particulate Emissions

1. Particle Collection and Analysis

The submicron particles that occur in combustion processes often escape most common collection methods. Those particles less than 0.4 micron are also invisible. In order to study particles of this size range, indirect techniques based on light scattering properties have been developed. Unfortunately, these devices cannot disciminate particle size or distributions in the gas stream accurately. This is because light scattering depends on particle structure as well as size. There is also a scattering maxima which occurs at about 0.2 micron. Therefore, many small particles (less than 0.1 micron) could be masked by a few particles of 0.2 micron.

For these tests the particles in the combustor exhaust gases were collected by a Thermal Precipitator (1 - 4*). In this collection device, a strong thermal force field is created by a hot wire heated by an electric current. The sample is drawn between the heated wire and a cooler surface (a Formvar coated screen) separated by .02 inch, by a small vacuum pump. When the small particles approach the wire, they are repelled and deposited on the cooler surface by the strong thermal gradient (about 10,000°F/in.). The efficiency of the thermal precipitator has been shown to be 100% for all particle sizes when the air downstream of the precipitator is observed by light scattering instruments. When testing for submicron particles, a special settling column is placed over the sample intake of the precipitator preventing particles larger than 5 microns from entering the precipitator.

---

*Numbers refer to references in Section VIII.

In order to investigate the size and shape of particulate material in the exhaust gases, it was collected on small electro-mesh nickel screens suitable for use in an electron microscope. The screen is .001 inch thick with 200 openings per inch. Each opening is about 60 microns across. The screens are coated with a thin film of Formvar (in 0.15% ethylene dichloride) which bridges the openings in the electromesh screen. This Formvar film is only a few Angstroms thick and serves as the collection surface.

After collection, the microscope screens are removed from the precipitator. To produce a three-dimensional image, they can be "shadow cast" with vaporized paladium metal. The metal is vaporized in a high vacuum by a large electric current. By shadow casting at about 15° above the horizontal, a uniform overlay of metal is placed on the microscope screen, except when a raised particle causes a "shadow". The height of the raised particle is proportional to the length of the shadow. Shadow casting also shows the shape and structure of the particle better.

The screens, either with or without shadow casting, are examined with the electron microscope. The microscope operates by the same principle as optical microscopes. The object to be examined (screen with deposit) is placed between an electron source and fluorescent screen. The beam of electrons is absorbed or scattered by the object and becomes dark spots on the fluorescent screen. The image of the fluorescent screen can be photographed to produce prints or slides. Particles appear white, the Formvar film appears gray, and holes in the film appear black. The resolution of the electron beam is much higher than a light beam (.001 vs. .2 micron). This allows each particle to be studied individually if desired. Typical magnifications used in atmospheric studies have been 1300; 10,000; and 18,000. The micrographs presented in this report are magnified 5,400 and 18,000 times.

2. Sampling System

Particulate samples were taken at two points in the gas flow system: (1) in the exhaust pipe just downstream of the gas sample station, (2) immediately upstream of the third heat exchanger or water bath. The sampling system is diagrammed in Figure 34.

The exhaust air is drawn into a box* (1) containing the precipitator by means of the vacuum pump (2). Once the air enters the box, the air is circulated by a blower (3) to prevent stratified air within the box. A heat source (4) is provided in the box to keep the air above its dew point. A thermometer (5) is mounted on the precipitator (6) to allow direct temperature readings. The air is drawn through the Thermal Precipitator by means of the vacuum pump (2). The flow of air drawn through the precipitator is monitored and regulated by means of a flow meter (8). An electrical source supplies current to a wire (9) which creates the strong thermal force field required for precipitation. A current meter (10) is built into the precipitator. In order to sample continuously, a slide block mechanism (11) is driven by an electric motor (12), allowing the slide block and microscope screens to advance across under the hot wire at a constant, predetermined speed. Calibration of the flow meter (8) and the slide advance (11) are needed to calculate the particle loading per cubic foot of air.

The operation of the precipitator involves preheating the precipitator box to prevent condensation of the water in the comoustor exhaust. The blower, heater, and pump are turned on before the sampling begins to stabilize the environment of the box and sample lines. When a sample of exhaust is desired, the hot wire and slide advance motor are turned on simultaneously. A stop watch is used to determine the time required for one slide to cross under the hot wire.

One microscope slide was used for each combustor condition evaluated. The micrograph print represents a section of the area contained within one opening of a grid. To ensure that the precipitator box contained a representative sample of exhaust at each condition, the pump was operated for several minutes before a sample was taken.

3. Data Collection and Counting Technique

Exhaust samples are presented as photographs enlarged from negatives exposed by the electron beam of the electron microscope. From the micrographs it is possible to calculate the number of particles per unit volume of exhaust gas. This is done by knowing the volume of gas sample, the area of the deposit, the rate of travel of the slide, the magnification of the photograph, the area of the deposit encountered, the number of particles counted and the amount of excess air (5). With the aid of a graticule, the size of the particles is determined. Statistical information is plotted on log probability paper to obtain the geometric mean (50%) size and the standard deviation. The amount of excess air is determined from the CO_2 concentrations. The equation representing the concentration of particles is:

---

*Numbers in parentheses refer to numbers shown in Figure 35.

$$\frac{\#\text{ of particles}}{\text{cubic meter}} = \frac{A_1 \times \frac{\text{count}}{\text{field}} \times 11.0 \times 10^{12}}{A_2 \times R \times T} \times \Phi$$

where: A_1 = area of deposit on slide in precipitator (mm^2)

= ($w \times s \times T$) for moving slide

w = width of precipitator slide (mm)

s = speed of travel of precipitator slide (mm/sec)

T = time of precipitator slide travel; sample taking (sec)

A_2 = area of deposit counted on micrograph print $(\text{microns})^2$

R = rate of gas stream flow (cc/min)

$\Phi = \frac{\text{(stoichiometric + excess) air}}{\text{stoichiometric}}$

$\frac{\text{Count}}{\text{Field}}$ = # of particles counted in A_2 of micrograph print

$11.0(10)^{12}$ = constant conversion factor giving dimensional equivalence including magnification factor

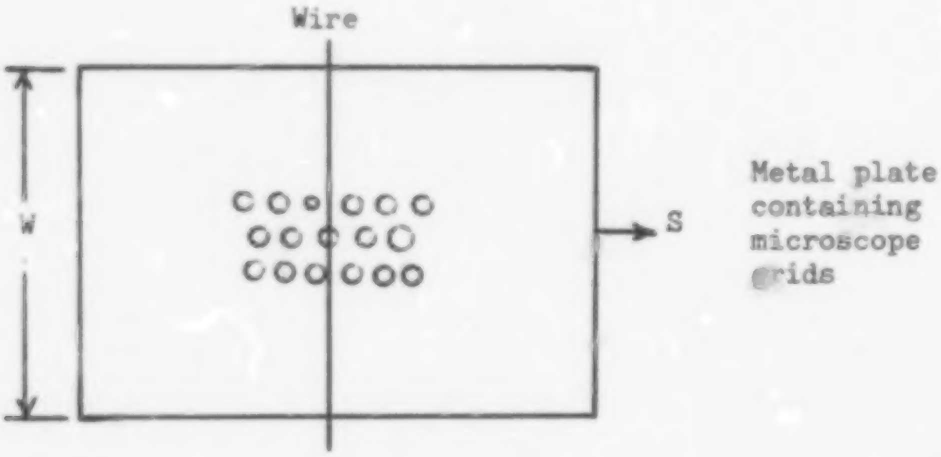

The "percent less than" size distribution plot is a simple graphical solution of the geometric mean particle size. This is obtained by plotting the % of particles less than a given size vs. that size. Particle size of small fairly uniform particles is taken as the largest flat cross section on the micrograph. For large, irregularly shaped particles, the particle size was arbitrarily defined as .8 of the largest flat cross section on the micrograph.

The frequency of occurrence of each particle size range is also plotted by dividing the number of particles of the particular size by the total number of particles. The geometric mean size and size of greatest frequency generally are not the same. The geometric mean size is:

$$Mg = \text{antilog} \frac{\Sigma n \log_{10} d}{\Sigma n}$$

d = particle diameter
n = particle number

and by definition bisects the symmetrical frequency curve yielding the mean or 50% size directly.

The standard geometric deviation defined by:

$$\sigma g = \frac{84\% \text{ size}}{50\% \text{ size}} = \frac{50\% \text{ size}}{16\% \text{ size}}$$

indicates the range of the geometric particle sizes. The geometric mean size and standard geometric deviation define the logarathmic probability curve (symmetrical normal probability) and determine all average diameters (geometric arithmetic, volume, surface) giving complete description of a non-uniform particle sample.

Using the mean particle size, an approximate weight equivalence can be obtained by assuming that the particles are spherical and of known density. This is a fair assumption for uniform tightly packed particles. However, the large chains and grossly non-spherical particles are not accurately represented by this assumption. Therefore, the mass approximations are considerable over estimated for the samples yielding large mean particle sizes and irregularly shaped chains.

In a given sample the volume of particles suspended equals the mean particle size (diameter defining volume) times the total number of particles. The mass then equals the density times the volume of particles. For 2,2,5-trimethylhexane, the fuel used in the combustor, the particles are assumed to be carbon (2.2 gms/cc). For automobile exhaust, 10% by number of the particles $.1 \rightarrow 1\mu$ are assumed to be lead (11.0 gms/cc) with the remainder carbon. Typical data reduction techniques and sample calculations are given in Appendix E.

4. Data Evaluation

Typical photomicrographs and particle size distributions are shown in Figures 36 thru 41 and the data are summarized in Table IV.

a. Particle Size

Particle size is determined from the x18,000 magnification prints when particles are small. Particle size ranged from 0.033 to 0.66 micron. The minimum particle size occurred for vaporized fuel at 3/4 fuel flow scale, Figures 37, 38 & 39. For the liquid kerosene, the minimum particle size was 0.20. micron which occurred at 1/2 fuel flow, Figures 40 & 41. In general, the particle sizes correspond to the expected sizes for continuous flow combustion processes. However, there is a wider range of particle sizes within each sample and from sample to sample than usually found with other combustion processes. The minimum particle size occurred at mid range fuel flow conditions for both liquid and vaporized fuels. Vaporized fuels yielded smaller particles at equivalent fuel flows. Run 14 at 3/4 fuel flow and Run 19 at 1/2 fuel flow yielded different particle sizes at different conditions suggesting that the ratio of primary to secondary air is important in determining the particle size distribution. The overall amount of excess air is not related to particle size. Particle size increased at full fuel flow conditions and at low ($\leq$1/10) flow conditions. At full flow conditions, inadequate residence time in the flame front prevents complete oxidation. In Run 11, the combustion was intermittant causing bimodal size distribution; i.e., the small particles were produced during burning while the large chains resulted from the "flame-out" periods, Figure 36.

b. Particle Count

The particle count data is all taken from the x5,400 magnification prints which give a larger visual field and presumably a more representative sample of the deposit. They are also measured downstream of the water bath as discussed below in Section e(1). Considerable variation in particle counts per unit volume are evident. They do, however, agree with the expected values for combustion gas particulate concentration. The liquid kerosene produced slightly fewer particles (52 to 94 x 10^9 part/cu.ft.) than vaporized TMH (83 to 210 x 10^9 part/cu.ft.) and showed smaller spread. The maximum particle counts occurred for the 3/4 fuel flow condition using vaporized fuel, Figure 40. The concentration of automobile exhaust is between 90 and 270 x 10^9 particles per cubic foot.

c. Particle Mass (calculated from observed particle concentrations)

Mass emissions estimated from the mean particle size, count and particle density is only a rough approximation of the particulate mass. For large particles, the density is inaccurate because of the void space

TABLE IV

SUMMARY OF PARTICULATE DATA

Sample	Run	Cond.	Inject; Fuel	Fuel Flow	ϕ_P ‡	ϕ_O ‡	Count Part/ft^3 x 10^9	Count Part/M^3 x 10^{12}	$\frac{\mu gm}{m^3}$	$\frac{\mu gm}{gm\ fuel}$	Mean Size(μ)	St'd. Dev. (σ)	Observe Smoke
2285D 2286C	11	1	I_{V_1} TMH	1/10	0.8	0.6	9.6	3.4	8.9 x 10^5	1.3 x 10^4	.60	2.50	No
2287C 2287D	11	3	I_{V_1} TMH	1/30	0.8	0.6	170	5.9	1.3 x 10^6	1.9 x 10^4	.56	2.34	No
2292C	14	7	I_{V_2}	3/4	1.2	0.6	210	7.5	3.2 x 10^2	3.2	.033	2.36	No
2292D			TMH	3/4	1.2	0.6	160	5.7	2.4 x 10^2	2.4			No
2293A	14	8	I_{V_2}	3/4	1.0	0.6	100	3.6	1.5 x 10^3	1.5 x 10^1	.07	2.70	No
2293B			TMH	3/4	1.0	0.6	170	6.0	2.5 x 10^3	2.6 x 10^1	.07	2.70	No
*2294C	18	9	I_{V_1}	1	1.2	0.8	46	1.6	2.0 x 10^5	2.6 x 10^3	.47	2.61	No
2295C	18	9	TMH	1	1.2	0.8	83	2.9	3.2 x 10^5	4.0 x 10^3	.45	1.56	No
2297A	18	11	I_{V_1} TMH	1/4	1.2	0.6	41	1.5	6.0 x 10^3	6.0 x 10^1	.15	2.18	No
*2298C	19	1	I_{L_2}	1/2	0.8	0.6	41	1.5	1.6 x 10^4	2.0 x 10^2	.21	2.24	No
2299C	19	1	Jet A	1/2	0.8	0.6	78	2.8	2.5 x 10^4	3.2 x 10^2	.20	2.25	No
3000C	19	3	↓	1/2	0.6	0.6	74	2.6	1.1 x 10^5	1.2 x 10^3	.33	1.76	Intermittant
3001C	19	4		1/2	1.0	0.6	94	3.4	2.6 x 10^5	3.1 x 10^3	.40	2.15	No
3002C	19	5		1/2	1.0	0.8	60	2.1	2.4 x 10^5	3.7 x 10^3	.45	2.15	Intermittant
3003C	19	10		3/4	1.0	0.6	93	3.3	3.9 x 10^5	4.3 x 10^3	.46	2.30	
3004A	19	11		1	1.0	0.8	54	1.9	6.8 x 10^5	9.4 x 10^3	.66	2.07	Heavy
3005A	19	13		1/4	0.8	0.6	52	1.9	3.3 x 10^5	4.3 x 10^3	.53	1.80	Light
3006A	19	15		1/4	0.6	0.6	65	2.3	4.1 x 10^5	5.2 x 10^3	.36	2.25	No

*Ahead of Water Bath (sample point 2)

‡ϕ_p and ϕ_o based on flow rates; rounded off

in the particles. For elongated particles, the assumption of spherical form is incorrect. However, given these assumptions, the minimum mass emissions were .32 mgm/m^3 and occurred for 3/4 scale fuel flow with vaporized TMH. This resulted from the very low mean particle size (.033 μ) which defines the average particle diameter. The maximum mass emission (1.3 x 10^3 mgm/m^3) occurred for the large carbon clumps of Run 11. Typical mass emissions are between 16 and 400 mgm/m^3. At equal conditions, the liquid fuel produced larger mass emissions due to the larger mean particle size characteristic of the liquid fuel.

d. Residual Ash (calculated from observed particle concentrations)

The estimate of residual ash is as high as 2% by weight for the Run 11 conditions. The minimum range is as low as .0002% ash for conditions of Run 14. The typical ash content is in the range of .02% to .2%.

e. Special Studies

(1) Effect of Heat Exchanger on Particulate Emissions

Most samples were taken downstream of the final heat exchanger (water bath) since this is the final combustor effluent. Two samples were taken upstream of the water bath to investigate whether particulates were being effected. No effect was found in mean particle size. However, on Run 18, a sharp drop in standard geometric deviation resulted downstream of the water bath indicating a smaller range of particle sizes. This suggests both agglomeration of small particles and precipitation of large particles. The total particulate count, however, was increased downstream of the water bath in both Run 18 and Run 19. This rather surprising observation is attributed to the configuration of the sample port at the upstream sample point. The end of the sample line is connected to a small diameter tube which is flush to the inside wall of the exhaust pipe. The sample line downstream is larger and pointed into the direction of gas flow. The combination of small flush-fitted tubing probably caused the abnormally small particle counts upstream. The total particle count upstream is about 1/2 the count downstream for both Runs 18 and 19, and the numerical values for the two runs are similar.

(2) TMH vs. Kerosene

The vaporized trimethylhexane generally produced smaller particles but greater total particle counts.

(3) External Combustor Compared to Internal Combustion Engines in Automobiles and Other Combustion Sources

Total particle counts generally were lower than from automobiles while the mean particle size was generally larger. Automobiles have particle size between .15 and .25 micron (see Table V and Figures 42 & 43). The external combustor normally operates in the .2 to .5 micron range, with optimum combustion producing particles less than .1 micron. Mass emissions of automobiles are difficult to evaluate because of the uncertainty of lead particulate concentration in the exhaust stream. If 10% lead is assumed, the particle mass emissions are in the range of 35 to 140 mgm/m^3 compared to 16 to 500 mgm/m^3 for the external combustor's usual performance. The optimum mass emissions of the combustor is less than 1 mgm/m^3. Emission standards are usually less than 300 mgm/m^3 for most stationary combustion processes (Stern, 1968).(5)

f. Physiologic Effect of Inhaled Particulates

Particles larger than 5 microns are trapped in nasal passages. One to 5 micron particles are deposited in the mid respiratory tract. Those less than 1 micron reach the alveoli (Surgeon General, 1962).(6) Therefore, almost all particulate material from both automobiles and the external combustor will enter the alveoli. Of those which reach the alveoli, Dautrebande (1962)(7) reports that 90% by count will deposit with a minimum deposition of 40% at about 0.1 micron. Deposition increases with decreasing size from .1 micron to .01 micron. The degree of damage is related to number of particles rather than particle size. Hence efforts to control particle emissions by reducing mass will not be effective in reducing lung insult if particle size is reduced rather than the number of particles.

g. Conclusions

(1) The external combustor produces particulate material somwhat larger in size and lower in concentration than found with internal combustion engines.

TABLE V

TYPICAL PARTICULATE DATA

(Thermal Precipitator and Electron Microscope)

	Particle Count x 10^9 particles/cubic foot	Mean Particle Size microns
CONTINUOUS FLAME		
Coal		
Direct Discharge	40 - 125	.1 - .15
Baghouse	500 - 6000	.04 - .1
Natural Gas	30 - 100	<.1 - .1
Oil	20 - 1200	.1 - .2
Marquardt Combustor	40 - 200	.03 - .66
AUTOMOBILE		
1957 Chevy	90 - 180	.14 - .23
1968 Plymoutn	160 - 270	.17 - .23
SMOGGY AIR (Downtown L.A.)	0.5 - 10	≈.03
CLEAR AIR	.001 - .10	≈.03

(2) The range of sizes within each sample and from sample to sample is greater for the external combustor than for other combustion sources except incinerators.

(3) Smaller particles are produced when operated on prevaporized fuel than on liquid fuel.

(4) Particle size is not dependent on amount of excess air but appears related to ratio of secondary air to primary air.

(5) Particle count is not related to excess air.

h. Recommendations

(1) Dynamic tests of the combustor are needed to evaluate transient response. Similar particulate data is available from automobiles for direct comparison.

(2) Design and operation of the combustor to produce large particle agglomerations would aid particle emission control. The effect of the final heat exchanger as a particle collection or agglomeration agent should be further investigated.

D. Heat Exchanger Interface

The interface between the combustion system and the complete power plant is the heat exchanger. The combustion process cannot be considered completely independent of the heat exchanger, as the sensible heat from the combustion gases must be transferred to the heating fluid both efficiently and in a manner not to increase emissions. For example, consideration of heat transfer favors high gas temperatures to minimize surface area, volume, weight and cost of the exchanger limited by material considerations. Excessively lean burning would reduce the gas temperature sharply which, in turn, reduces the heat transfer rate (increasing the required heat exchanger surface area and size), and also reduces the thermal efficiency for a fixed exhaust temperature. Large excess air rates also increase the power requirements to drive the blower and so increase its size. In another sense, the presence of relatively cold surfaces in the heat exchanger can have effects on the combustion process by freezing incomplete reactions or by affecting the destruction of unwanted, intermediate compounds. Burning should be completed prior to the time the gases enter the heat exchanger.

The rate at which the gas is cooled could affect the kinetics of the NO formation and CO destruction as described in the analysis. A typical temperature time profile in the heat exchanger is given in Figure 44. For this example, the gases are cooled below 2000°F in less than 15 milliseconds. At this temperature the gas composition is, for practical purposes, frozen and will not change in the ensuing passage to the sampling station. For very low flow rates, the cooling is much less rapid and some reactions may continue past the burner exit. The conditions existing for the maximum burning rate are shown in Table VI.

For comparison, the data for a Rankine cycle boiler designed by The Thermo Electron Corporation is shown in Table VII. In this design, an additional stay time of 9.4 milliseconds at constant temperature occurs in a transition section between the burner outlet and the boiler inlet. The residence time for the maximum design load in the first row of heat exchanger tubes where the temperature is reduced from 3300 to 1900°F is about 5 milliseconds.

TABLE VI

COMBUSTION TEST RIG

HEAT EXCHANGER CHARACTERISTICS

MAXIMUM BURNING RATE CONDITION

STAGE	GAS TEMPERATURE, °F INLET	OUTLET	RESIDENCE TIME Milli seconds	HEAT REMOVAL RATE BTU/Hr
1	3040	2060	12.3	180,000
2	2060	1540	20.4	91,000
3	1540	519	76.0	165,000
TOTALS	--	--	108.7	436,000

TABLE VII

RANKINE ENGINE BOILER CHARACTERISTICS

THERMOELECTRON DESIGN

MAXIMUM BURNING RATE CONDITION

STAGE	GAS TEMPERATURE, °F INLET	OUTLET	RESIDENCE TIME Milliseconds	HEAT REMOVAL RATE BTU/Hr
Transition	3330	3330	9.4	--
Vaporizer	3330	1900	5	834,000
Superheater	1900	1190	--	383,000
Preheater	1190	490	--	359,000
TOTAL	--	--	--	1,576,000

VII. DESIGN CRITERIA

A. Experimental Results

1. Steady State Emission Criteria

The principal basis for the design of the Rankine engine burner is the reduced emissions of carbon monoxide, hydrocarbons, oxides of nitrogen, and particulate matter. In very general terms, hydrocarbons, carbon monoxide, and smoke (unburned carbon) are due to incomplete combustion and reflect fuel injection, vaporization, and mixing problems, plus insufficient air and too short a burning time. Oxides of nitrogen (NO) are formed in any combustion process at a rate usually insufficient to achieve full equilibrium and are destroyed at a negligible rate. Thus, the kinetics are of major importance in determining at what levels NO will exist, with the major factors affecting initial reactions being peak temperatures and durations, available oxygen, and rates of cooling. The burner design variables that have a major bearing on the emissions have been shown to be:

Temperature	(Equivalence ratio, ϕ)
Residence Time	(Lengh/velocity)
Injector Characteristics	(Atomization, vaporization)
Turbulent Mixing	(Burner geometry)
Air Staging	(Burner geometry)
Quenching	(Cold surfaces, air addition)
Fuel Burning Characteristics	(Fuel)

a. Temperature

The temperature of the reaction, both in the primary and secondary burning zones, has a major effect on the formation and destruction of the air pollutants. It appeared that rich burning ($\phi_0 = 1.2$), followed by air addition to bring the overall equivalence ratio to somewhere between $\phi_0 = 0.6$ and $\phi_0 = 0.8$ gave the optimum results. Gas temperatures in this range of fuel-air ratios are also desirable to maximize the thermal efficiency of the vapor generator and keep the air pumping requirement to a minimum. From the analysis, a slight preheat of the inlet air appears desirable to minimize unburned hydrocarbons and more readily oxidize the carbon monoxide.

b. Residence Time

Residence time requirements are extremely important and it was shown there is a distinct trade-off in the afterburner between minimizing NO formation and increasing CO oxidation. The kinetic calculations also indicate that the primary zone in the experimental test rig could possibly be reduced, as the reaction was calculated to be complete in less than the full length. The afterburner section was shown to have two conflicting requirements: (1) with less time allowed for afterburning, the NO emissions showed a sharp drop, (2) however, with less time available, the oxidation of the CO to CO_2 could not be completed. This was confirmed by the experimental results where NO emissions continued to drop with higher flows through the combustor, whereas the CO stayed about the same up to a point where the time was insufficient to complete the oxidation step and the values climbed sharply. From the data, this minimum time appeared to be of the order of 20 milliseconds.

c. Injector Characteristics

The method of injection and fuel preparation prior to injection had a significant effect on the steady state emissions. The use of vaporized fuel produced lower emissions at higher heat release rates. The injection of liquid kerosene or TMH through pressure atomizing nozzles produced low emissions up through one-half of design flow. The time required for vaporization of the fuel droplet was apparently of sufficient magnitude to significantly reduce the time available for the complete burning of the fuel. Carbureting fuel injection where the vaporized fuel and air are premixed produced the best results.

d. Turbulent Mixing

The burner used in all the tests produced a strong recirculation zone in the corner of the step that aided significantly in gas phase mixing. The inlet velocities and velocities through the primary zone and in the afterburner were sufficiently high to produce highly turbulent flow conditions. The secondary air inlet holes were also sized to produce vigorous mixing boundaries. The completeness of burning is enhanced by strong mixing of the fuel and air that avoids pockets or over-rich ar over-lean mixtures. This is expecially important where the fuel is not premixed with the air. In the SUE burner configuration, the injection of the fuel at right angles to the high velocity air jet in the corner of the step provided the best possible mixing.

e. Air Addition

It was shown by analysis and experiments that a fuel rich reaction followed by air introduction and afterburning produce the minimum NO. It was possible to burn at a higher temperature and avoid a rise in NO formation by staging the air addition such as to produce a deficiency of oxygen in the high temperature primary burning zone. Introduction of the secondary air produced a fairly rapid completion of burning with the CO reaching equilibrium values. Too much air in the afterburner produced a condition where the velocity was increased (residence time decreased) and the reaction temperature brought down too quickly to fully oxidize the CO.

f. Quenching

Quenching can occur: (1) locally from cold walls, (2) from heat extractions from the gases, and (3) by introduction of cold air. To prevent quenching and creation of unburned fuel, the walls of the burner were always operated hot (500°F and higher). Heat transfer away from the gas was limited to radiation to a water cooled outer chamber and by convection to the slow moving secondary air. For a typical run at 100 percent design load, the heat transferred away from the burner was approximately 10 percent. This produced a reduction in the actual gas temperature by approximately 150°F. As mentioned previously, downstream air addition was very helpful in completing the combustion reactions, but the amount and method of introduction are critical with respect to freezing the CO composition.

g. Fuel Burning Characteristics

There is a wide range of hydrocarbon fuel candidates which might be considered for the external combustion system based on combustion performance. These are discussed in Appendix B. Very little difference in emission characteristics were noted between a commercial grade of kerosene and a pure hydrocarbon, 2,2,5-trimethylhexane having comparable molecular weights, in the tests. Combustion tests made with methane and computer runs using pyrolized fuel fragments strongly indicate that hydrocarbon fuel blended with lighter fractions than kerosene types could have significantly lower emissions (including oxides of nitrogen) if used in an external combustion engine.

2. Other Emission Criteria

In addition to selecting a combustion process that inherently produces low emissions, consideration must be given to the following in the design:

a. Level of emissions during a typical drive cycle with either on-off or modulating control.

b. Level of emissions during startup and shutdown.

c. Possible degradation of emission levels with time.

d. Possible inspection and maintenance that may be required by State or Federal Laws.

Only the first two are considered to be within the scope of the present program.

a. Fuel Modulation

The results obtained at 10:1 and 30:1 turndown with premixed vaporized fuel strongly suggest that very low emissions at high fuel turndown can only be obtained with a secondary, or pilot, burner designed specifically for the lower flow rates. Two types of problems result in any burner design where large turndowns are required. The first is the combustion problem of maintaining the stability over a wide range of flows and the second one is simply that of introducing small amounts of fuel with good mixing. For example, a 100:1 turndown for the burner corresponds to a minimum fuel flow of 0.16 gal/hr. As a comparison, a "small" conventional atomizing nozzle used in oil burners flows 3/4 gal/hr. In Figure 45 the results from three nozzles flow tested during the current program are shown. The pressure atomizing nozzle has a cutoff point of 40-50 psi; below which the atomization pattern is unsatisfactory. Air atomizing nozzles can operate at lower pressures and are reported to have good characteristics for 10:1 turndown(8). However, they require a source of high pressure air and considerable parasitic power. The air atomizing nozzle tested in the current program did not appear to have satisfactory atomization at 10:1 turndown, but was not combustion tested. Assuming a burner can be made to operate over a large turndown ratio, a practical problem arises of controlling the fuel-air ratio to maintain good combustion at all points and during rapid transients.

Controlling the fuel-air ratio in transient operations was not a part of the current program. However, qualitative observations made during the testing in changing from one condition to the next indicated large emission peaks could occur where the fuel and air were independently changed and excursions in equivalence ratio occurred. This showed the need for a control system that could follow rapid demands for both fuel and air in transient operation. In general, the combustor gas exit temperature and wall temperature responded rapidly to change in fuel flow due to the thin wall, low heat capacity burner can.

b. Startup and Shutdown

The startup and shutdown emissions are chiefly a function of the particular hardware design. For example, in the current program, no emission overshoot was observed on starting except in the unusual case where ignition did not occur immediately. In these cases, the hydrocarbon reading quickly rose to several thousand PPM. On shutdown, the CO and NO meters decreased to zero in 2-3 seconds with hydrocarbon instrument showing slightly slower response. Overshoots in CO and CH (but not NO) often occurred on stopping. The difference between these results and the data observed by others (9 - 11) on fuel oil heaters is due to the responses of the fuel and air system and the thermal lag in the combustion chambers. In the test rig, the fuel flow is controlled by a bypass and fast acting solenoid valve closely coupled to the fuel injector. The response time between the valve opening and full fuel flow is very short. The air flow is brought up prior to fuel injection. In addition, the thin wall burner can will heat up in seconds. In oil burners, the air and fuel flow responses are linked to the rate at which an electric motor driving the blower and pump comes up to speed and to the filling time of a fairly large diameter fuel line. The thermal response in the oil burner combustion chamber is very slow (5-10 minutes in some cases).

For clean startup and shutdown the following criteria would apply:

(1) Solenoid shutoff valve

(2) Minimize fuel line volume

(3) Air flow to lead fuel on startup

(4) Preheated wall surfaces

3. Summary of Design Criteria

The recommended criteria and features for a low emission Rankine burner, based on present knowledge, are summarized in Table VIII.

TABLE VIII

RECOMMENDED DESIGN CRITERIA FOR LOW EMISSION BURNERS

A. PERFORMANCE FEATURES

1. Type of Burner - Staged with primary recirculation zone
2. Fuel - Kerosene (Aviation Turbine Fuel)
3. Maximum Heat Release Rate - 2.0×10^6 BTU/Hr-Ft^3
4. Pressure - Atmospheric (8.3 - 14.7 psia)
5. Inlet Air Temperature - Ambient (-40°F to 120°F)
6. Burner Pressure Loss - 5 in. H_2O
7. Fuel Pressure - 50 psia maximum
8. Fuel Equivalence Ratio - 0.6 to 0.8
9. Fuel Injector - Carbureting (premixed fuel and air)
10. Ignition - High voltage spark electrodes
11. Gas Temperatures - 3200°F maximum

B. DESIRED SYSTEM FEATURES

1. Low Emissions - Expected levels of emissions will be below 1980 Federal Research Goals.
2. Compact Size - A heat release set by low emission criteria will determine burner size for a given maximum power output.
3. Low Noise - Noise levels will depend on velocities and muffling by vapor generator. High heat release burners can be noisy.
4. Positive Ignition - Continuous spark ignition and/or optical flame detector for positive fuel shutoff.

Table VIII - (Continued)

B. Desired System Features - (Continued)

5. Fast Startup - Startup time for burner will depend on response of blower and fuel pump.

6. Wide Turndown - >10:1

7. Environmental Adaptability - Burner should not be sensitive to change in ambient conditions.

8. Low Manufacturing Costs - Cannot be estimated at this time.

9. Minimum Maintenance - Ignition electrodes may require periodic replacement. Small orifices on fuel injectors should be avoided to prevent clogging, etc. Other parts of burner should be maintenance free.

10. Maximum Accessibility - Depends to a large extent on packaging of complete power plant.

11. Clean, Free of Odors - Efficient and complete combustion will prevent any carbon (soot) buildup and eliminate aldehyde or other odors.

VIII. REFERENCES

1. Bush, A.F., "Analysis of Airborne Particles by Count and Size Using Thermal Precipitation and Electron Microscopy," Presented at the Tenth Conference on Methods in Air Pollution and Industrial Hygiene Studies, San Francisco, February 19, 1969.

2. Bush, A.F., "Instrumentation for Sampling and Analyzing Combustion Particulates Using an Electron Microscope," Analysis Instrumentation, Plenum Press, 1964, pp. 267-278.

3. Bush, A.F., "Strange Airborne Particles, "AMA Archives of Industrial Health, Vol. 15, pp. 1-2, January, 1957.

4. Froula, H., A.F.Bush, and E.S.C.Bowler, "Use of Thermal Precipitator and Electron Microscope for Evaluation of Airborne Particles," Proceedings of the Third National Air Pollution Symposium, April 18-20, 1955, Pasadena, California.

5. Stern, Arthur C., Air Pollution, Vol. 3, 2nd Ed., Academic Press, 1965.

6. "Motor Vehicles, Air Pollution, and Health," a Report of the Surgeon General to the U.S. Congress, June, 1962.

7. Dautrebande, Lucien, Microaerosols, Academic Press, New York, 1962.

8. Vickers, P.T., "The Design Features of the GMSE-101 - A Vapor Cycle Powerplant," SAE Paper 700163, Presented at Automotive Engineering Congress, Detroit, Michigan, January 12-16, 1970.

9. Howekamp, D.P. and Hooper, M.H., "Effect of Combustion-Improving Devices on Air Pollution Emissions from Residential Oil-Fired Furnaces," Division of Process Control Engineering, National Air Pollution Control Administration, NOFI Workshop, September 17-18, 1968.

10. Wasser, J.H., et al, "Effects of Air Fuel Stoichiometry on Air Pollutant Emissions from an Oil-Fired Test Furnace," NPCA Journal, Vol. 18, No. 5, May, 1968.

11. Wasser, J.H., et al, "Effects of Combustion Gas Residence Time on Air Pollutant Emissions from an Oil-Fired Test Furnace," Presented at National Oil Fuel Institute Workshop, September 17-18, 1968.

12. Longwell, J.P. and Weiss, M.A., "Mixing and Distribution of Liquids in High-Velocity Air Streams," Industrial and Engineering Chemistry, 45, 667-677, 1953.

13. Bahn, G.S. and Builder, C.H., "The Application of High Speed Motion Pictures in Fuel Injection Studies," American Rocket Society, pp. 463-57, June, 1957.

14. Stern, Arthur C., "Air Pollution," Vol. II, Analysis, Monitoring, and Surveying, 2nd Ed., Academic Press, 1965.

15. "The Oxides of Nitrogen in Air Pollution," State of California, Department of Public Health, Bureau of Air Sanitation, January, 1966.

16. Peters, Max S., "Role, Sources and Control of Nitrogen Oxides in Air Pollution," Presented at the American Institute of Chemical Engineers, Southern California Section, 5th Annual Technical Exhibit and Meeting, Los Angeles, California, April 25, 1968.

17. ICRPG Sixth Thermochemistry Working Group Symposium Held at Huntington Beach, California, March 25-27, 1968.

18. Smith, D.S., Sawyer, R.F., Starkman, E., "Oxides of Nitrogen From Gas Turbines," Journal of Air Pollution Control Association, Vol. 18, No. 1, January, 1968.

19. Grumer, J., et al, "Effect of Recycling Combustor Products on Production of Oxides of Nitrogen, Carbon Monoxide, and Hydrocarbon by Gas Burner Flames," AICHE Preprint 37A, Presented at Symposium on Air Pollution Control Through Applied Combustion Science, New York, N.Y., November 26-30, 1967.

20. Moffat, R.J., "Gas Temperature Measurement," Paper 52. "Temperature, Its Measurement and Control in Science and Industry," Vol. III, Part 2, Rheinhold, New York, 1962.

21. McAdams, W.H., "Heat Transmission," 3rd Ed., McGraw-Hill, New York, 1954.

22. Dodge, B.F., "Chemical Engineering Thermodynamics," McGraw-Hill, New York, 1944.

V7892-3

CONTINUOUS FLOW COMBUTION SYSTEM FOR EXTERNAL COMBUSTION ENGINE

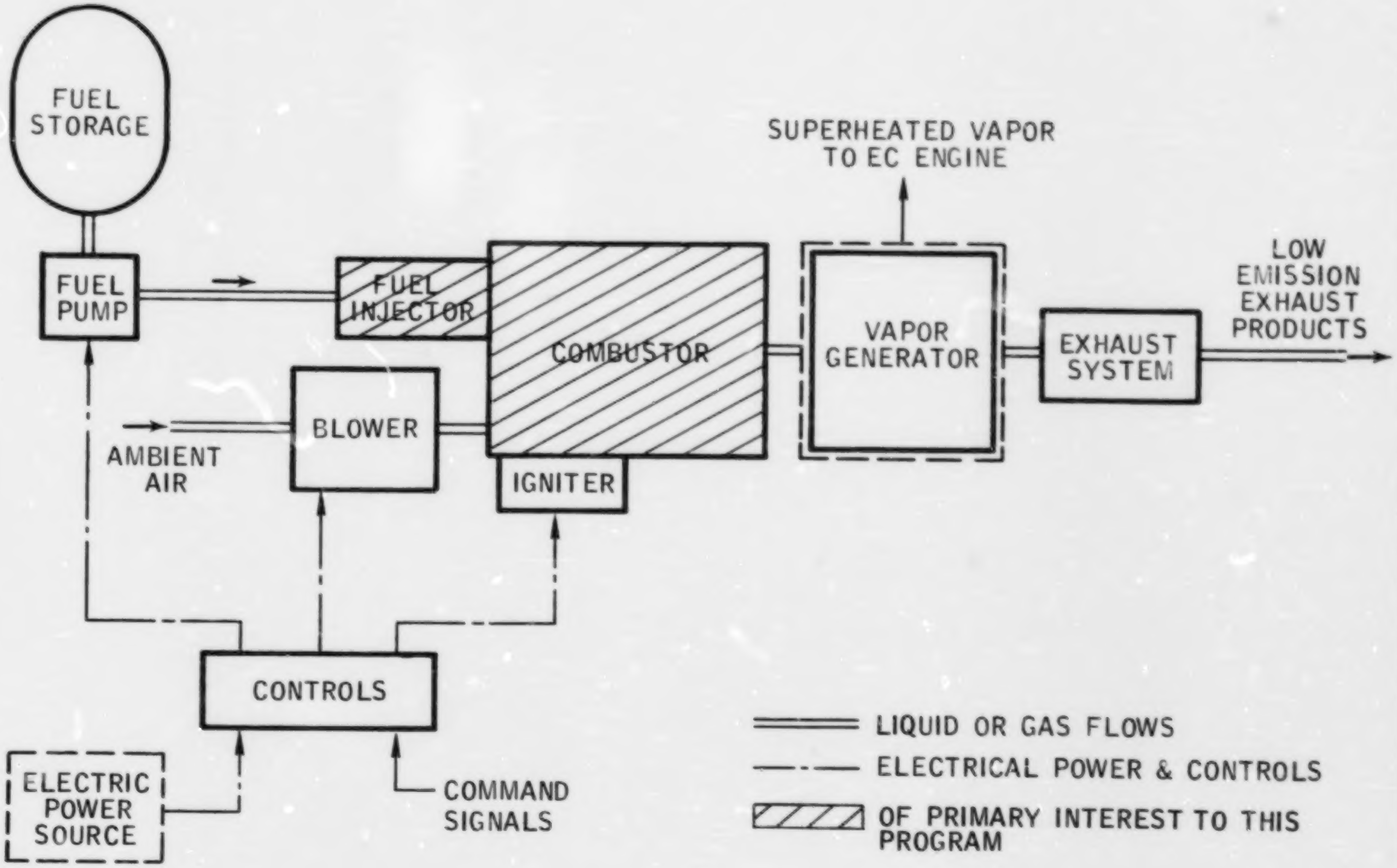
FUEL STORAGE
FUEL PUMP
FUEL INJECTOR
AMBIENT AIR
BLOWER
COMBUSTOR
IGNITER
SUPERHEATED VAPOR TO EC ENGINE
VAPOR GENERATOR
EXHAUST SYSTEM
LOW EMISSION EXHAUST PRODUCTS
CONTROLS
ELECTRIC POWER SOURCE
COMMAND SIGNALS
LIQUID OR GAS FLOWS
ELECTRICAL POWER & CONTROLS
OF PRIMARY INTEREST TO THIS PROGRAM

Figure 1

VALUES FROM THE STEADY-STATE SOLUTION FOR HYDROCARBON COMBUSTION

CONDITIONS: P = 1 ATM, ϕ = 1.5, 0.068 MOLES OF FRESH MIXTURE
DILUTING 1 MOLE OF BURNED MIXTURE FROM 3420°R TO 3240°R,
AND RECOVERY CALCULATED FROM 3240°R TO 3420°R

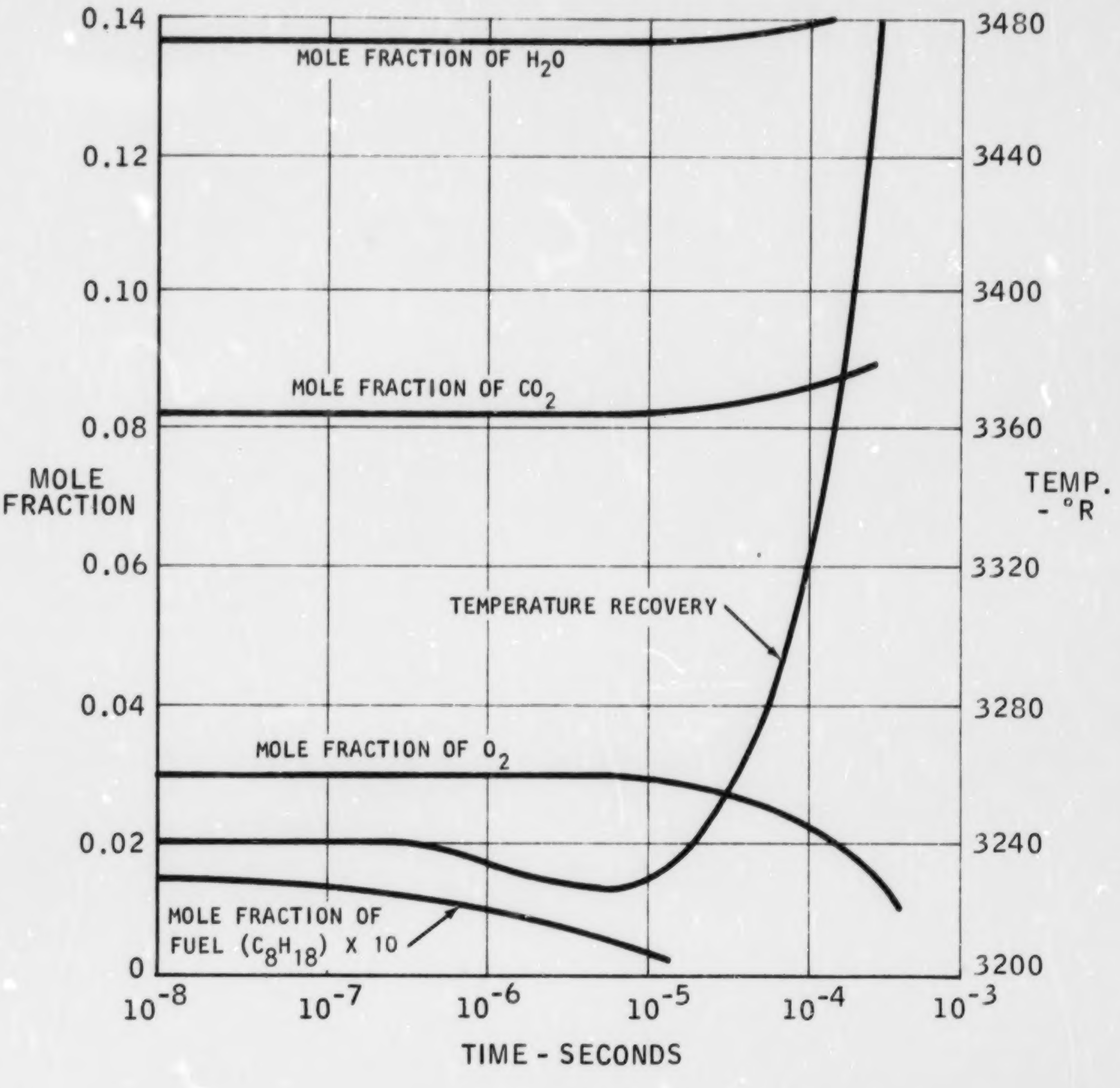

Figure 2

ANALYTICAL MODEL

a. MODEL FOR ANALYSIS

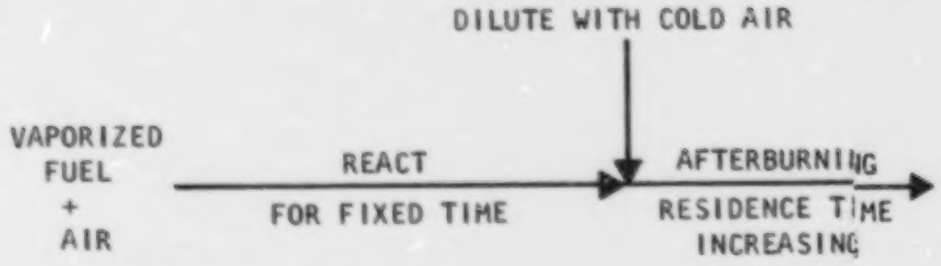
DILUTE WITH COLD AIR
VAPORIZED FUEL + AIR
REACT
FOR FIXED TIME
AFTERBURNING
RESIDENCE TIME INCREASING

b. EXPERIMENTAL BURNER

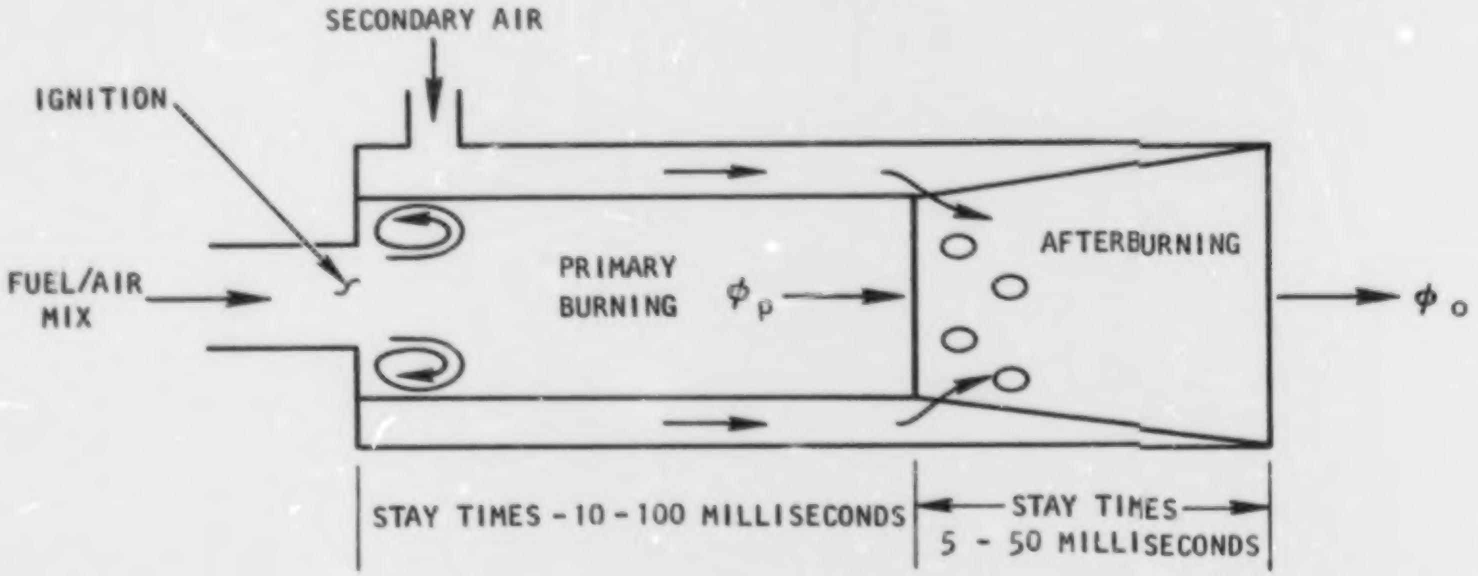
SECONDARY AIR
IGNITION
FUEL/AIR MIX
PRIMARY BURNING
ϕ_p
AFTERBURNING
ϕ_o
STAY TIMES - 10 - 100 MILLISECONDS
STAY TIMES 5 - 50 MILLISECONDS

Figure 3

INSTANTANEOUS TEMPERATURE OF RECIRCULATING HYDROCARBON/AIR FLAMES IN PRIMARY ZONE

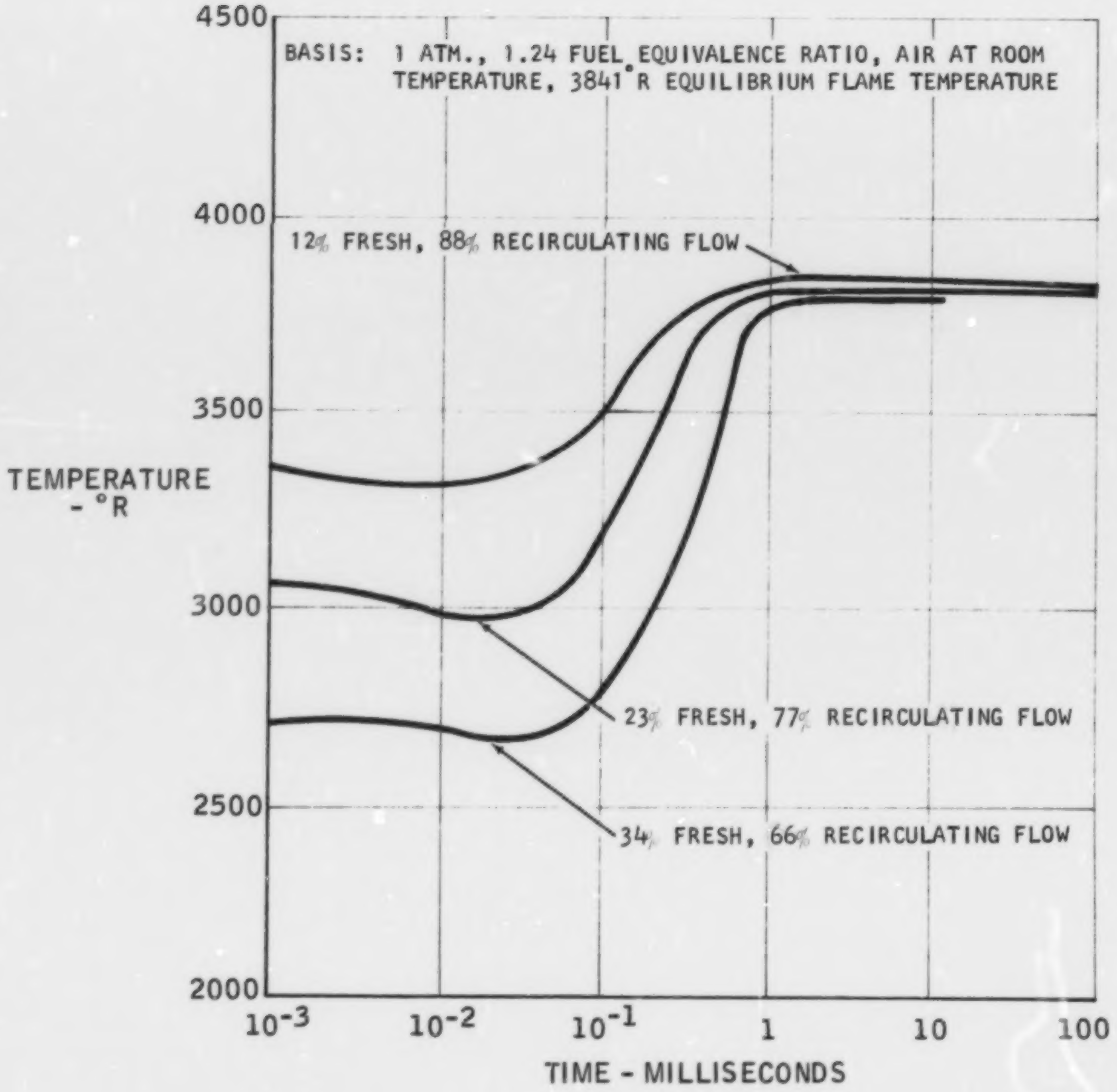

Figure 4

PERFORMANCE OF PRIMARY COMBUSTION ZONE

1.24 EQUIVALENCE RATIO
FRESH MIXTURE + RECIRCULATING PRODUCTS
REACTING FROM 2700°R

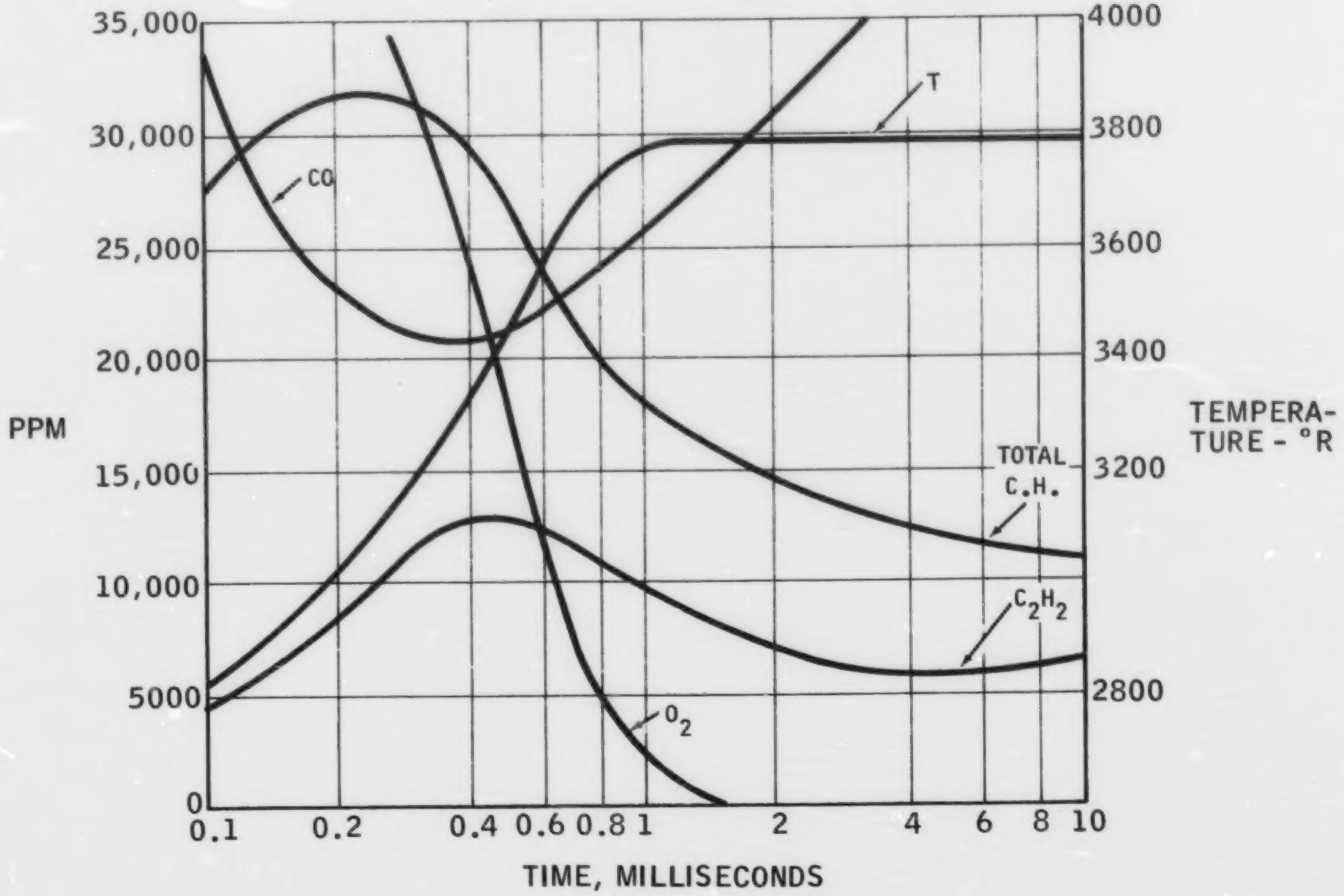

Figure 5

AFTERBURNING AT $\phi = 0.65$ OF FUEL/AIR MIXTURE AT $\phi = 1.24$ REACTED FOR 1 MILLISECOND, AND THEN DILUTED WITH AIR TO TEMPERATURE OF 2700°R

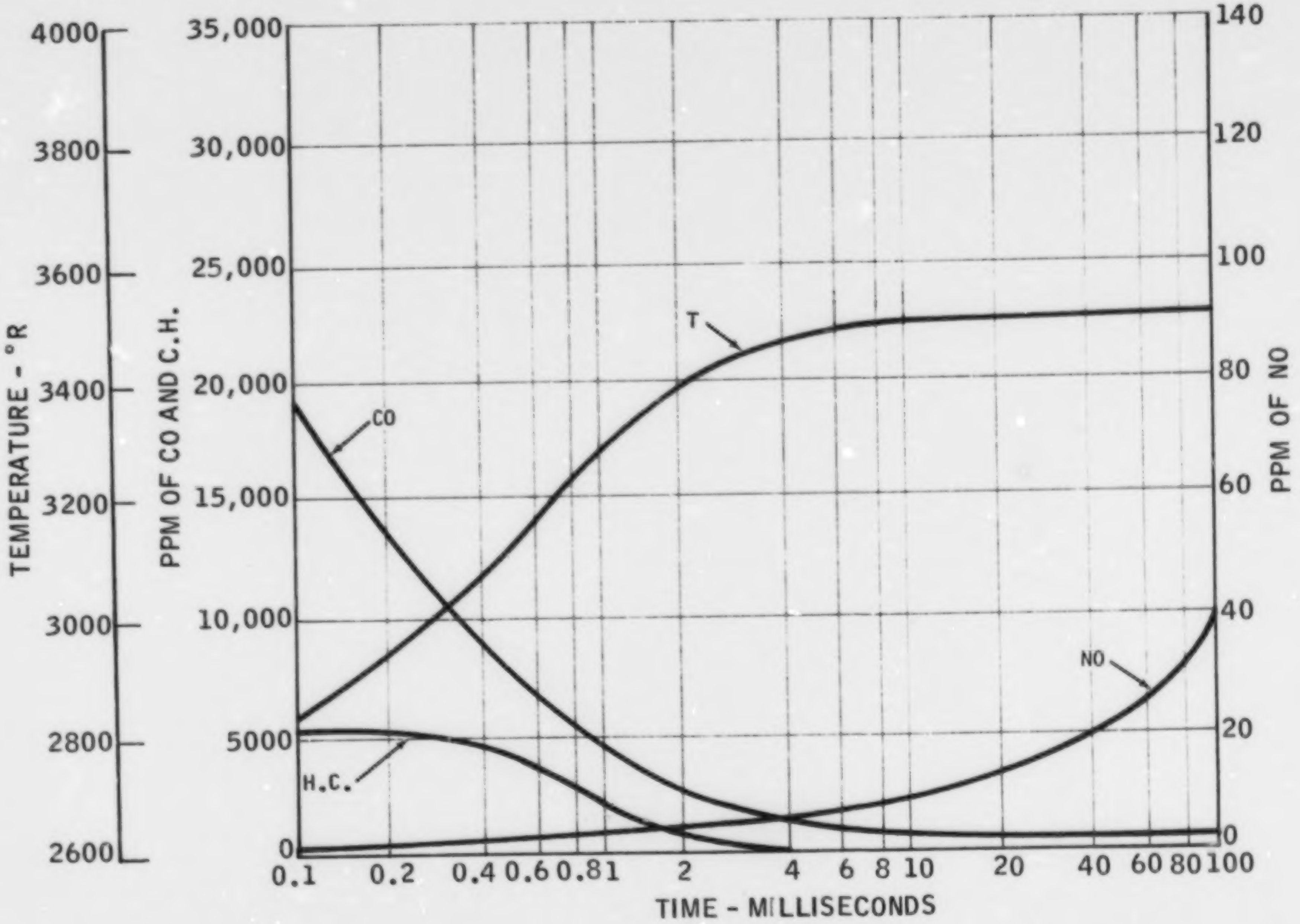

Figure 6

AFTERBURNING AT ϕ = 0.65 OF FUEL/AIR MIXTURE AT ϕ = 1.24 REACTED FOR 1 MILLISECOND, AND THEN DILUTED WITH AIR TO TEMPERATURE OF 2456°R

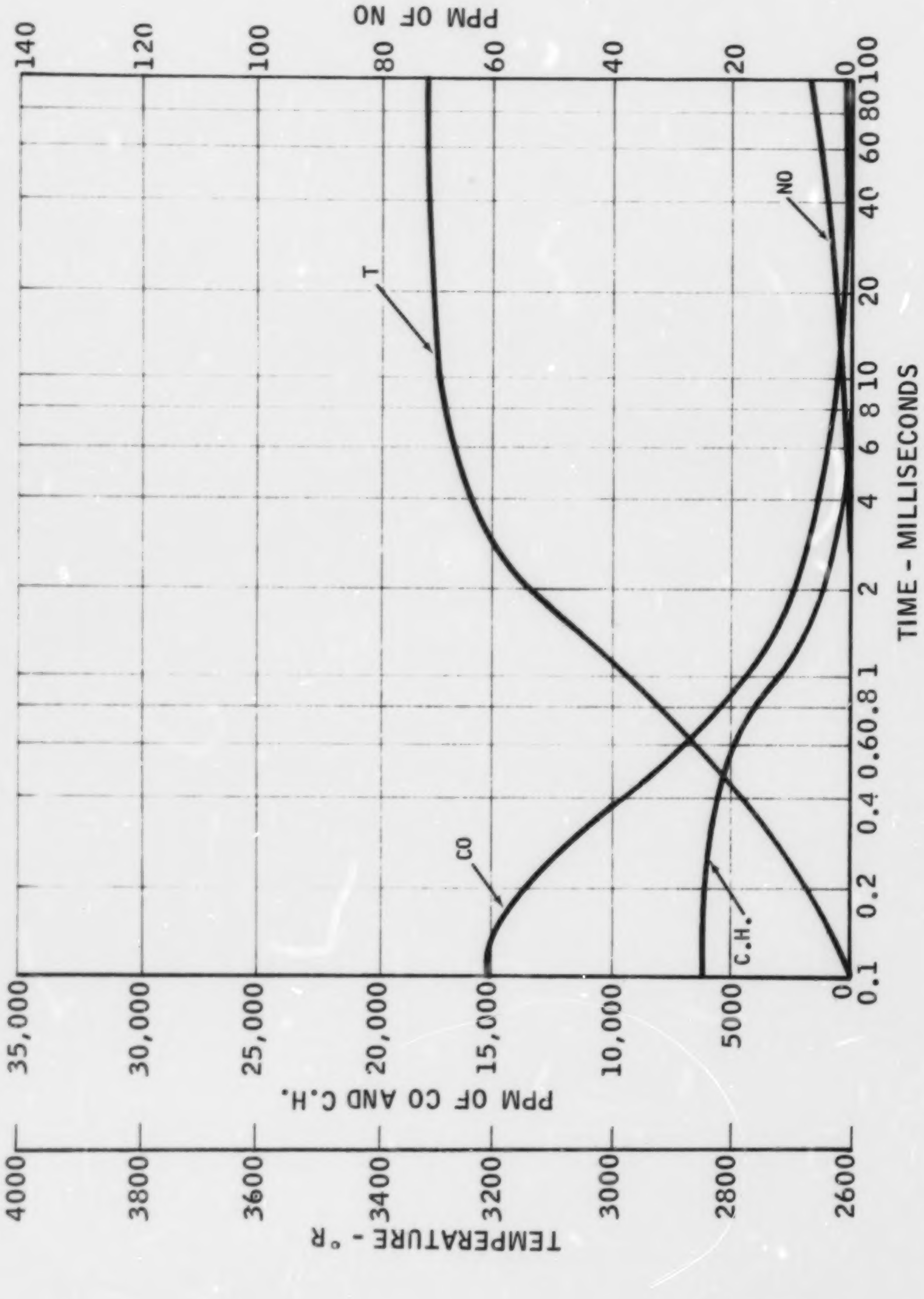

Figure 7

V7892-1

COMBUSTION TEST RIG SCHEMATIC

MAXIMUM HEAT RELEASE = 500,000 BTU/HR

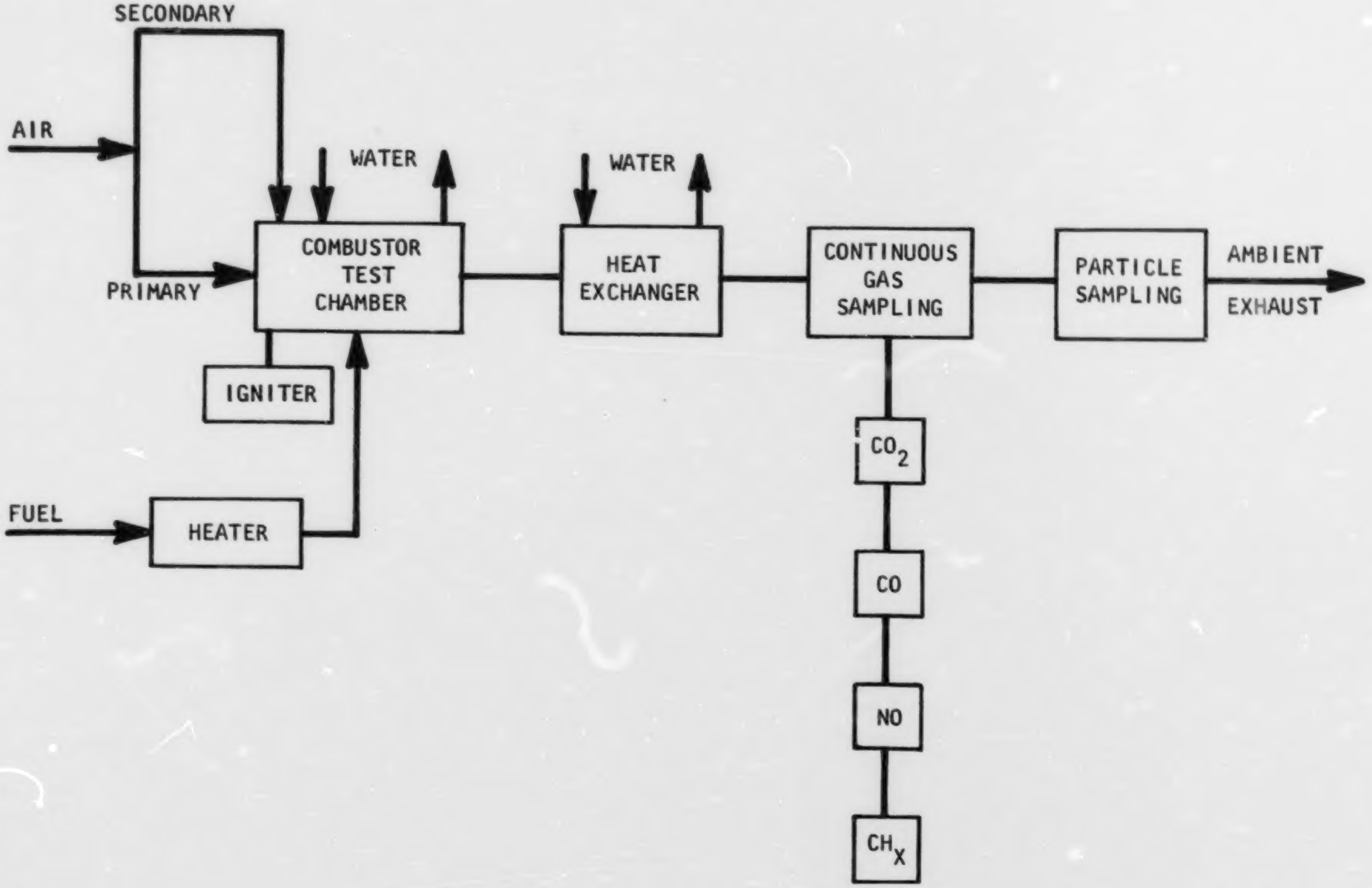
SECONDARY
AIR
PRIMARY
WATER
COMBUSTOR TEST CHAMBER
IGNITER
FUEL
HEATER
WATER
HEAT EXCHANGER
CONTINUOUS GAS SAMPLING
CO_2
CO
NO
CH_X
PARTICLE SAMPLING
AMBIENT EXHAUST

Figure 8

AIR SUPPLY SYSTEM

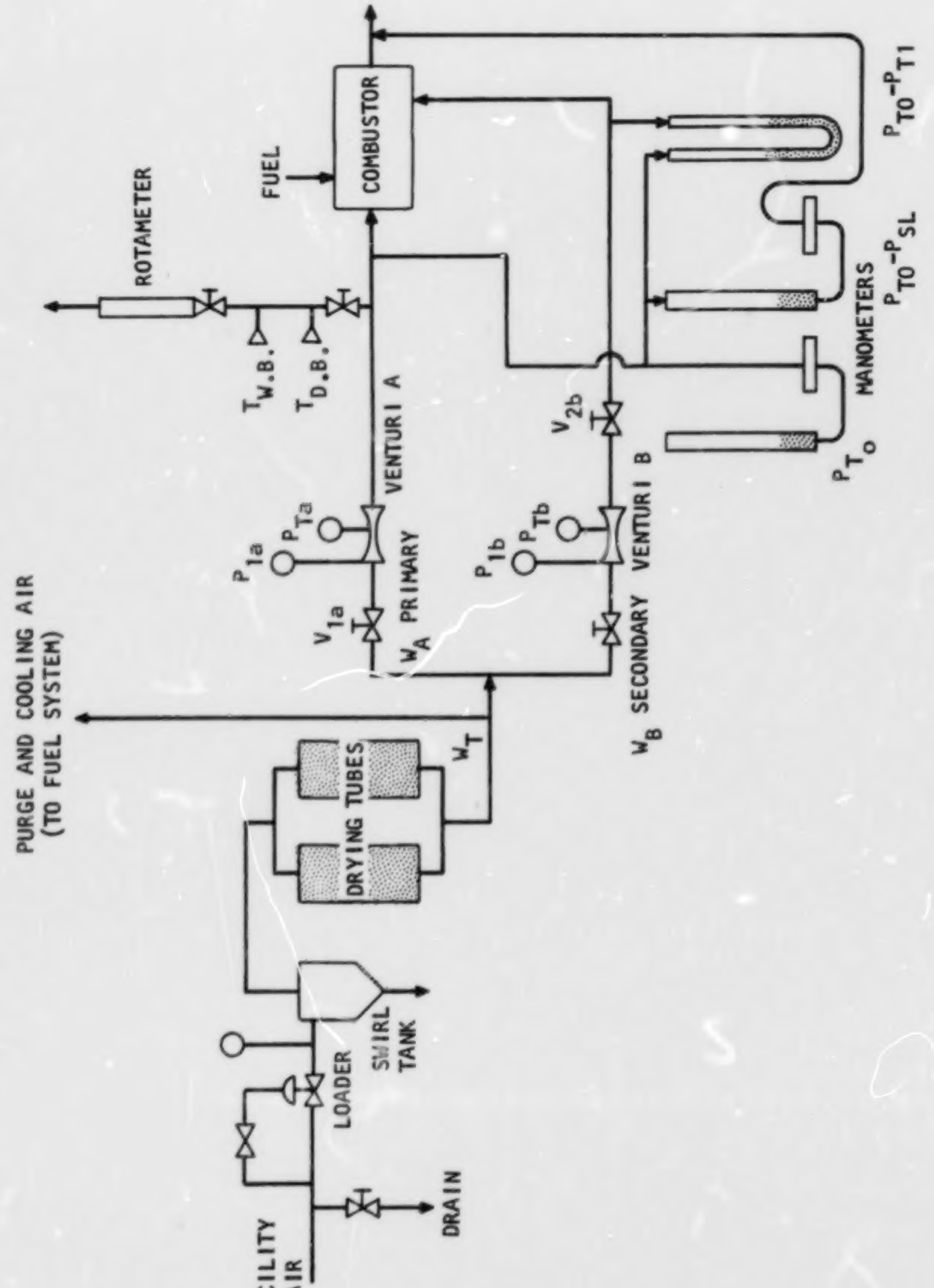
ROTAMETER
FUEL
COMBUSTOR
T_W.B.
T_D.B.
VENTURI A
P_1a
P_Ta
V_1a
W_A PRIMARY
PURGE AND COOLING AIR (TO FUEL SYSTEM)
DRYING TUBES
W_T
SWIRL TANK
LOADER
FACILITY AIR
DRAIN
W_B SECONDARY VENTURI B
P_1b
P_Tb
V_2b
MANOMETERS
P_TO-P_SL
P_TO-P_T1
P_To

Figure 9

V8150-38

FUEL SUPPLY SYSTEM

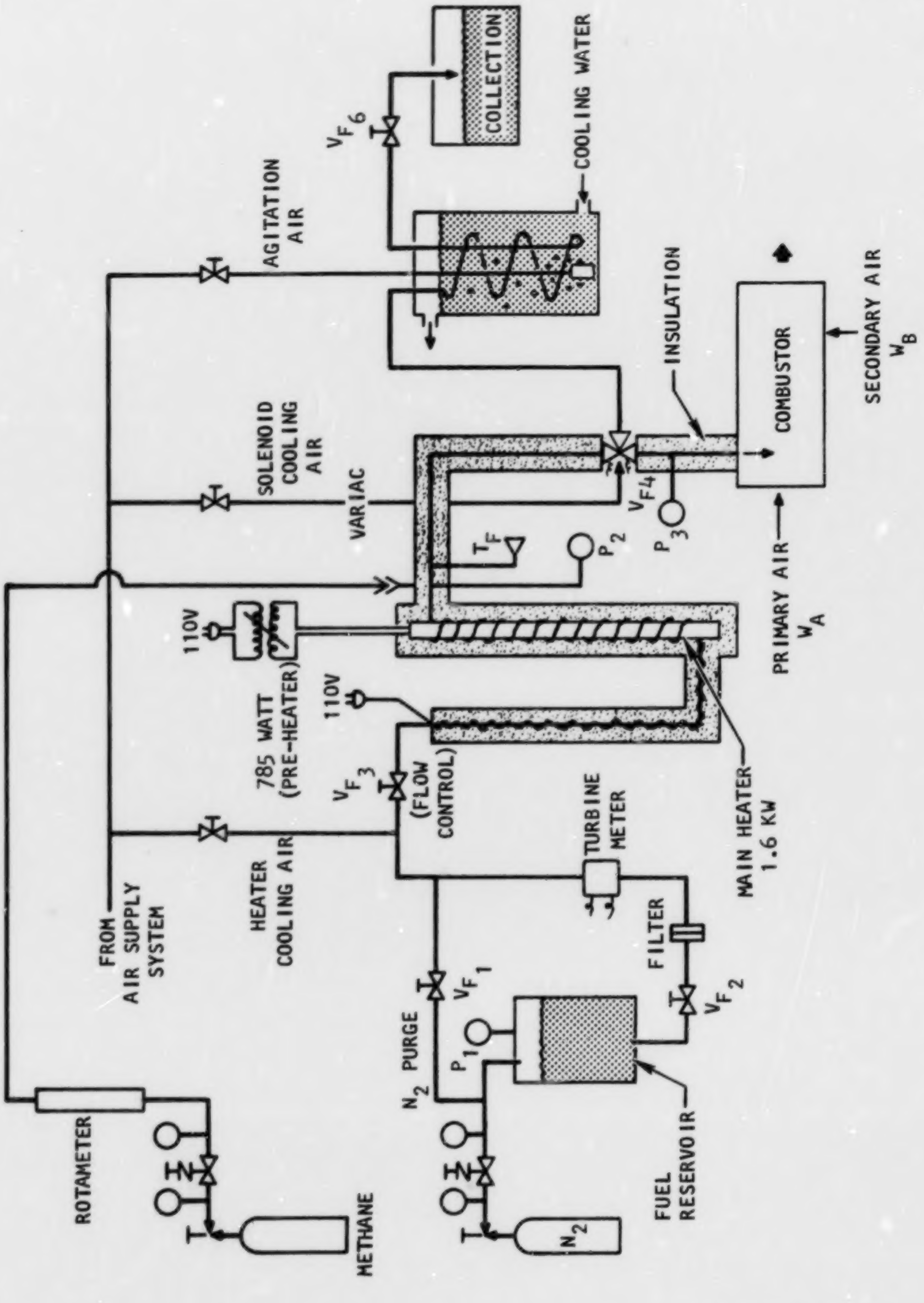
COLLECTION
COOLING WATER
V_{F_6}
AGITATION AIR
INSULATION
COMBUSTOR
SECONDARY AIR W_B
SOLENOID COOLING AIR
VARIAC
V_{F4}
P_3
T_F
P_2
PRIMARY AIR W_A
110V
785 WATT (PRE-HEATER)
110V
V_{F_3}
(FLOW CONTROL)
MAIN HEATER 1.6 KW
TURBINE METER
HEATER COOLING AIR
FROM AIR SUPPLY SYSTEM
FILTER
V_{F_1}
V_{F_2}
N_2 PURGE
P_1
FUEL RESERVOIR
ROTAMETER
METHANE
N_2

Figure 10

COMBUSTOR AND IGNITER SCHEMATIC

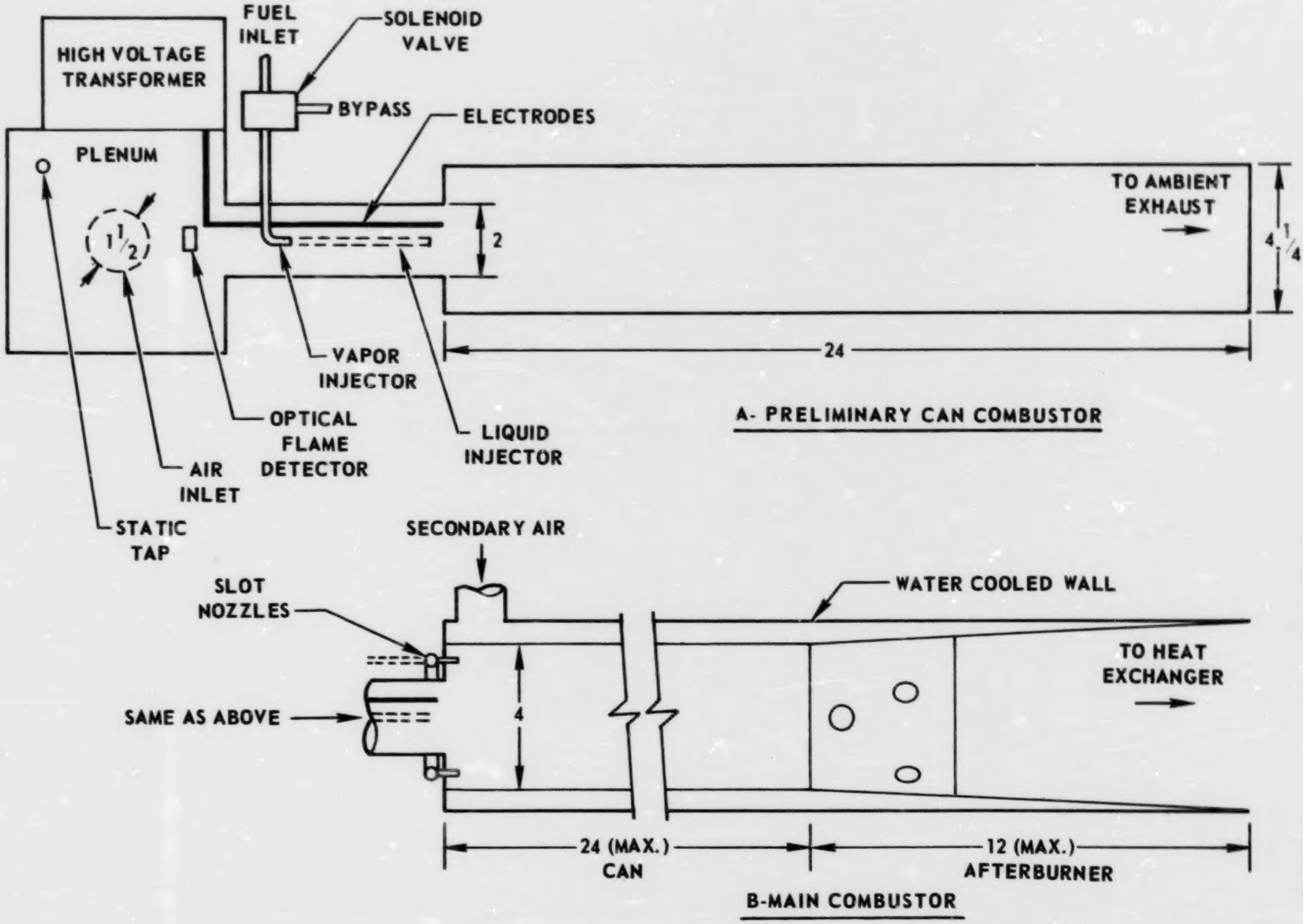
FUEL INLET
SOLENOID VALVE
HIGH VOLTAGE TRANSFORMER
BYPASS
ELECTRODES
PLENUM
TO AMBIENT EXHAUST
2
$4\frac{1}{4}$
$1\frac{1}{2}$
24
VAPOR INJECTOR
OPTICAL FLAME DETECTOR
LIQUID INJECTOR
AIR INLET
STATIC TAP
A- PRELIMINARY CAN COMBUSTOR
SECONDARY AIR
SLOT NOZZLES
WATER COOLED WALL
TO HEAT EXCHANGER
SAME AS ABOVE
4
24 (MAX.) CAN
12 (MAX.) AFTERBURNER
B-MAIN COMBUSTOR

Figure 11

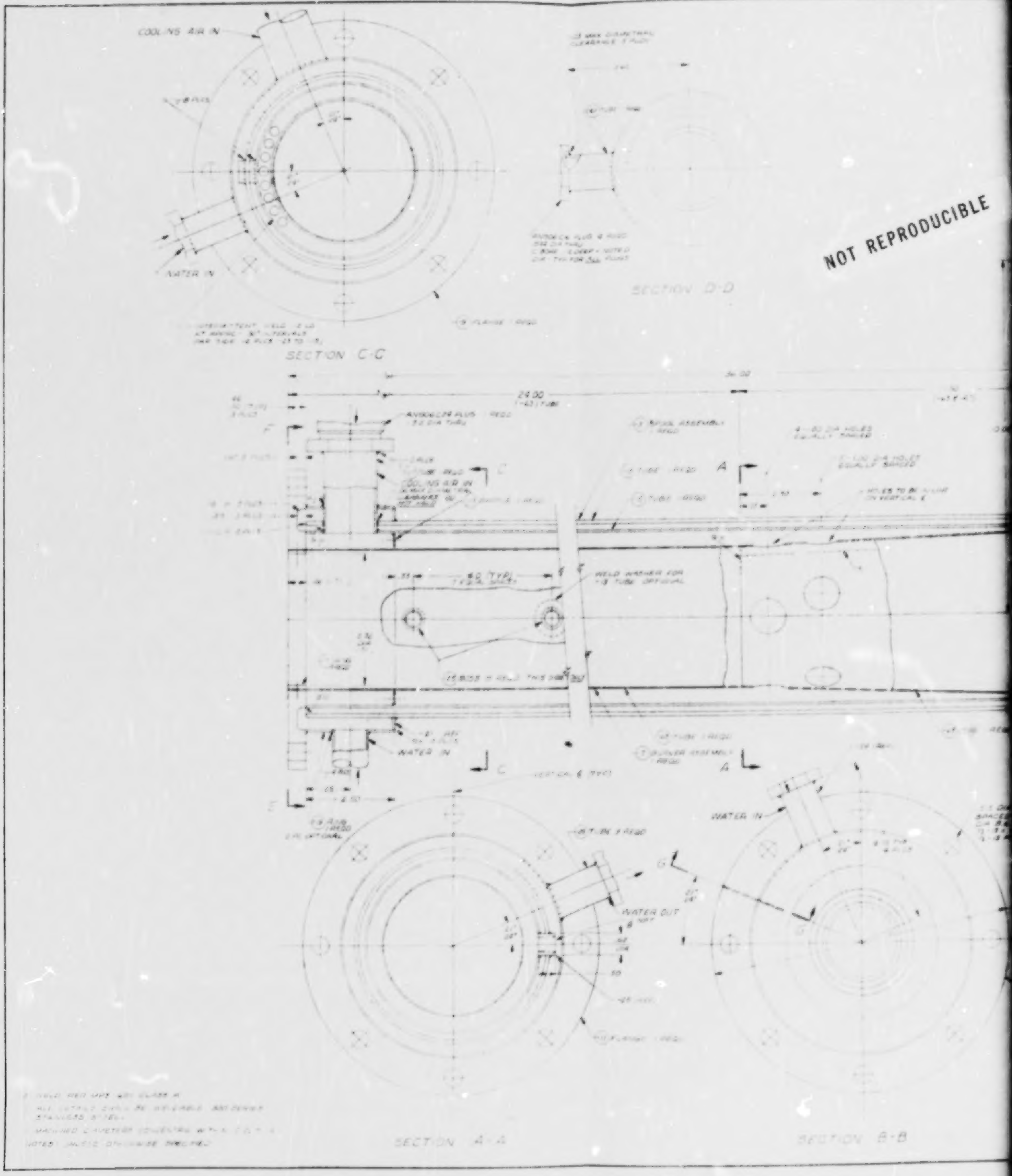
COOLING AIR IN
WATER IN
FLANGE 1 REQD
SECTION C-C
SECTION D-D
24.00
36.00
COOLING AIR IN
WELD WASHER FOR TUBE OPTIONAL
TUBE 1 REQD
BURNER ASSEMBLY 1 REQD
4 - .60 DIA HOLES EQUALLY SPACED
WATER IN
WATER OUT
WATER IN
A
C
F
E
G
SECTION A-A
SECTION B-B
NOTES: UNLESS OTHERWISE SPECIFIED

NOT REPRODUCIBLE

A

NOT REPRODUCIBLE

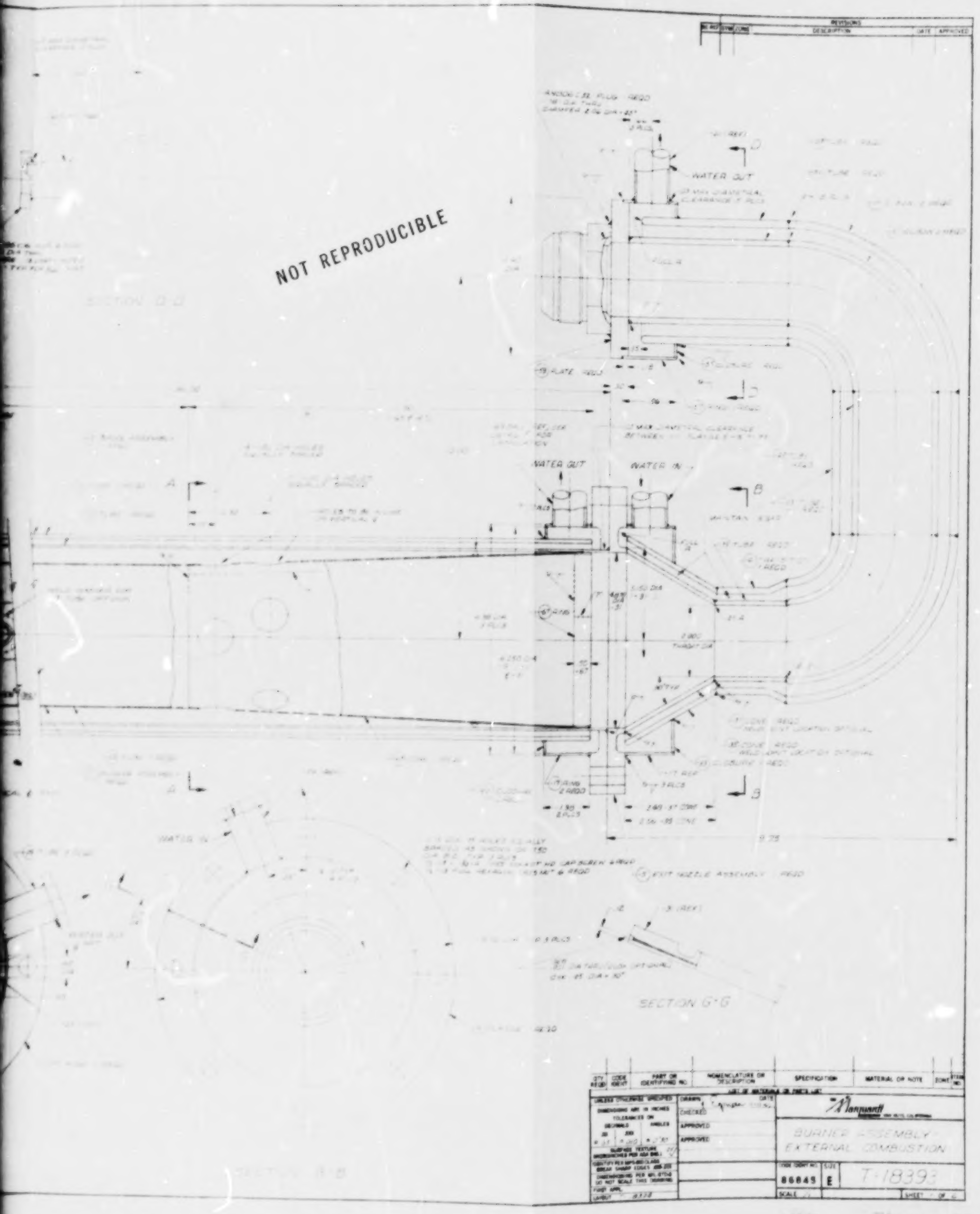
REVISIONS
DESCRIPTION
DATE
APPROVED
WATER OUT
WATER OUT
WATER IN
WATER IN
SECTION D-D
SECTION G-G
SECTION A-B
A
B
D
PLATE REQD
CLOSURE REQD
CONE REQD
WELD JOINT LOCATION OPTIONAL
THROAT DIA
EXIT NOZZLE ASSEMBLY 1 REQD
8.75
QTY REQD
CODE IDENT
PART OR IDENTIFYING NO.
NOMENCLATURE OR DESCRIPTION
SPECIFICATION
MATERIAL OR NOTE
ZONE
ITEM NO.
LIST OF MATERIALS OR PARTS LIST
UNLESS OTHERWISE SPECIFIED
DIMENSIONS ARE IN INCHES
TOLERANCES ON
DECIMALS
ANGLES
DRAWN
DATE
CHECKED
APPROVED
APPROVED
Marquardt
BURNER ASSEMBLY - EXTERNAL COMBUSTION
CODE IDENT NO.
86845
SIZE
E
T-18393
SCALE
SHEET
LAYOUT

B

70 Figure 12

COMBUSTOR ASSEMBLY

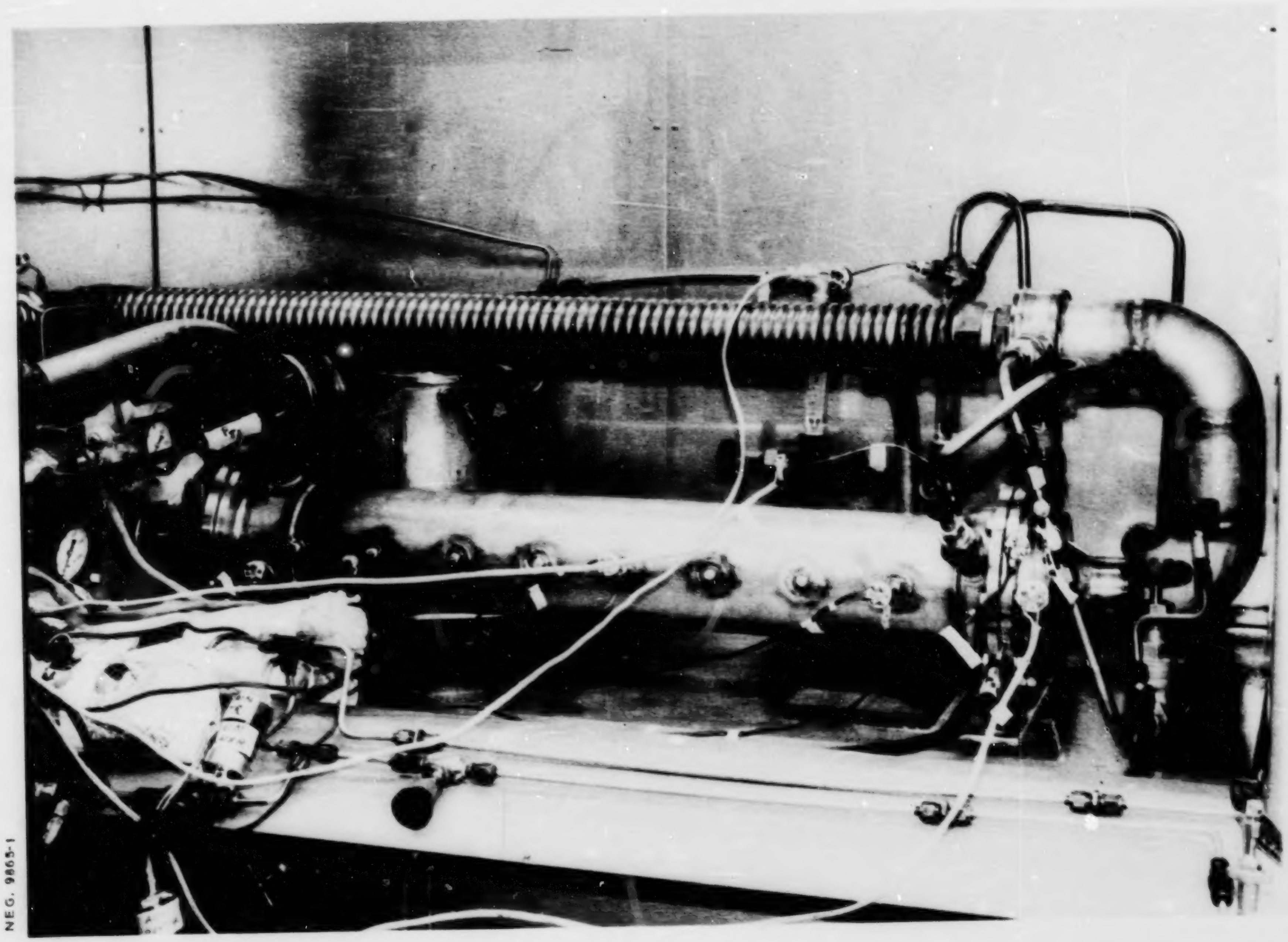

NEG. 9865-1

Figure 13

COMBUSTOR CONTROL AREA

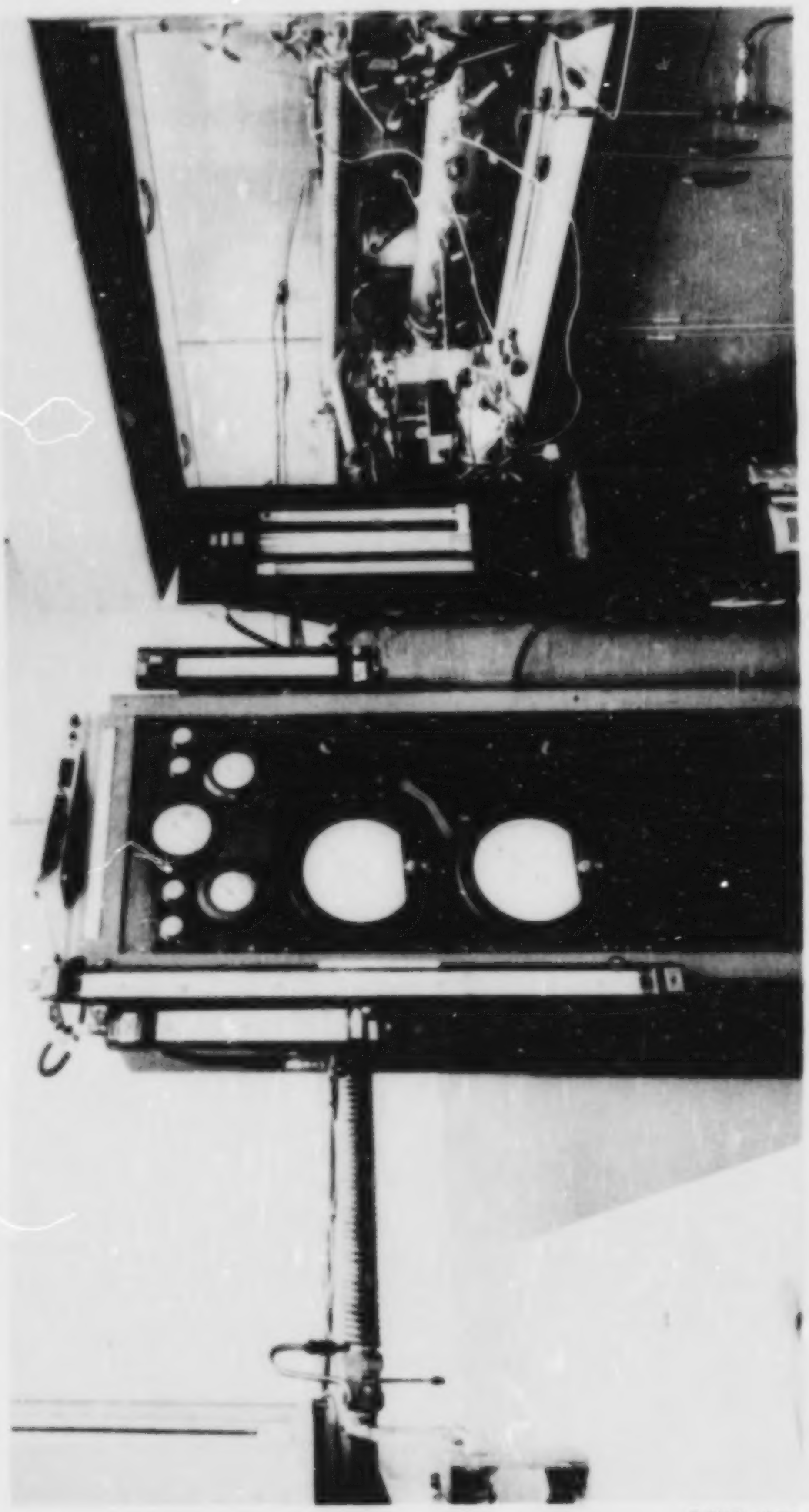

Figure 14

FUEL MANIFOLD
SUE BURNER CONFIGURATION
U.S. PATENT NO. 3,074,469

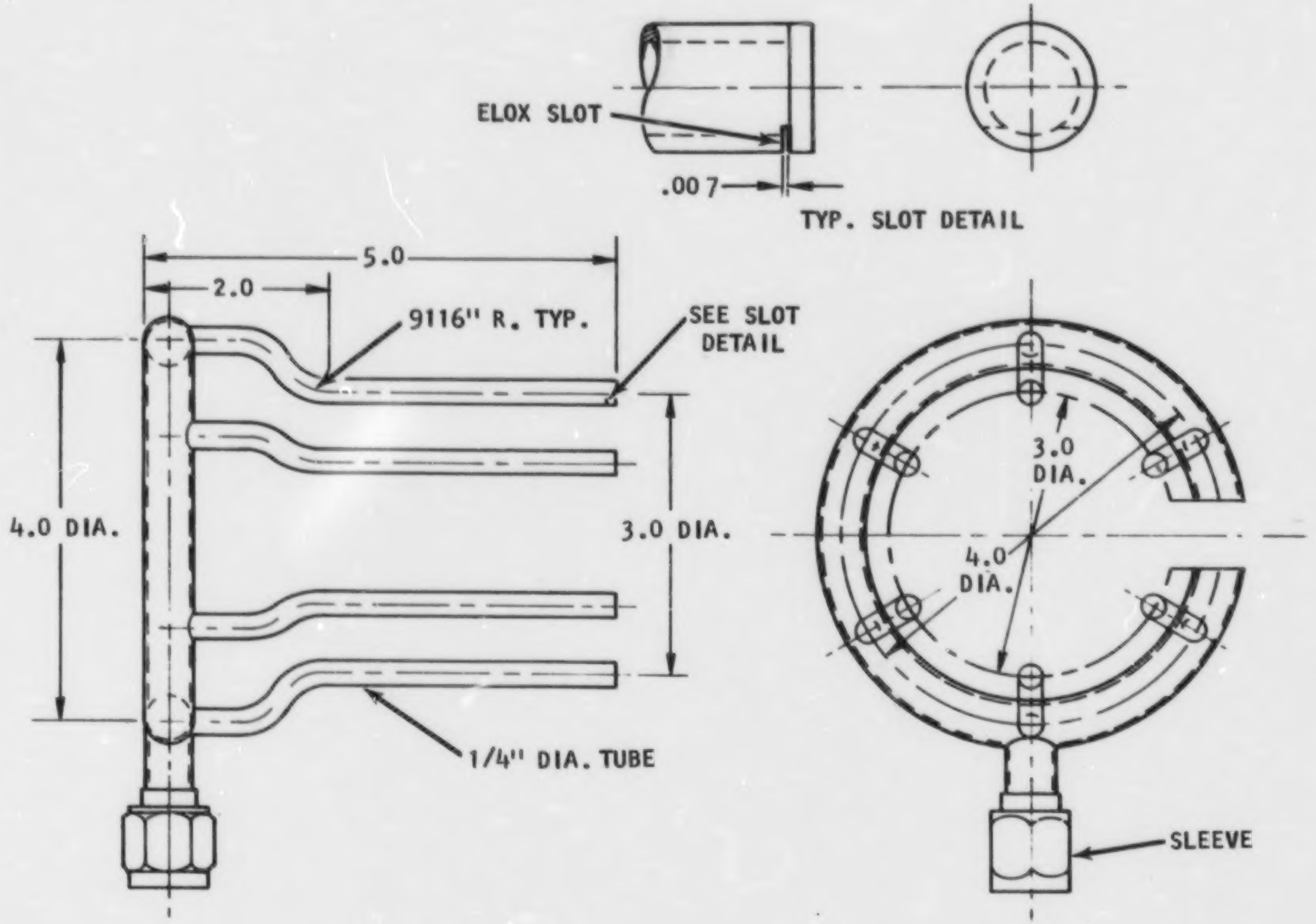
ELOX SLOT
.007
TYP. SLOT DETAIL
5.0
2.0
9116" R. TYP.
SEE SLOT DETAIL
4.0 DIA.
3.0 DIA.
1/4" DIA. TUBE
3.0 DIA.
4.0 DIA.
SLEEVE

Figure 15

GAS ANALYSIS INSTRUMENTATION SCHEMATIC

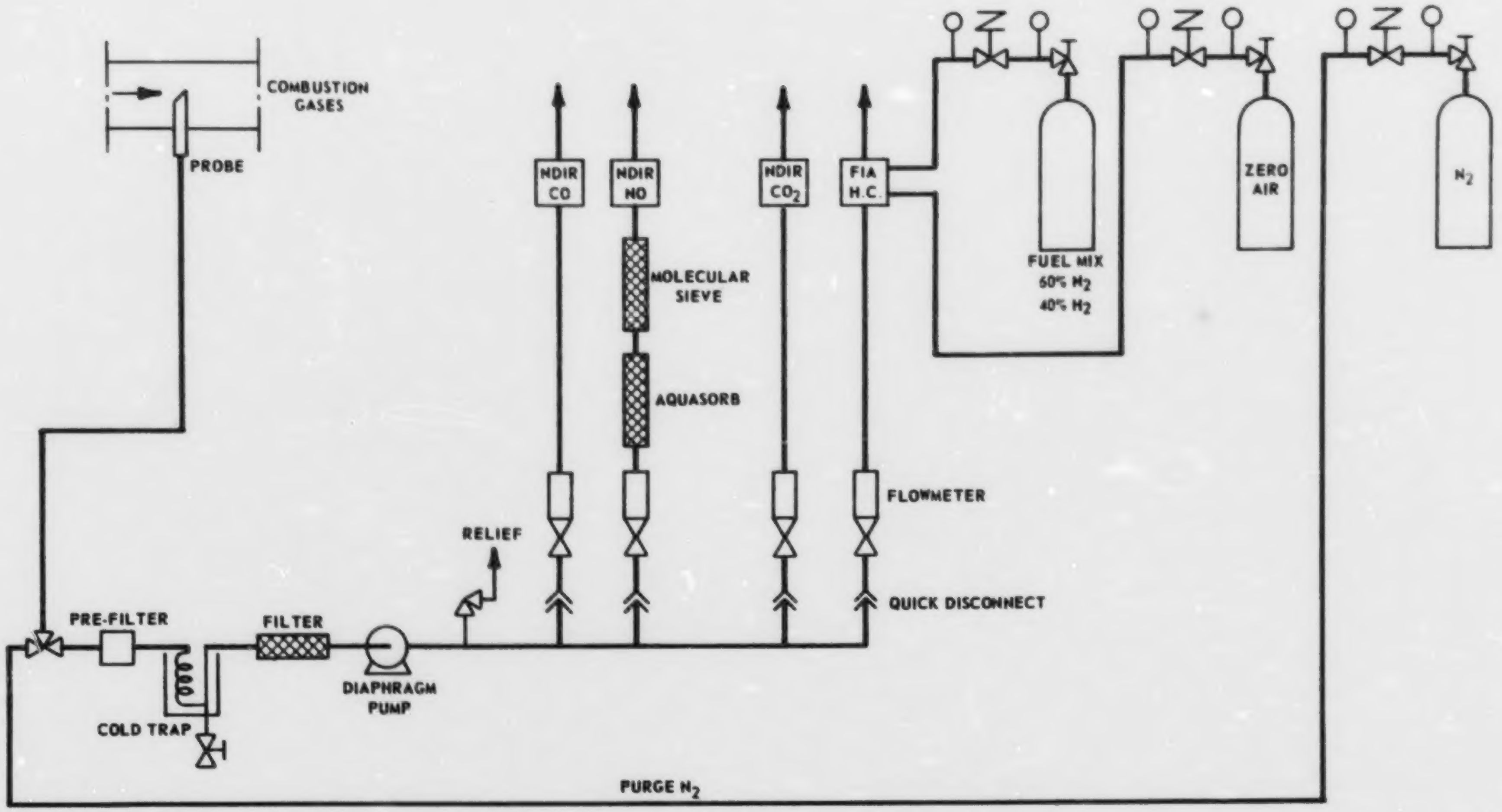
COMBUSTION GASES
PROBE
NDIR CO
NDIR NO
NDIR CO_2
FIA H.C.
FUEL MIX
60% N_2
40% H_2
ZERO AIR
N_2
MOLECULAR SIEVE
AQUASORB
FLOWMETER
RELIEF
QUICK DISCONNECT
PRE-FILTER
FILTER
DIAPHRAGM PUMP
COLD TRAP
PURGE N_2

Figure 16

IDEAL GAS TEMPERATURE RISE

HEATING VALUE = 18,600 BTU/LBM

$T_{INLET} = 60°F$

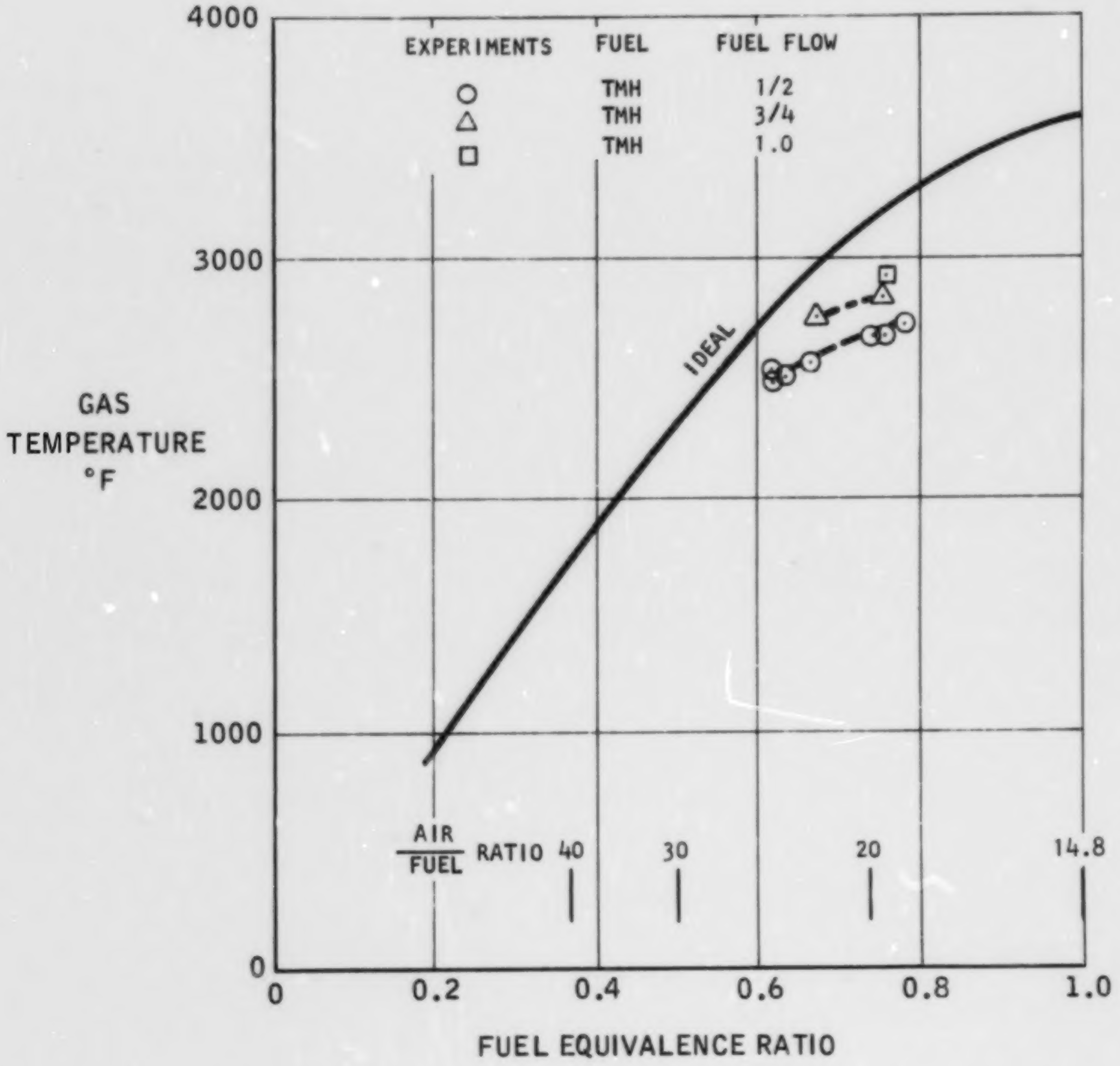

Figure 17

TYPICAL PRESSURE DATA
VAPORIZED TMH

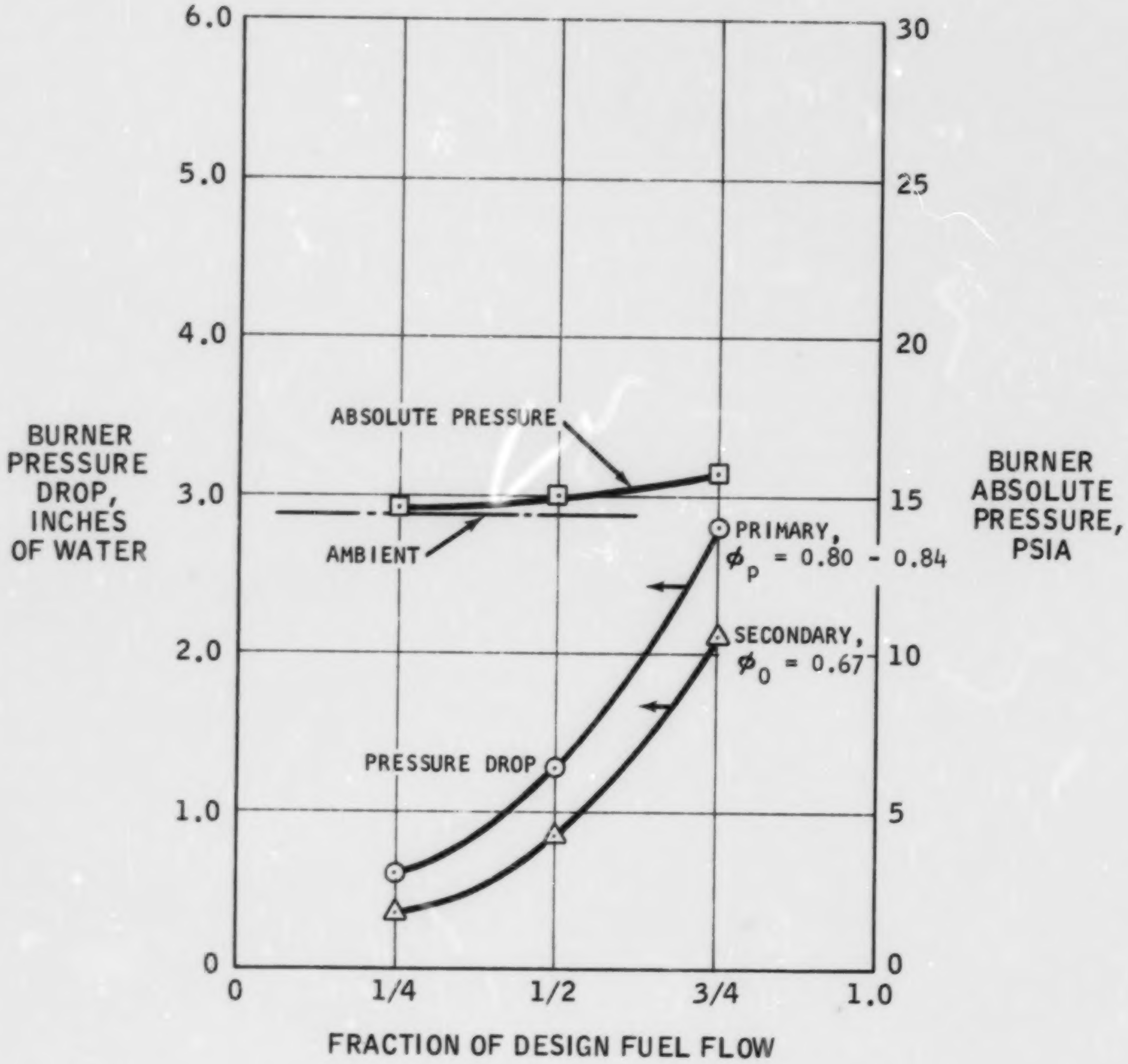

Figure 18

TYPICAL WALL TEMPERATURE DATA

FUEL FLOW = 1/2

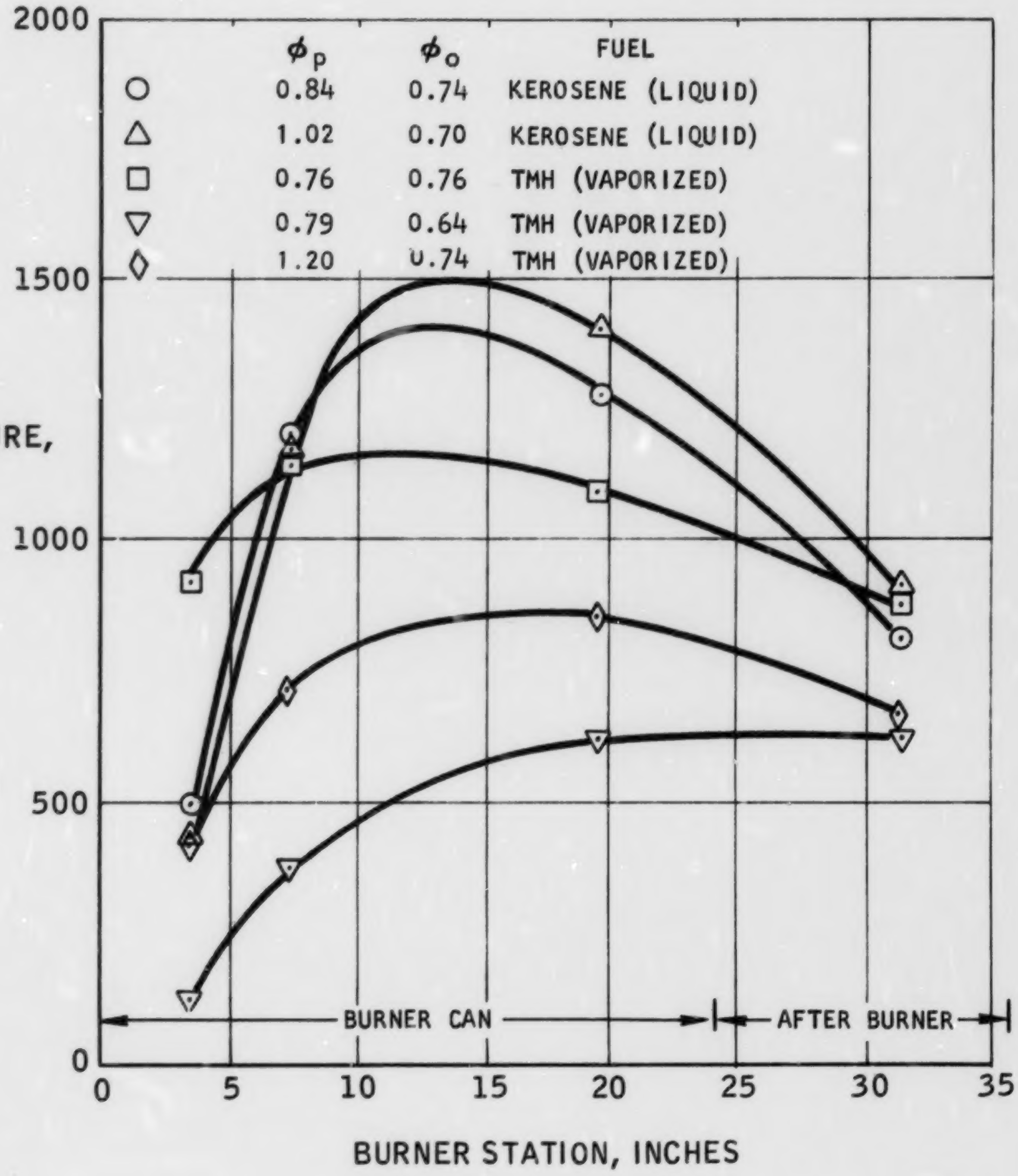

Figure 19

EFFECT OF OVERALL EQUIVALENCE RATIO

VAPORIZED PREMIXED INJECTION

TMH FUEL

1/2 DESIGN FLOW

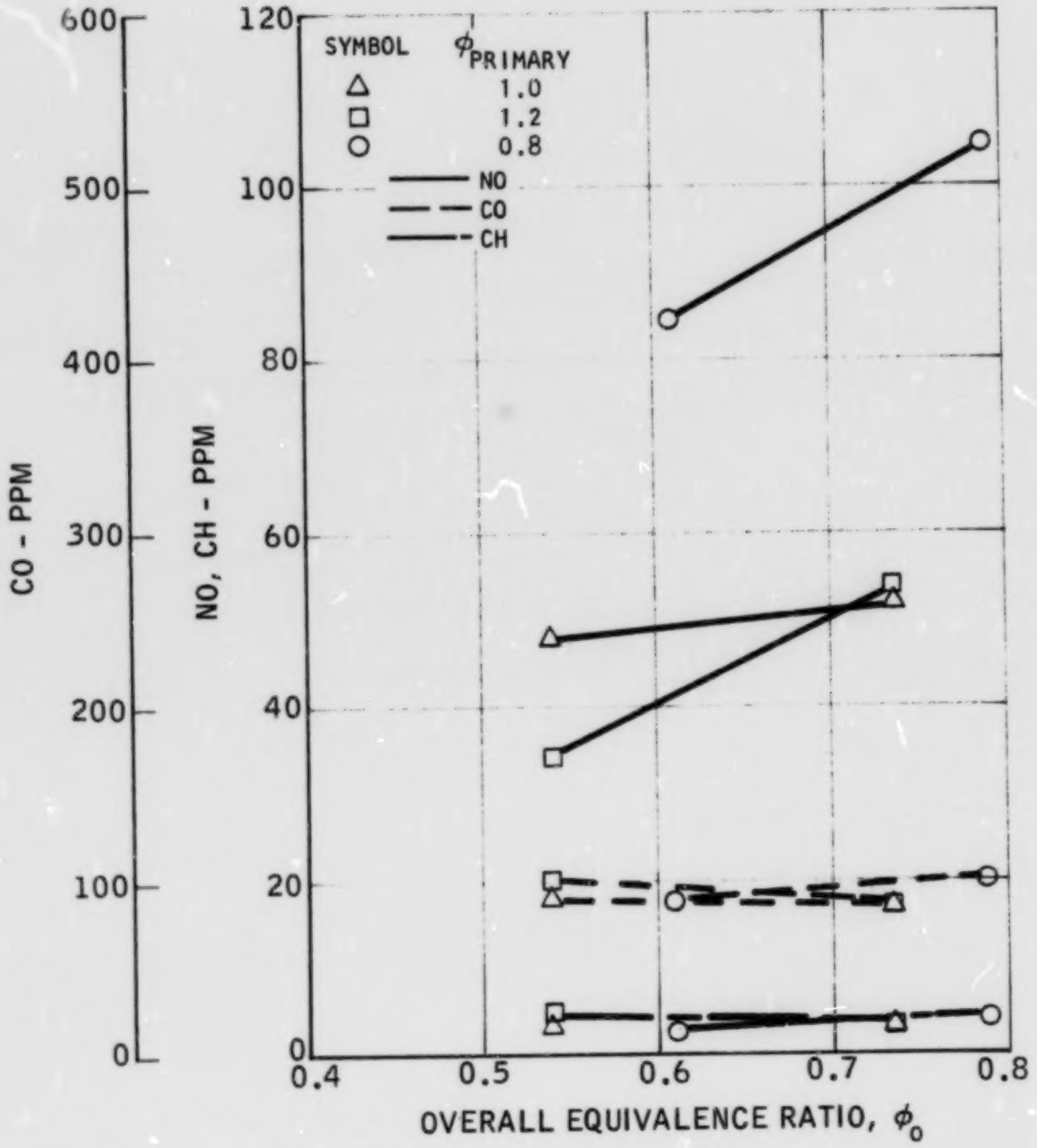

Figure 20

VARIATION OF EMISSIONS WITH HEAT RELEASE

VAPORIZED, PREMIXED INJECTION

TMH FUEL

$\phi_p = 0.8$ - CORRECTED TO STOICHIOMETRIC

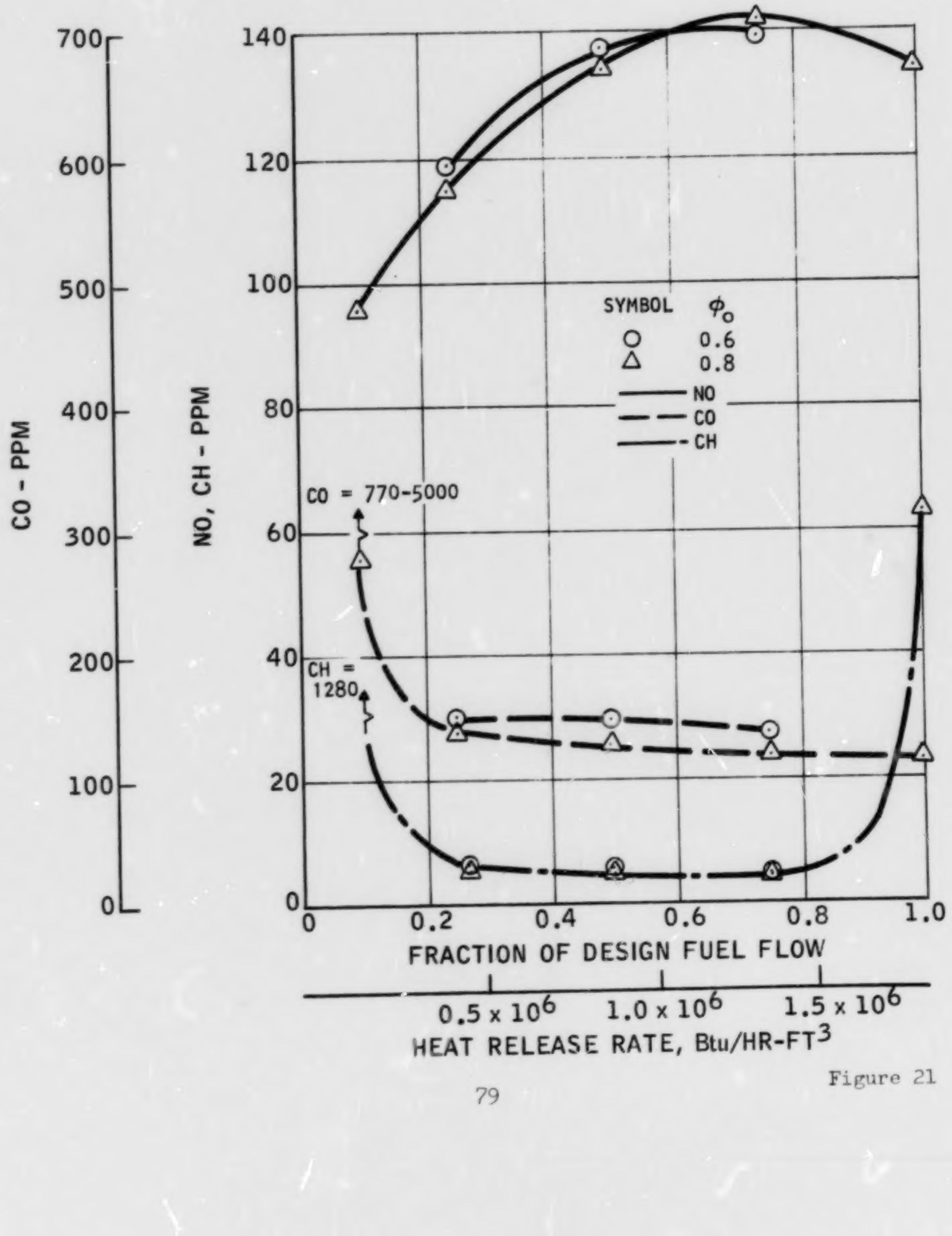

Figure 21

V8150-28

VARIATION OF EMISSIONS WITH HEAT RELEASE

VAPORIZED, PREMIXED INJECTION
TMH FUEL
ϕ_p = 1.0 - CORRECTED TO STOICHIOMETRIC

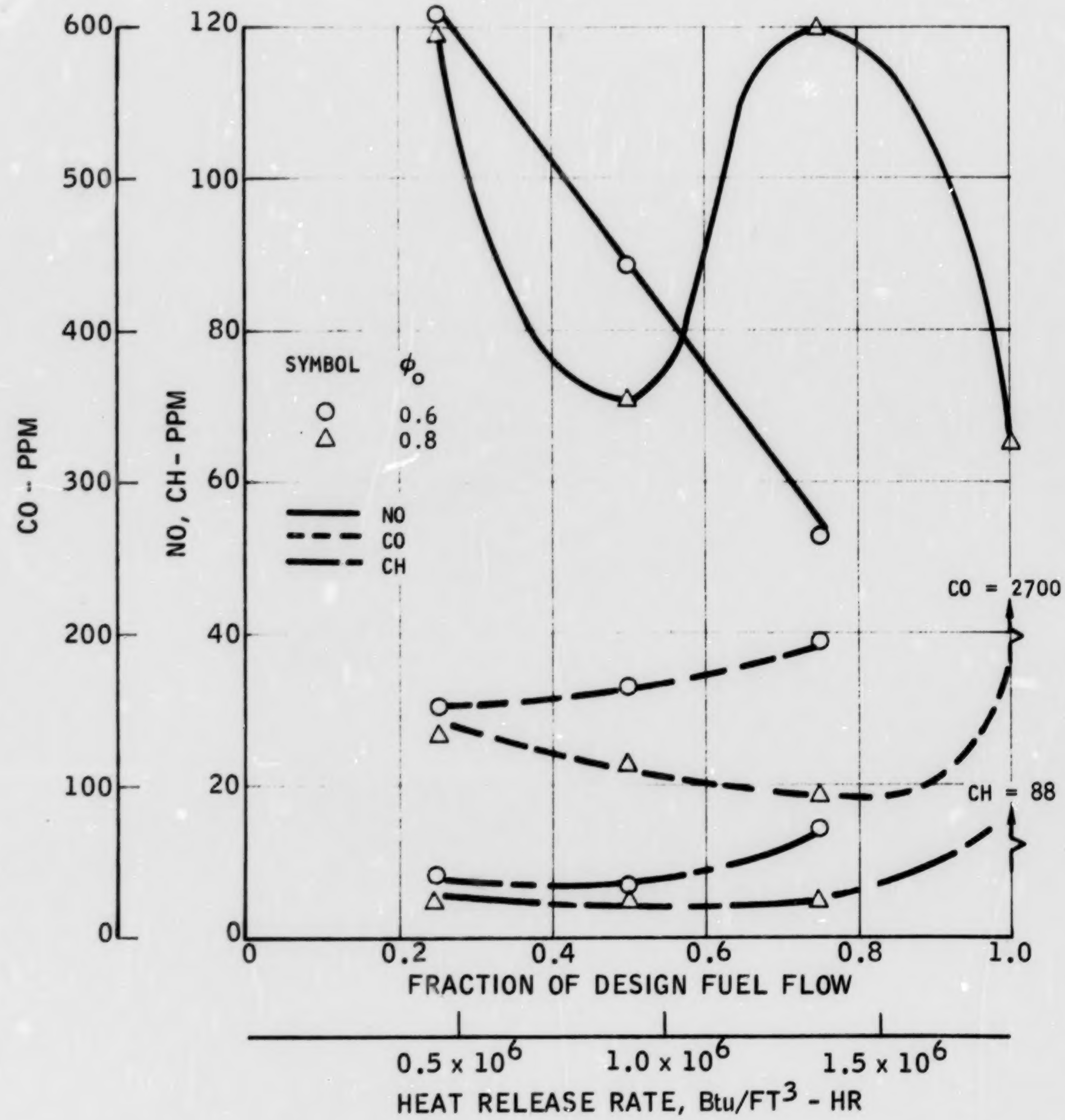

Figure 22

VARIATION OF EMISSION WITH HEAT RELEASE

VAPORIZED, PREMIXED INJECTION

TMH FUEL

$\phi_p = 1.2$ - CORRECTED TO STOICHIOMETRIC

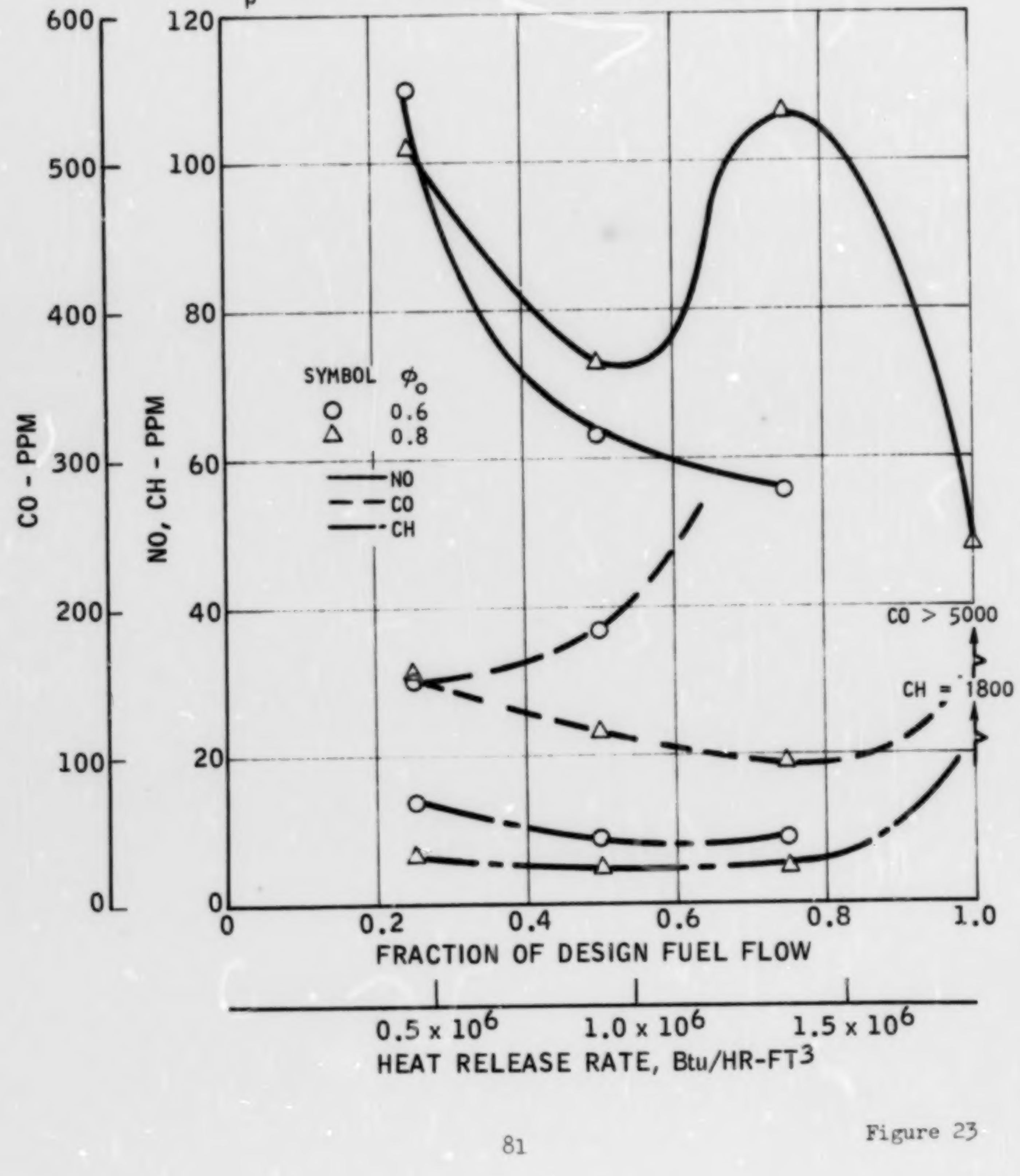

Figure 23

EFFECT OF OVERALL EQUIVALENCE RATIO

SUE BURNER CONFIGURATION
VAPORIZED TMH FUEL
1/2 DESIGN FLOW

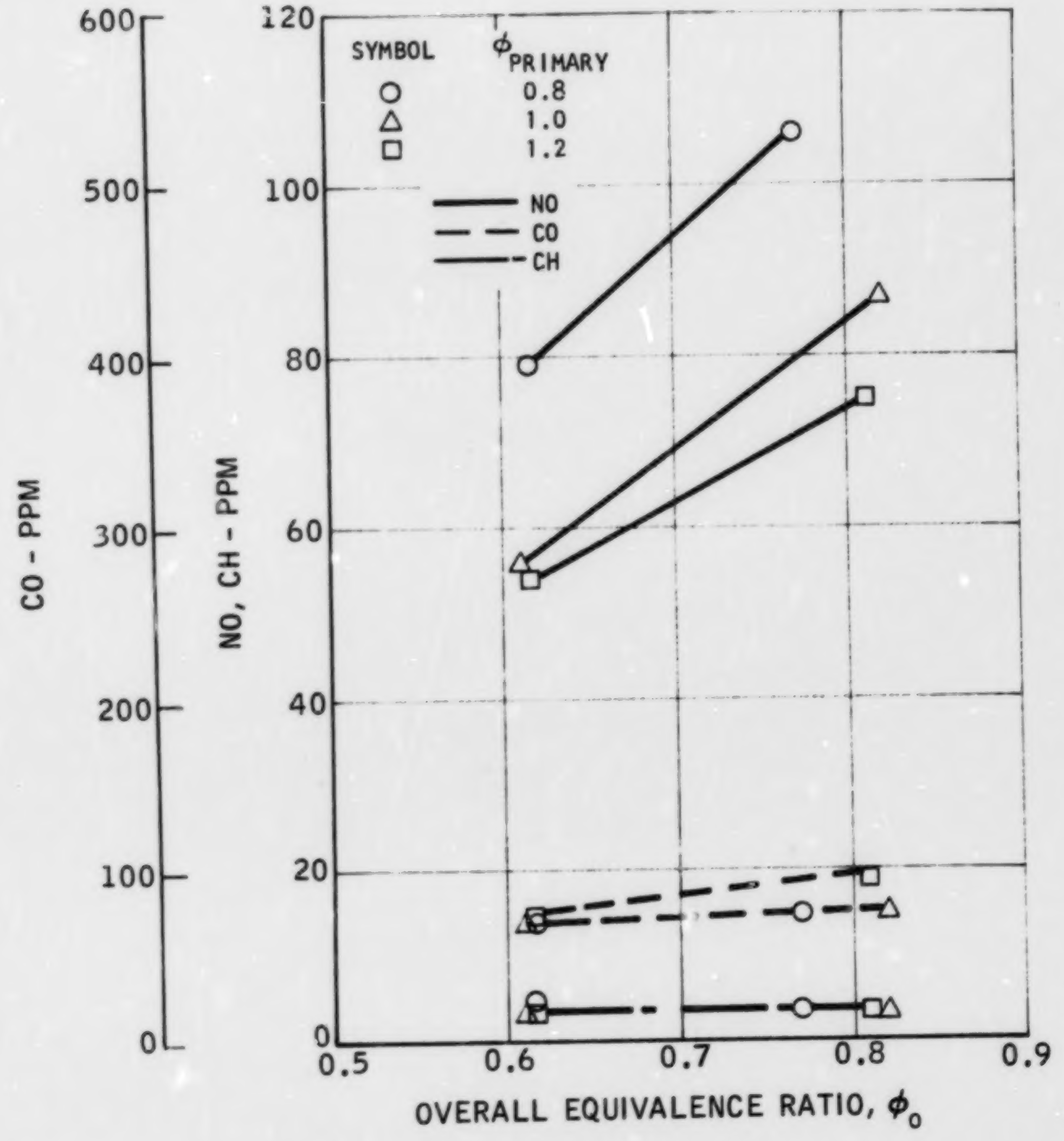

Figure 24

EFFECT OF PRIMARY EQUIVALENCE RATIO

SUE BURNER CONFIGURATION
VAPORIZED TMH FUEL
1/2 DESIGN FLOW
$\phi_o = 0.6$

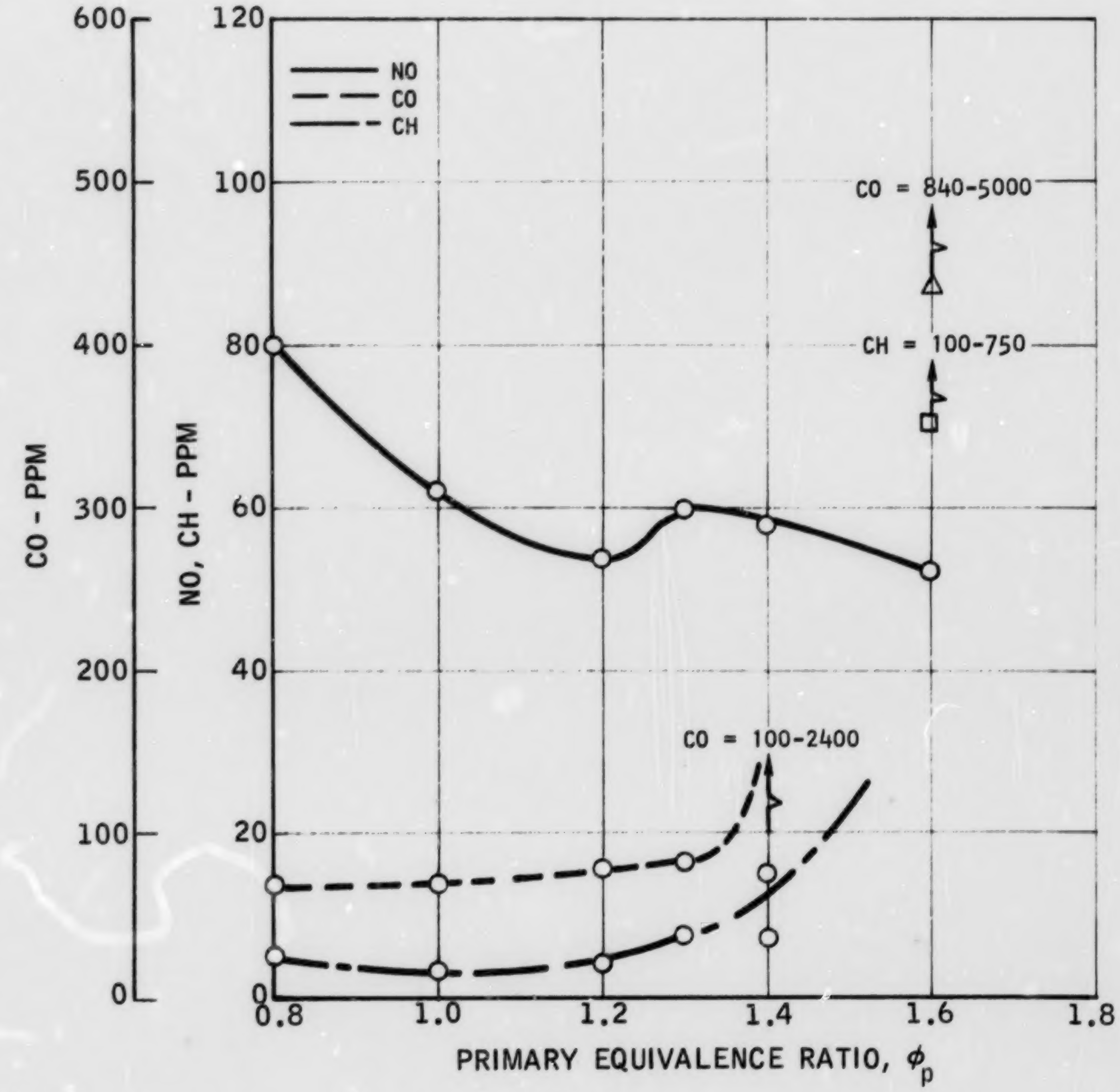

Figure 25

VARIATION OF EMISSIONS WITH HEAT RELEASE

SUE BURNER CONFIGURATION

VAPORIZED TMH FUEL

$\phi_p = 1.0$ - CORRECTED TO STOICHIOMETRIC

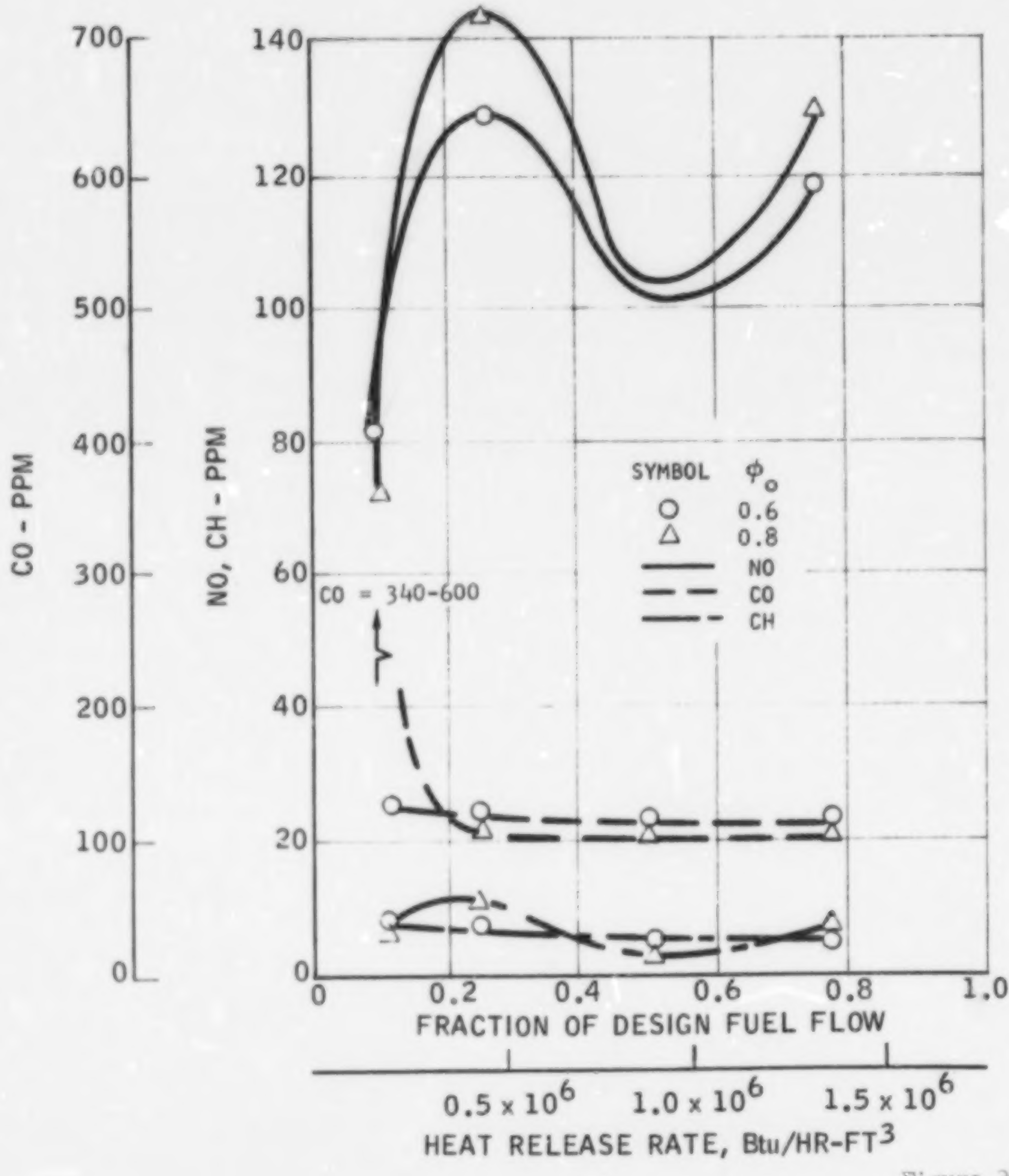

Figure 26

VARIATION OF EMISSIONS WITH HEAT RELEASE
SUE BURNER CONFIGURATION
VAPORIZED TMH FUEL
ϕ_p = 1.2 - CORRECTED TO STOICHIOMETRIC

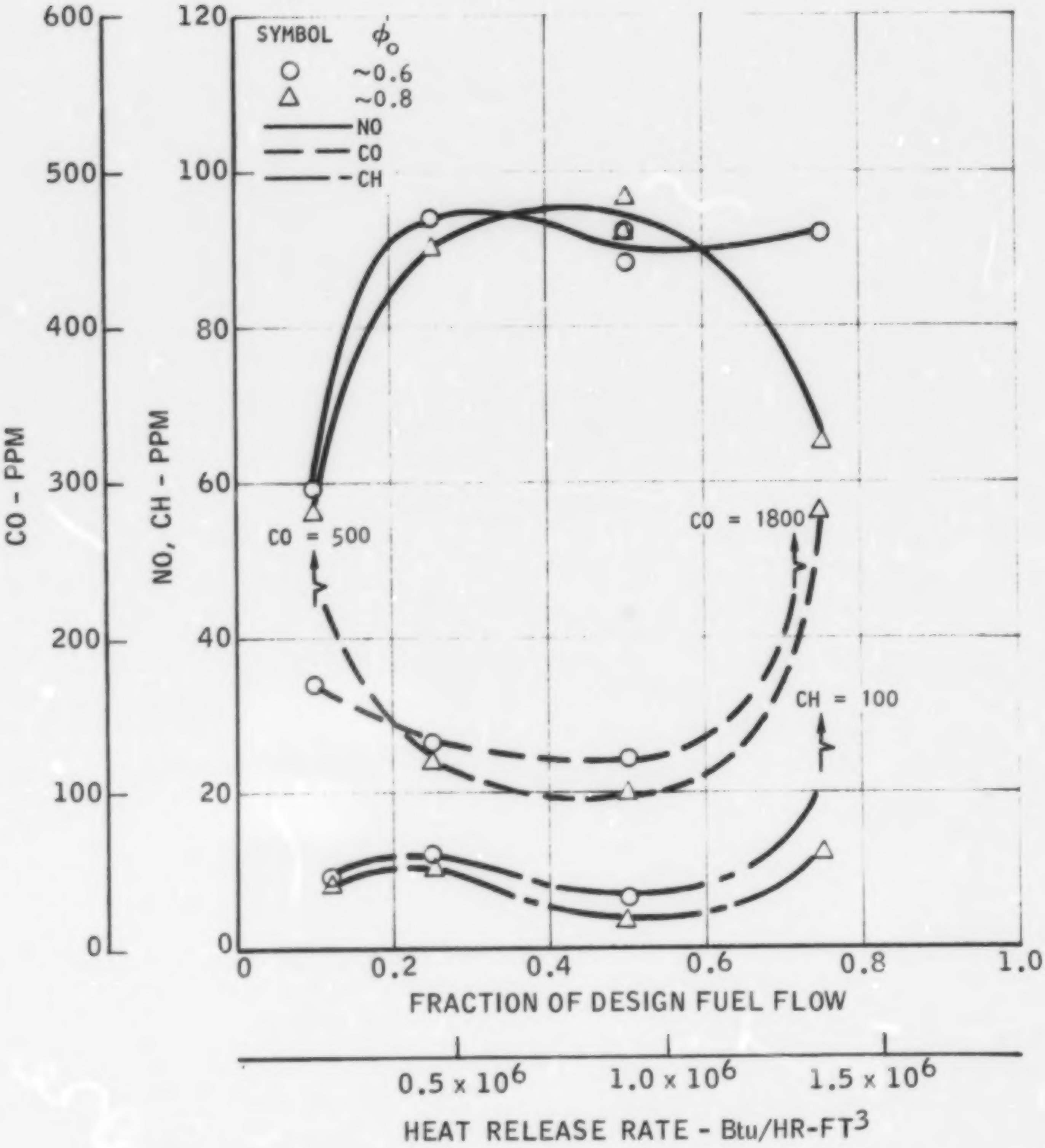

Figure 27

EFFECT OF PRIMARY EQUIVALENCE RATIO

LIQUID INJECTION

KEROSENE FUEL

1/2 DESIGN FLOW

LOW PRESSURE NOZZLE

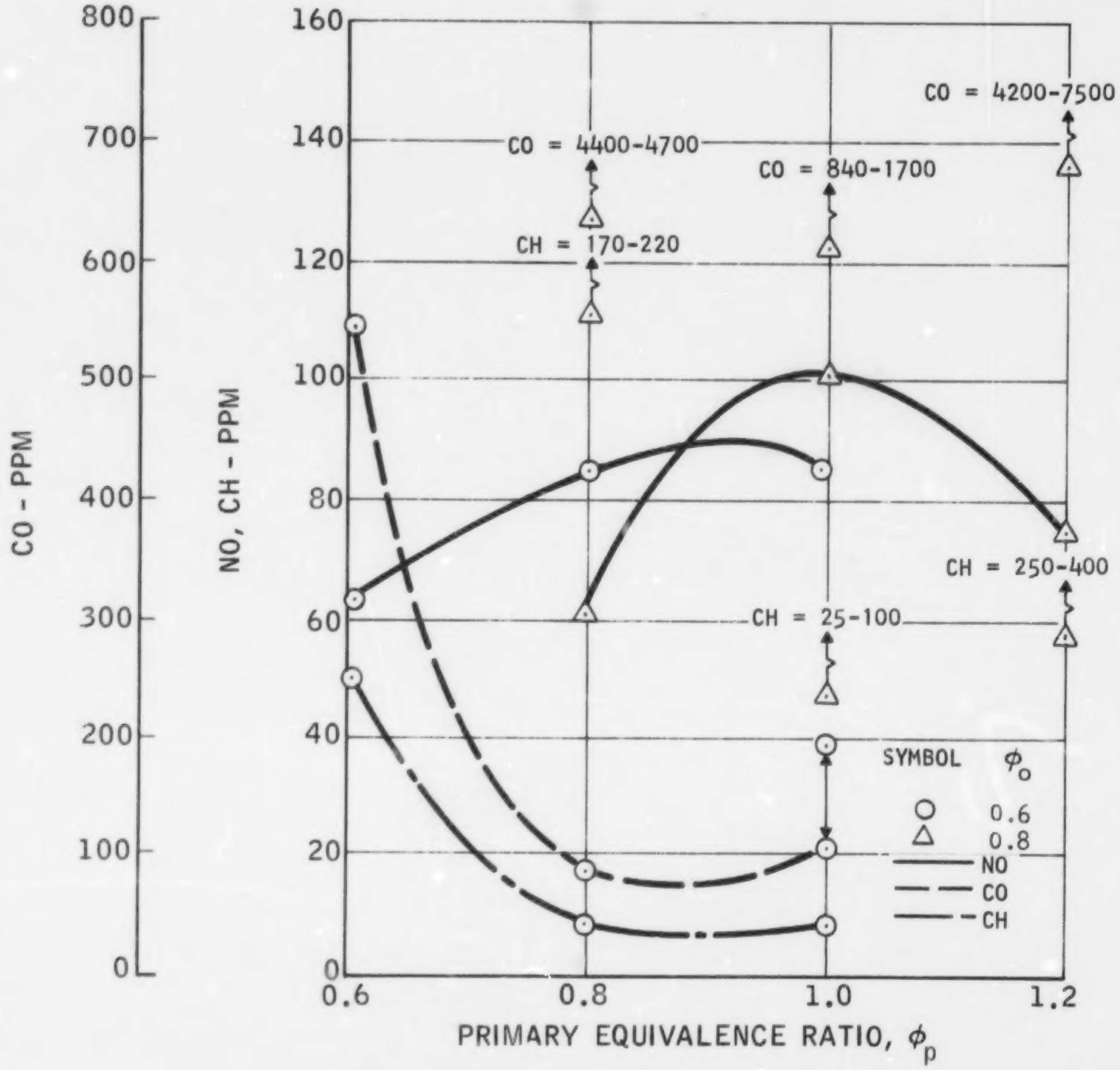

Figure 28

EFFECT OF OVERALL EQUIVALENCE RATIO

LIQUID INJECTION

KEROSENE FUEL

1/2 DESIGN FLOW

HIGH PRESSURE NOZZLE

$\phi_p = 0.87$

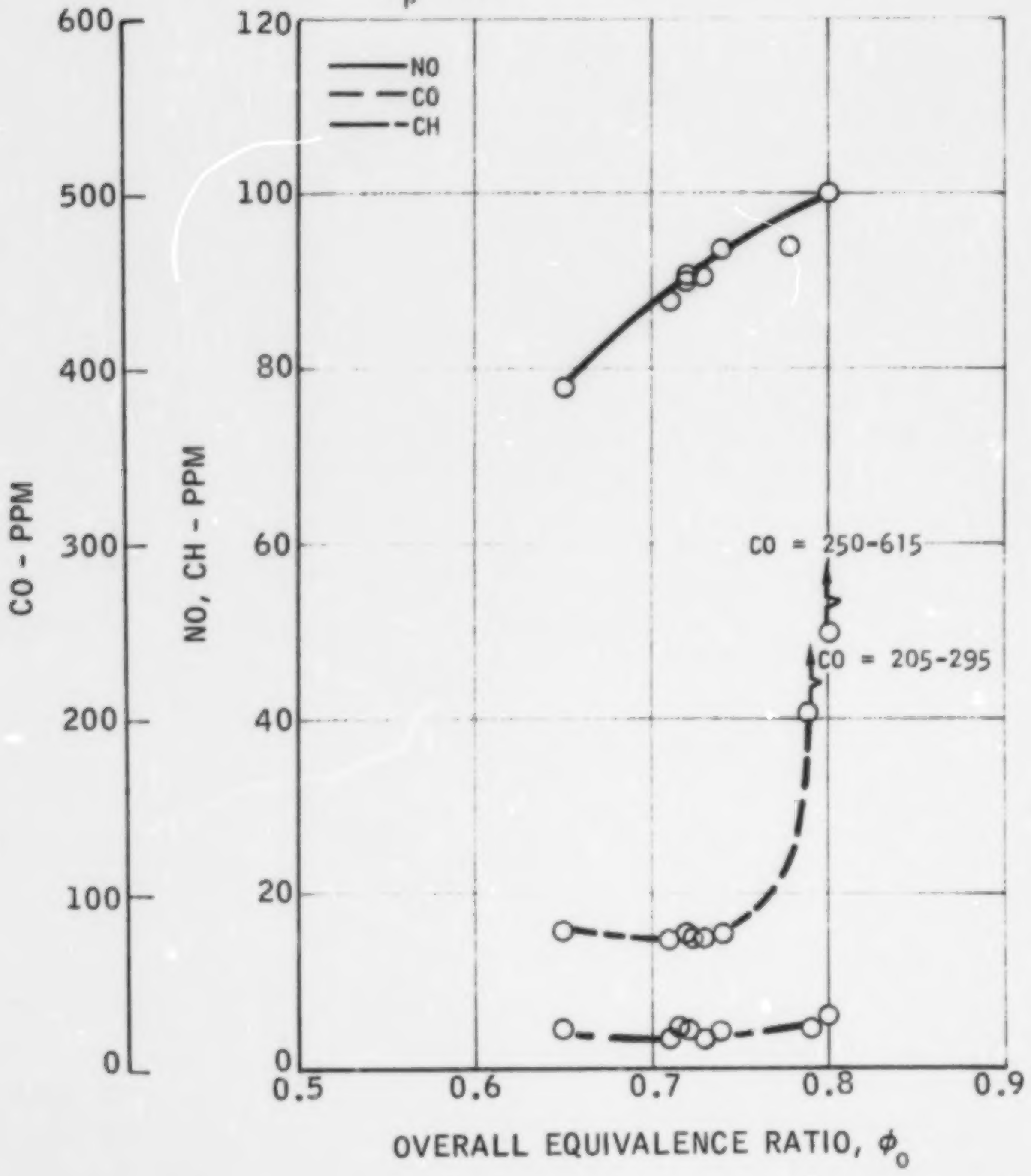

Figure 29

VARIATION OF EMISSIONS WITH HEAT RELEASE

LIQUID INJECTION

KEROSENE FUEL

$\phi_p = 0.8$ – CORRECTED TO STOICHIOMETRIC

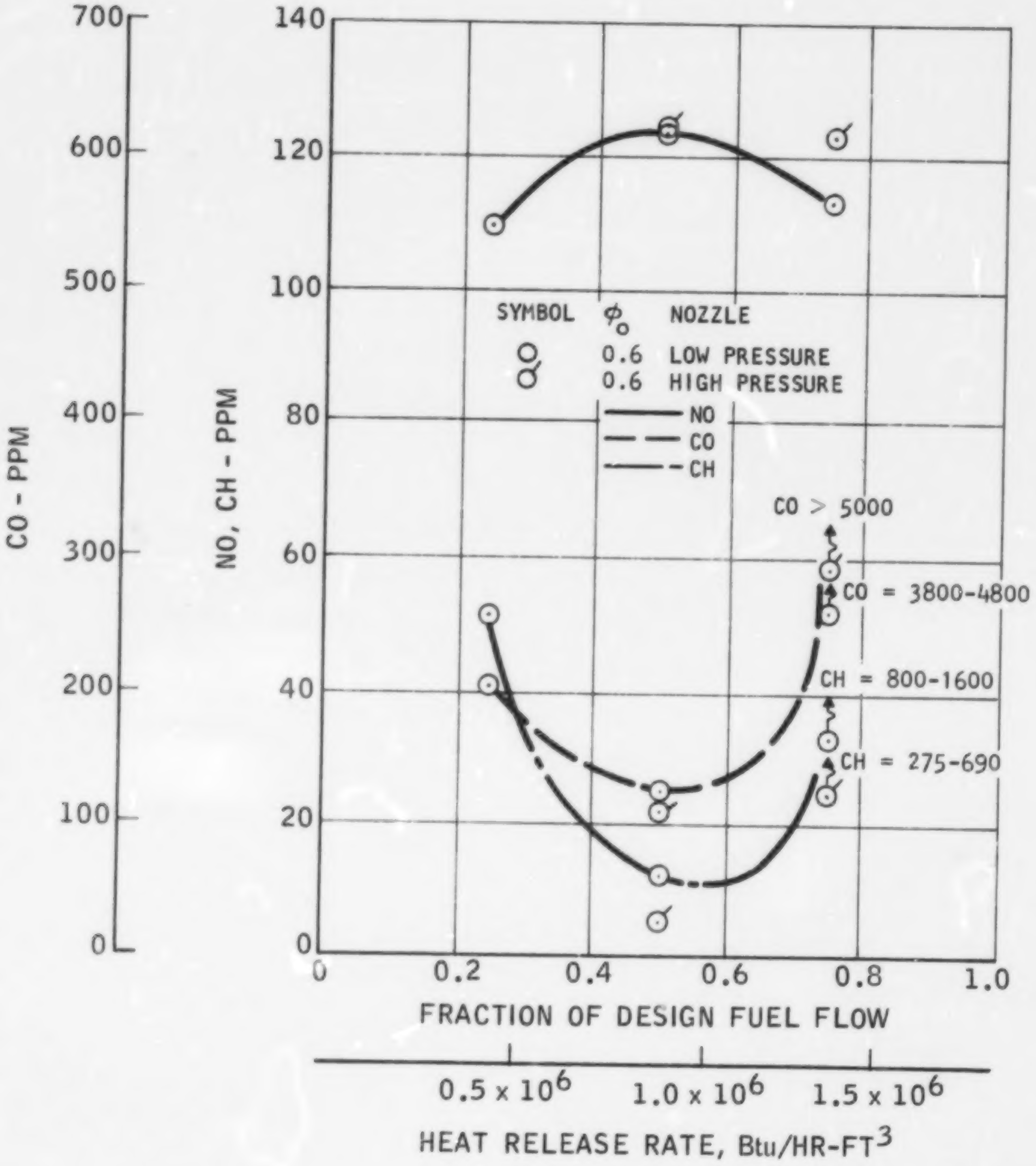

Figure 30

VARIATION OF EMISSIONS WITH HEAT RELEASE

LIQUID INJECTION, HIGH PRESSURE NOZZLE
TMH FUEL
$\phi_p = 0.87$ - CORRECTED TO STOICHIOMETRIC

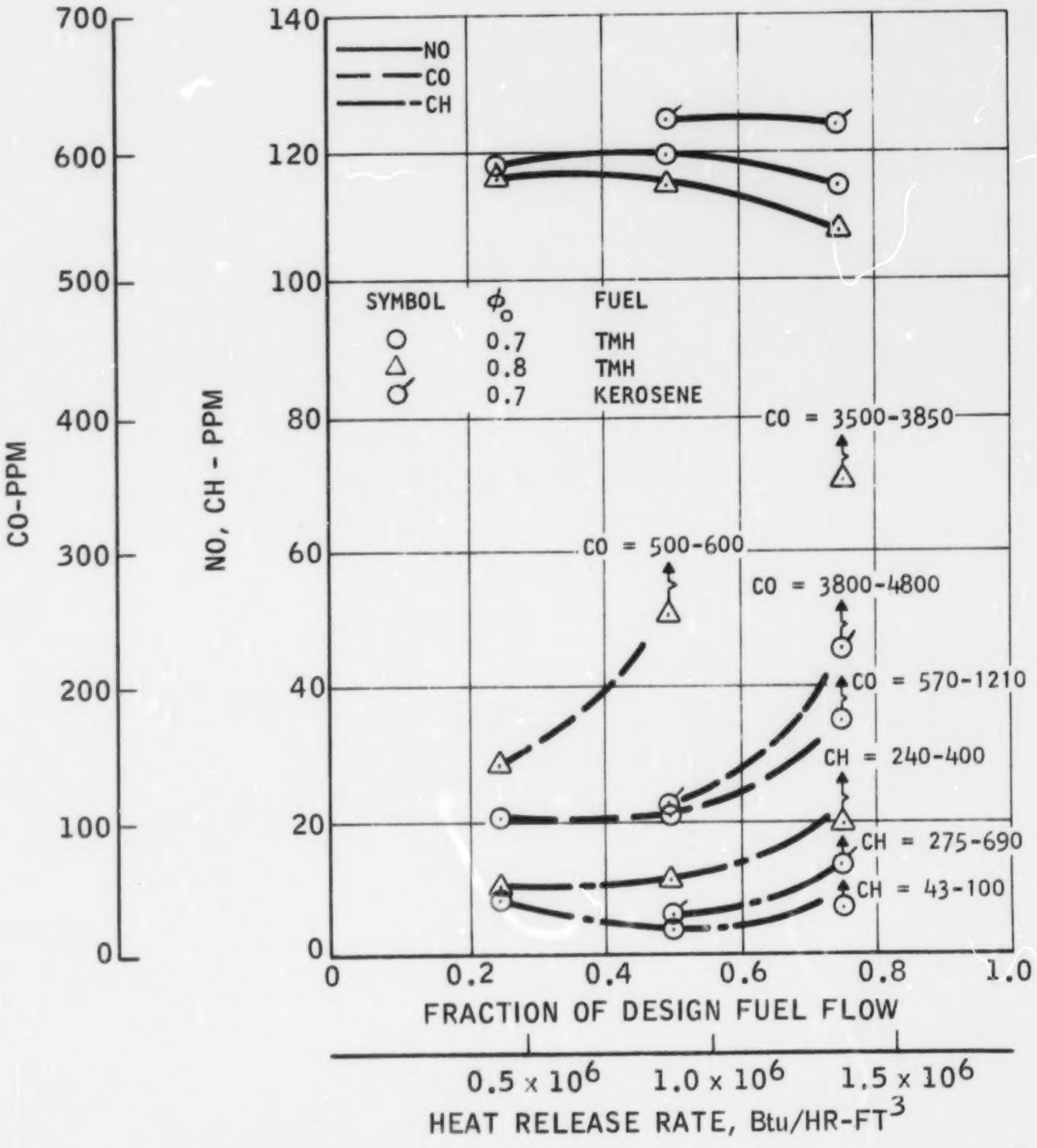

Figure 31

EFFECT OF OVERALL EQUIVALENCE RATIO

METHANE FUEL

SUE BURNER CONFIGURATION

1/4 DESIGN FLOW

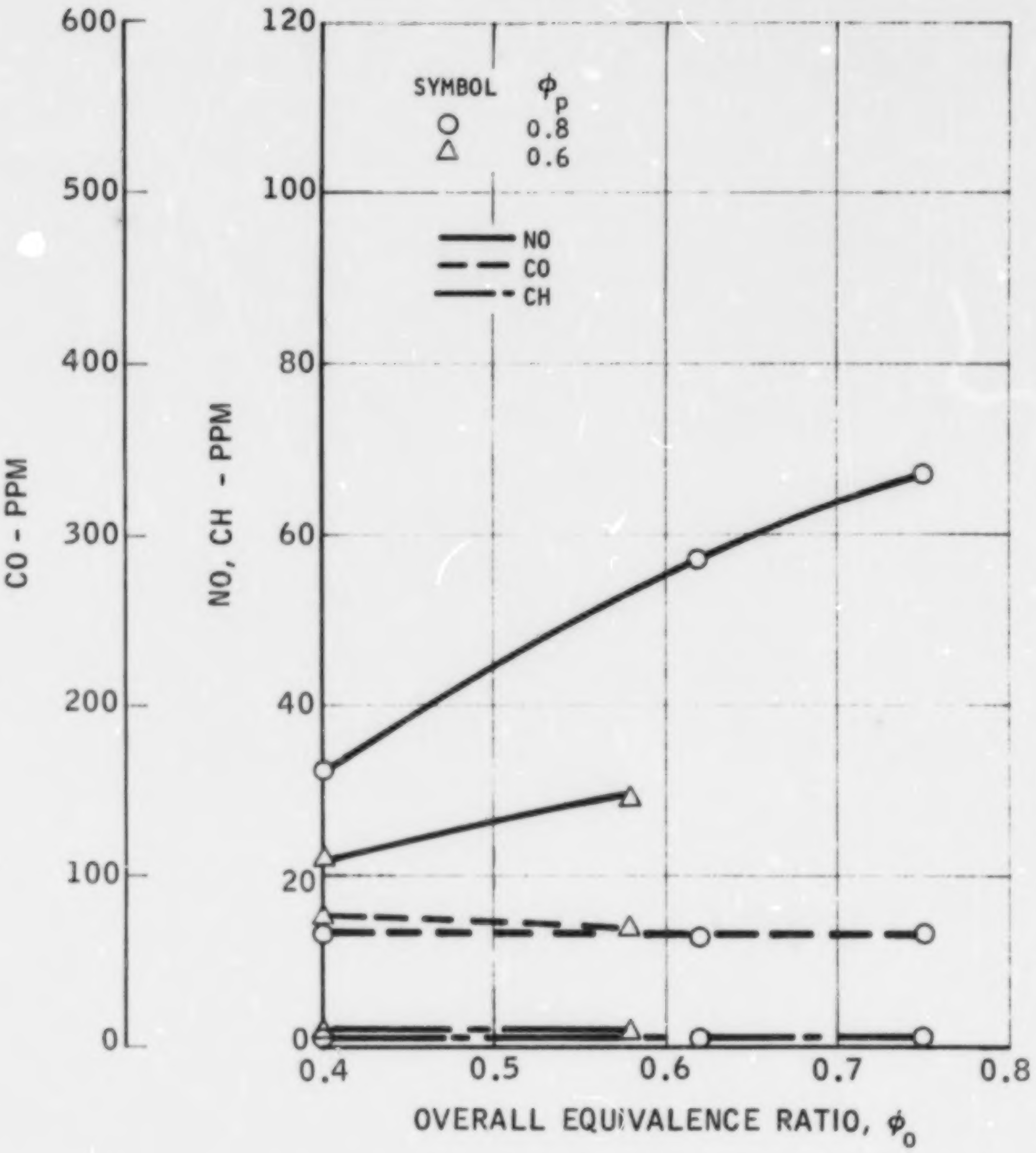

Figure 32

VARIATION OF EMISSIONS WITH HEAT RELEASE

METHANE FUEL

$\phi_p = 0.8$, $\phi_o = 0.62\text{-}0.70$

CORRECTED TO STOICHIOMETRIC

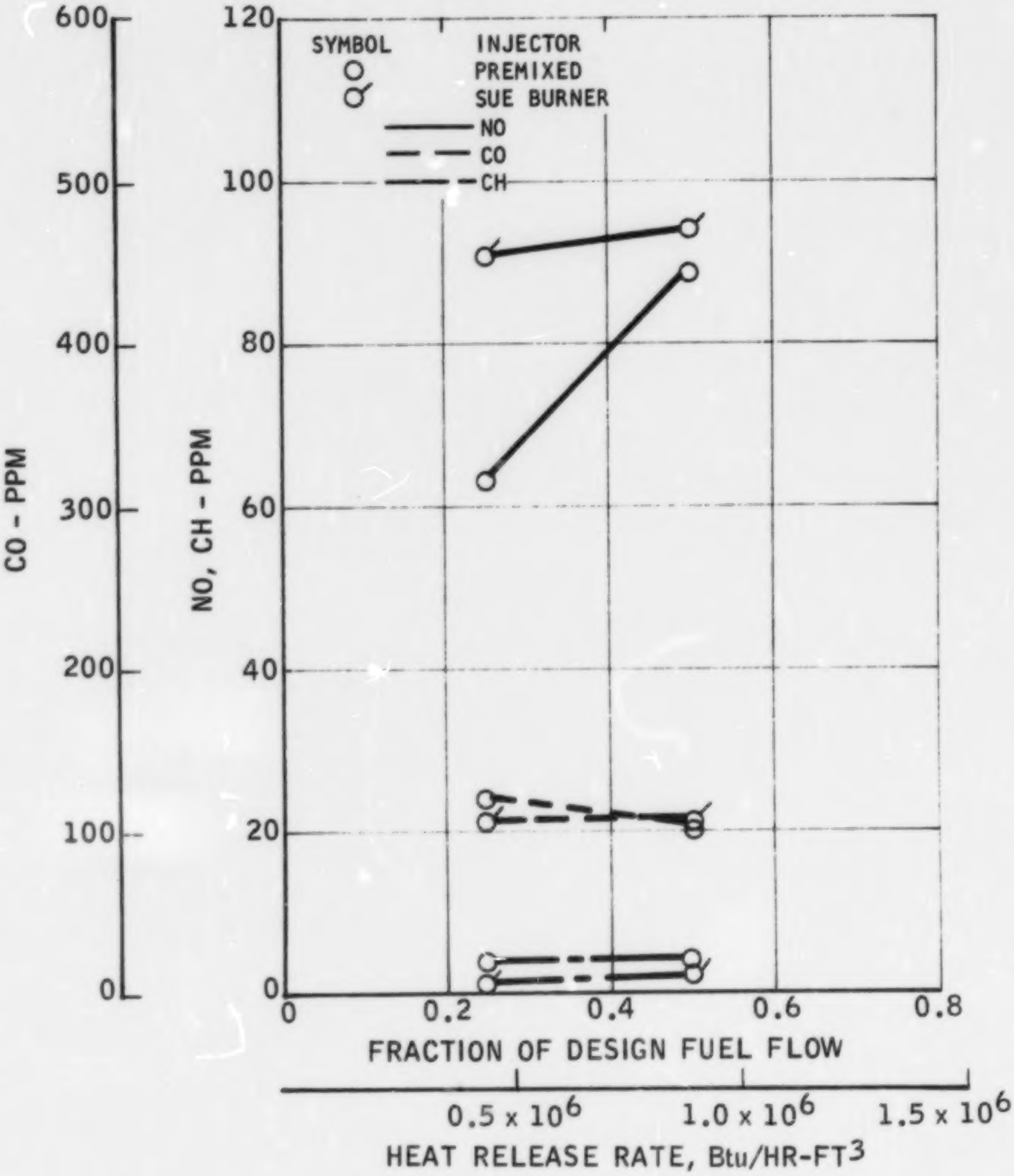

Figure 33

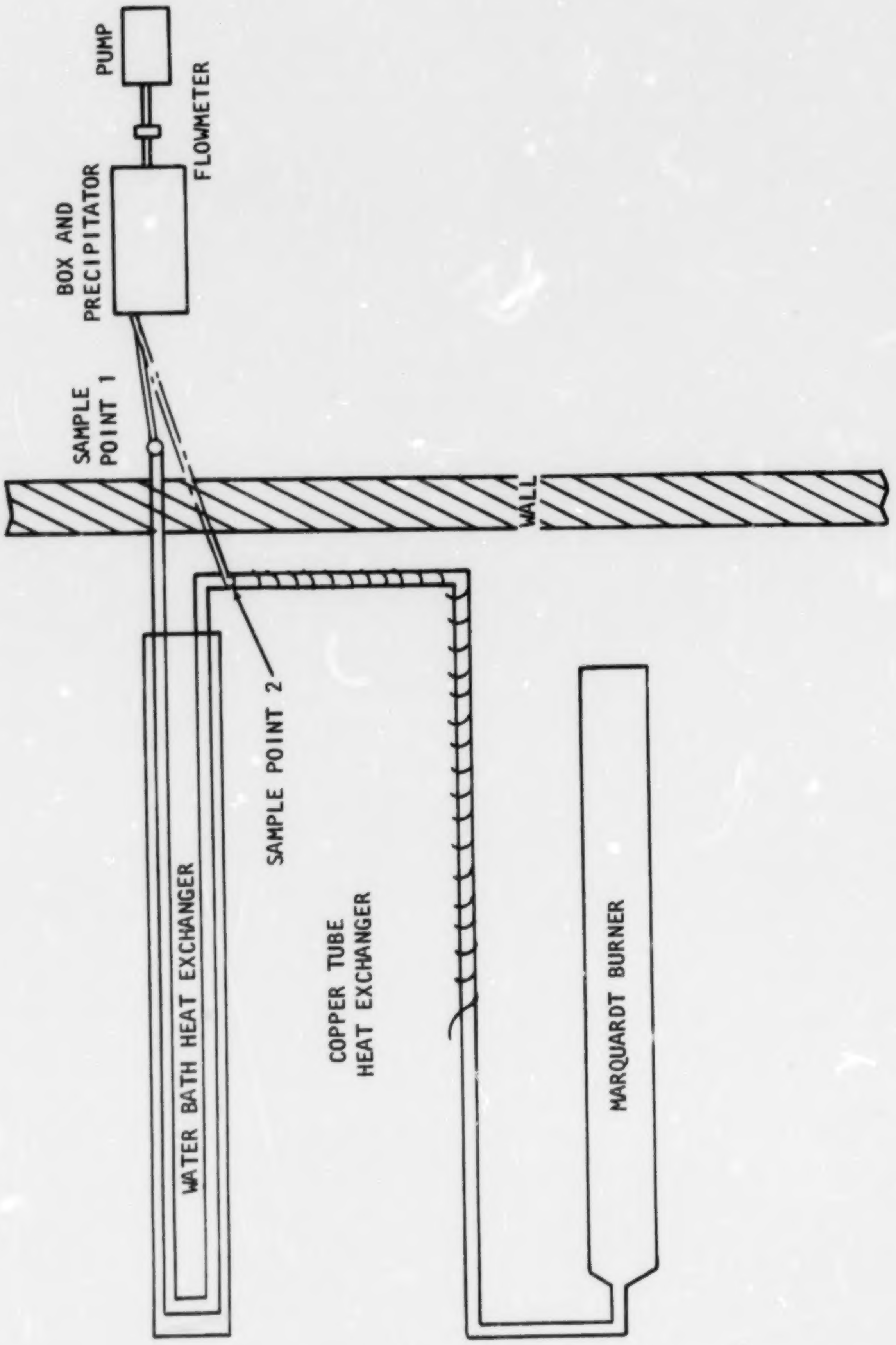
PUMP
FLOWMETER
BOX AND PRECIPITATOR
SAMPLE POINT 1
WALL
SAMPLE POINT 2
WATER BATH HEAT EXCHANGER
COPPER TUBE HEAT EXCHANGER
MARQUARDT BURNER

PARTICLE SAMPLING SCHEMATIC

Figure 34

PARTICLE COLLECTION SYSTEM

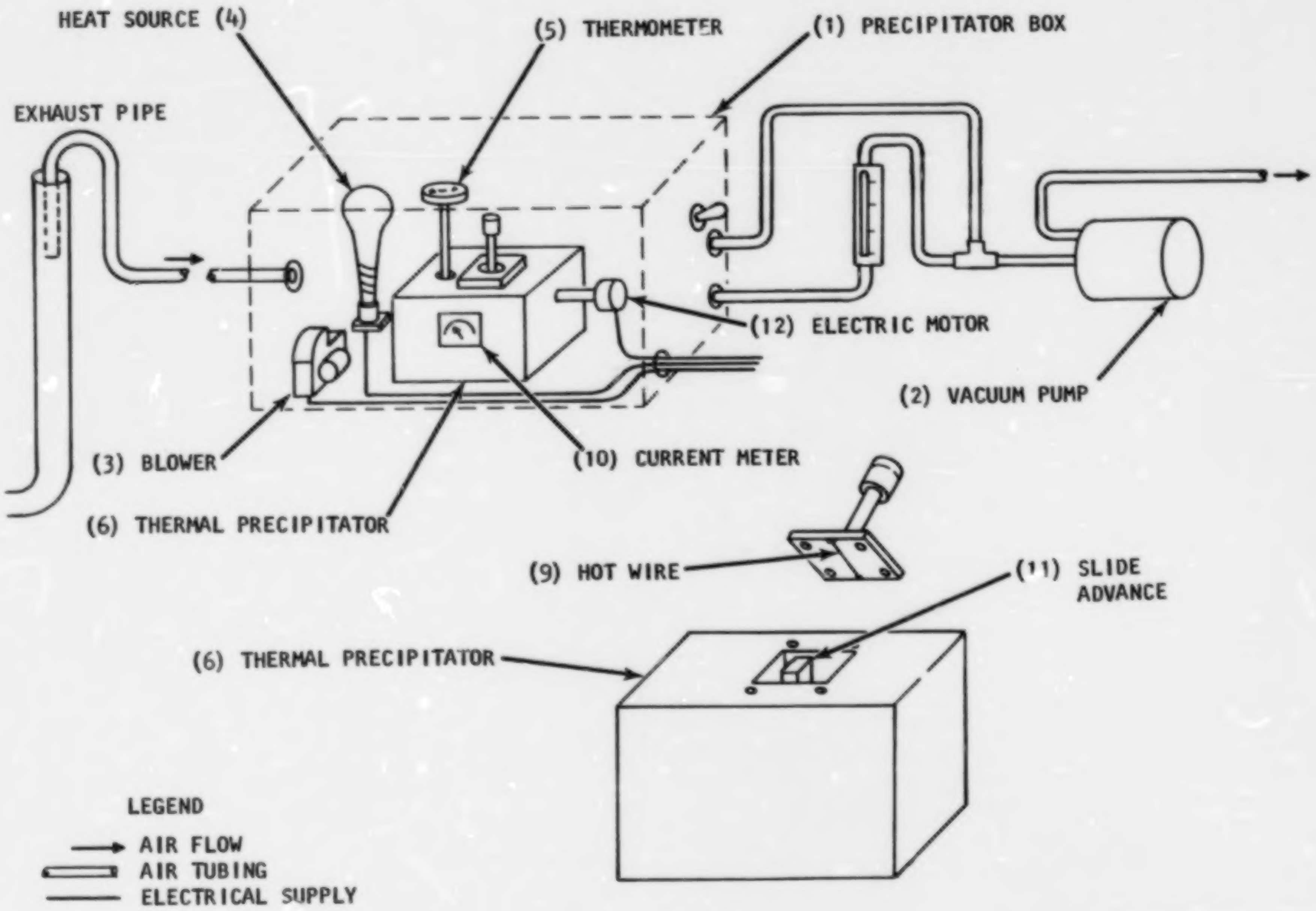
HEAT SOURCE (4)
(5) THERMOMETER
(1) PRECIPITATOR BOX
EXHAUST PIPE
(12) ELECTRIC MOTOR
(2) VACUUM PUMP
(3) BLOWER
(10) CURRENT METER
(6) THERMAL PRECIPITATOR
(9) HOT WIRE
(11) SLIDE ADVANCE
(6) THERMAL PRECIPITATOR
LEGEND
→ AIR FLOW
AIR TUBING
ELECTRICAL SUPPLY

Figure 35

PARTICULATE SAMPLE — EXTERNAL COMBUSTOR

SAMPLE 2287D

RUN #11 CONDITION 3

2,2,5 TRIMETHYLHEXANE (VAPOR)

1/30 FUEL FLOW

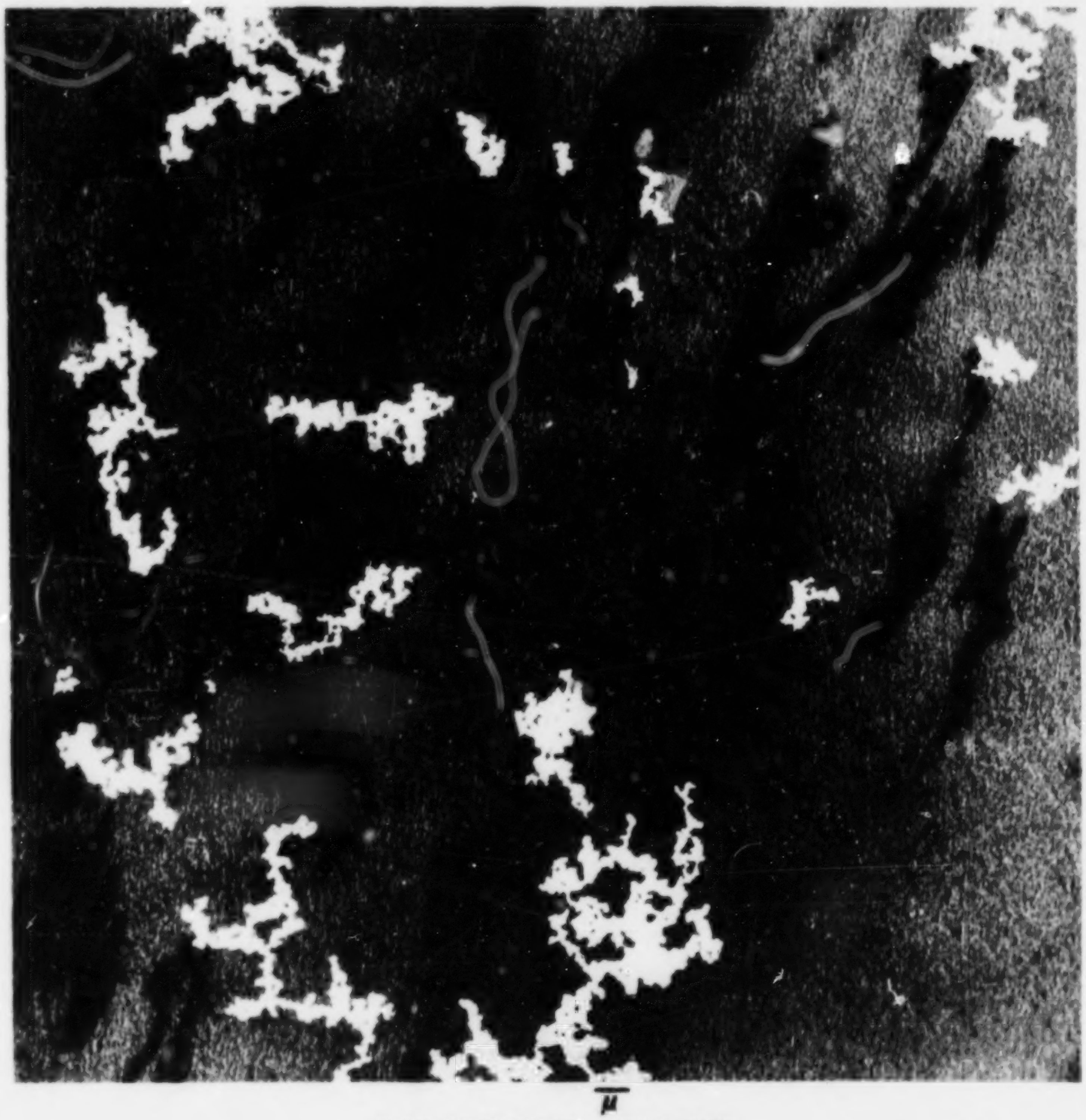

MAGNIFICATION = X18,000

Figure 36

PARTICULATE SAMPLE — EXTERNAL COMBUSTOR

SAMPLE 2293A

2,2,5 TRIMETHYLHEXANE (VAPOR)

RUN # 14 CONDITION 8

3/4 FUEL FLOW

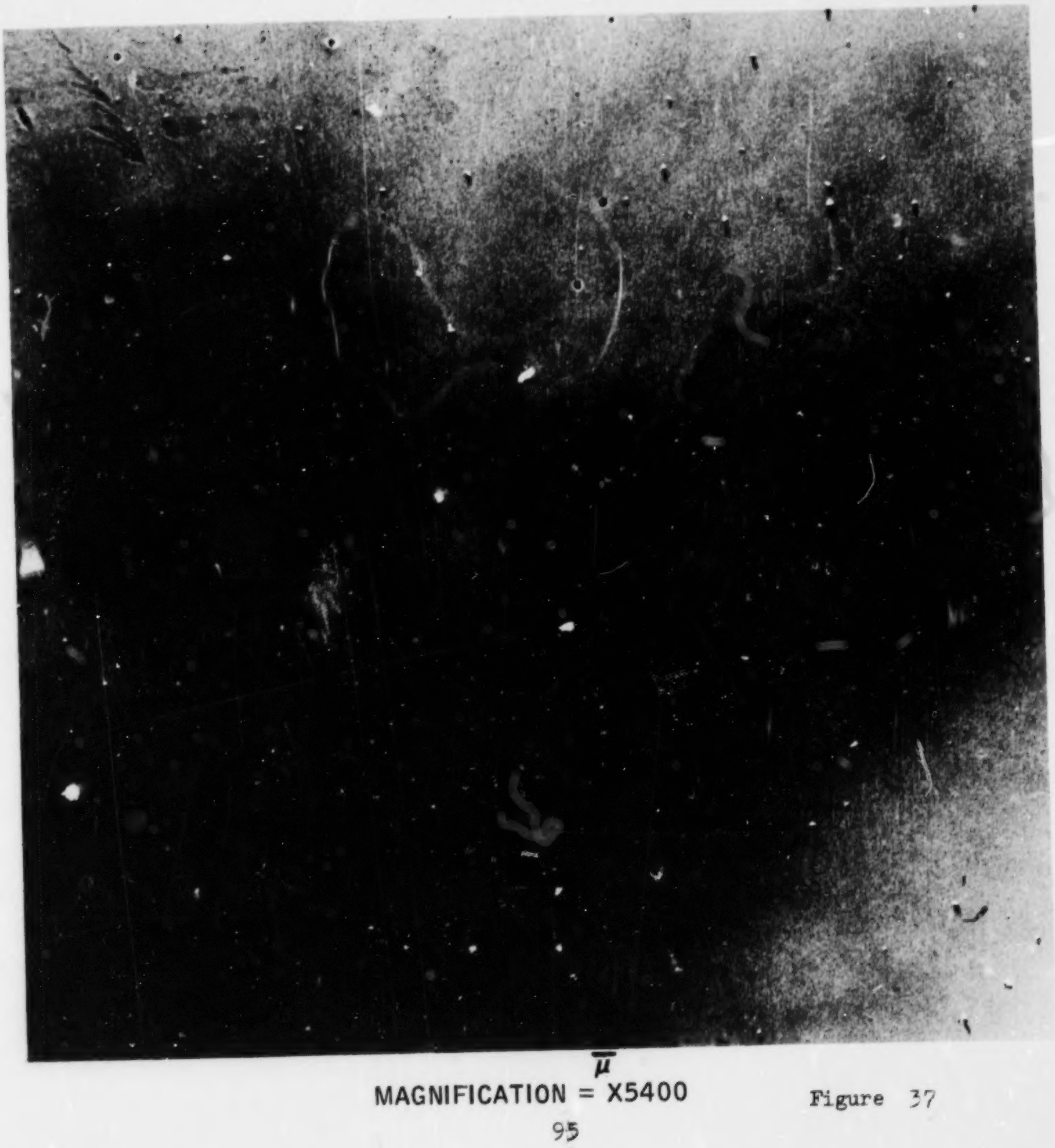

MAGNIFICATION = X5400

Figure 37

PARTICULATE SAMPLE — EXTERNAL COMBUSTOR

SAMPLE 2293B

RUN #14 CONDITION 8

2,2,5 TRIMETHYLHEXANE (VAPOR)

3/4 FUEL FLOW

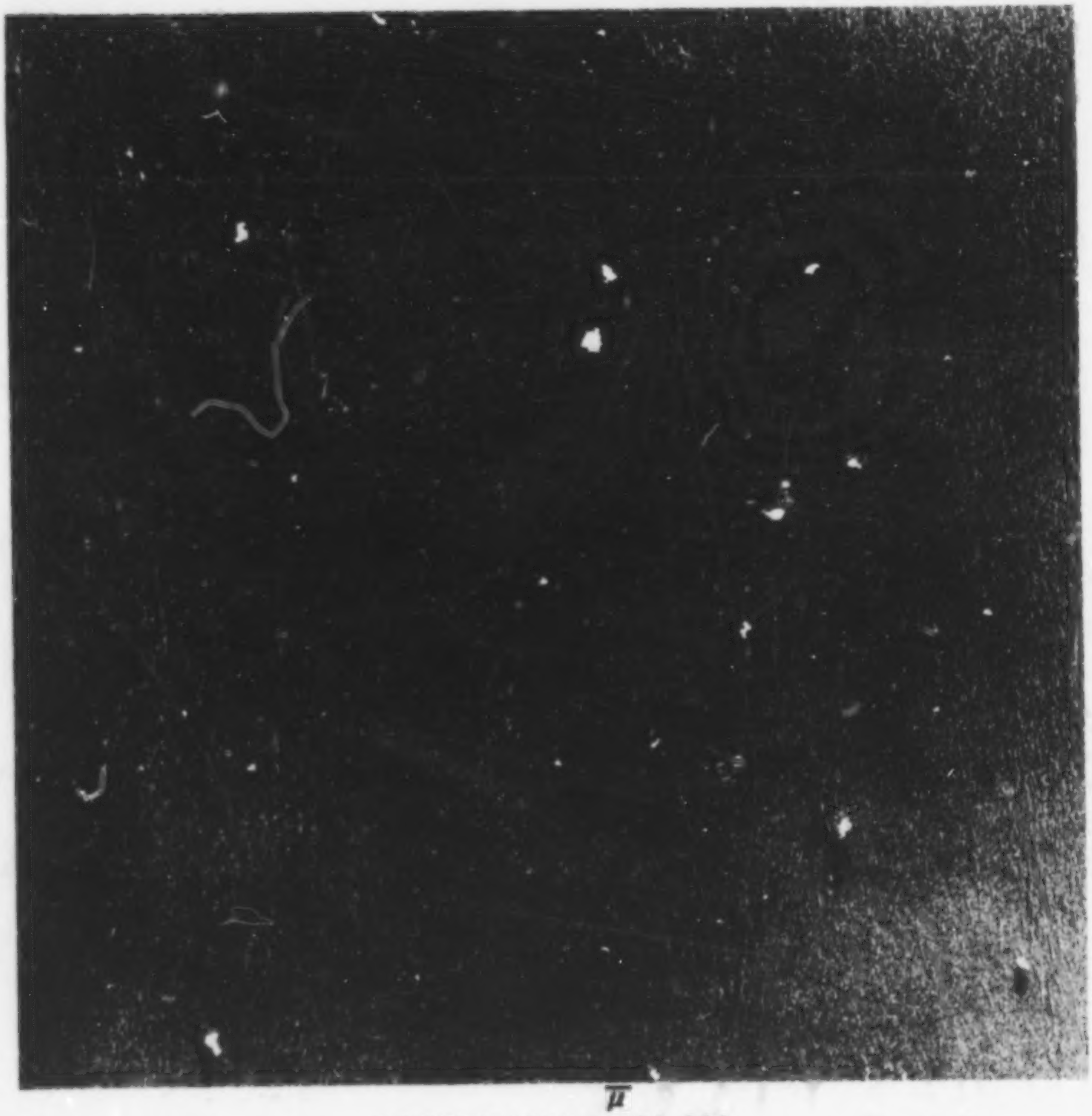

MAGNIFICATION = X18,000

Figure 38

PARTICULATE SAMPLE - EXTERNAL COMBUSTOR
SAMPLE 2293
SPECIMEN K-4
3/4 FUEL FLOW
RUN #14 CONDITION 8

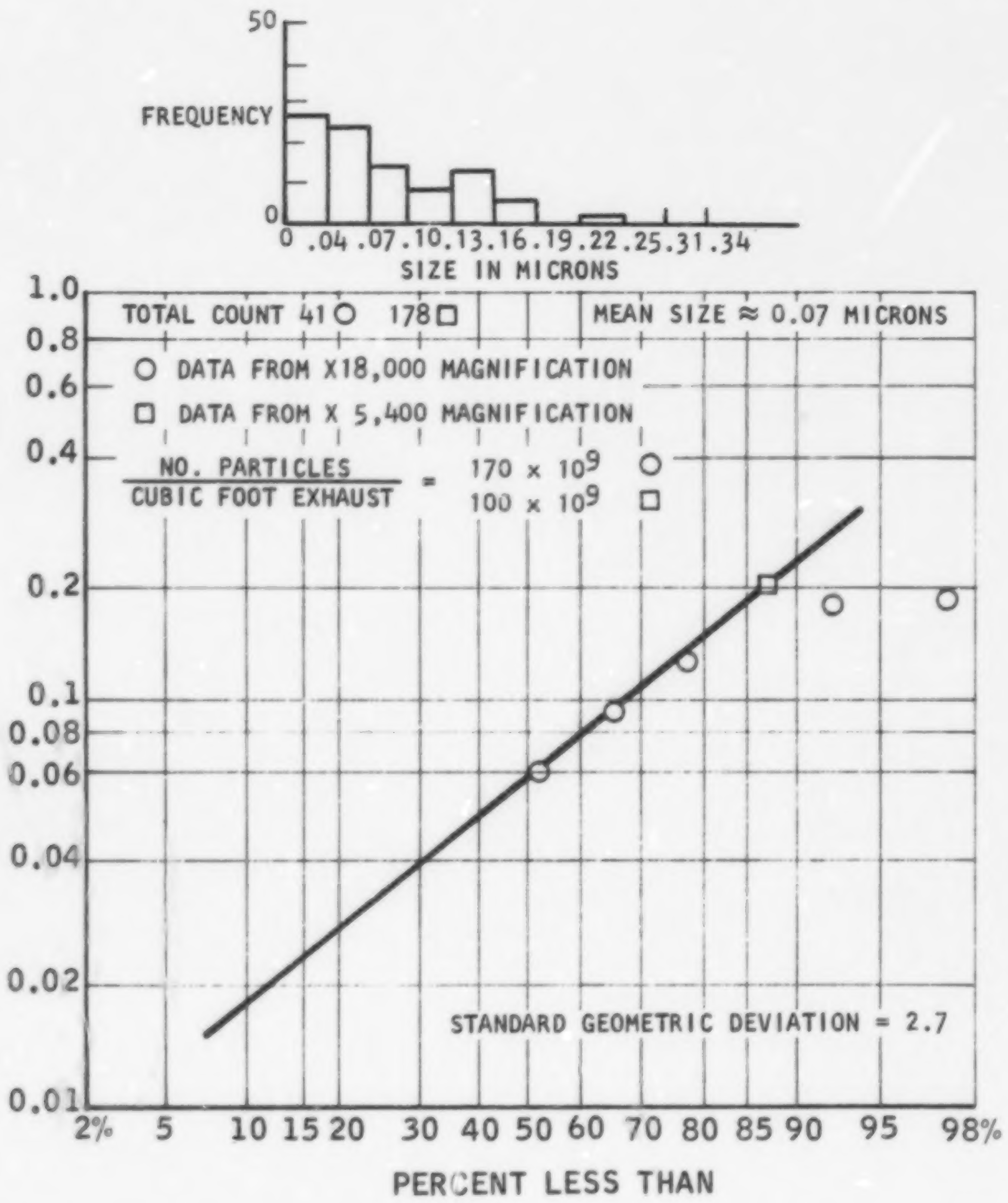

Figure 39

PARTICULATE SAMPLE – EXTERNAL COMBUSTOR

SAMPLE 2299C

RUN #19 CONDITION 1

JET A (LIQUID)

1/2 FUEL FLOW

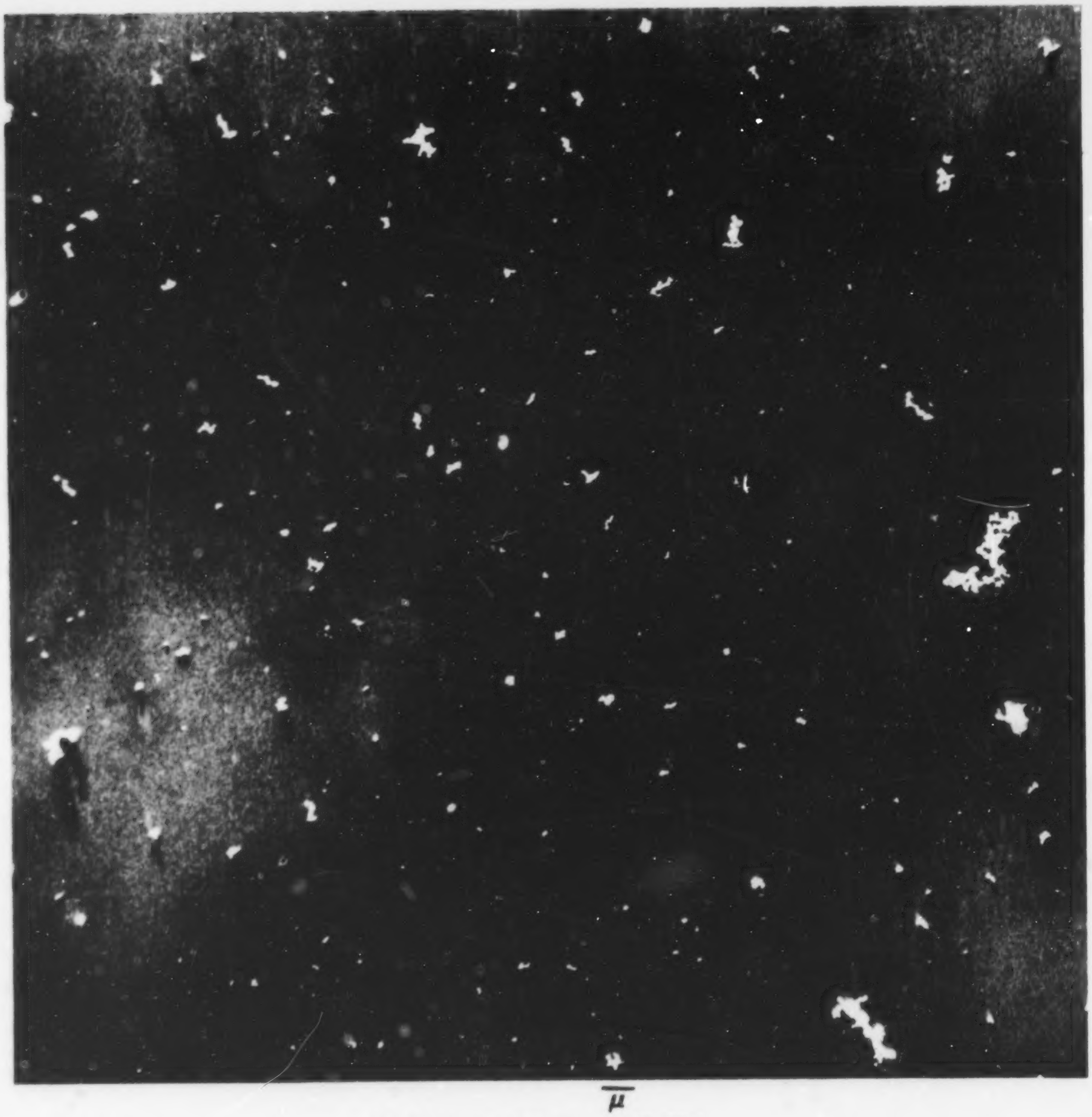

MAGNIFICATION = X5400

Figure 40

PARTICULATE SAMPLE - EXTERNAL COMBUSTOR

SAMPLE 2299C

SPECIMEN N-5
1/2 FUEL FLOW
RUN #19 CONDITION 1

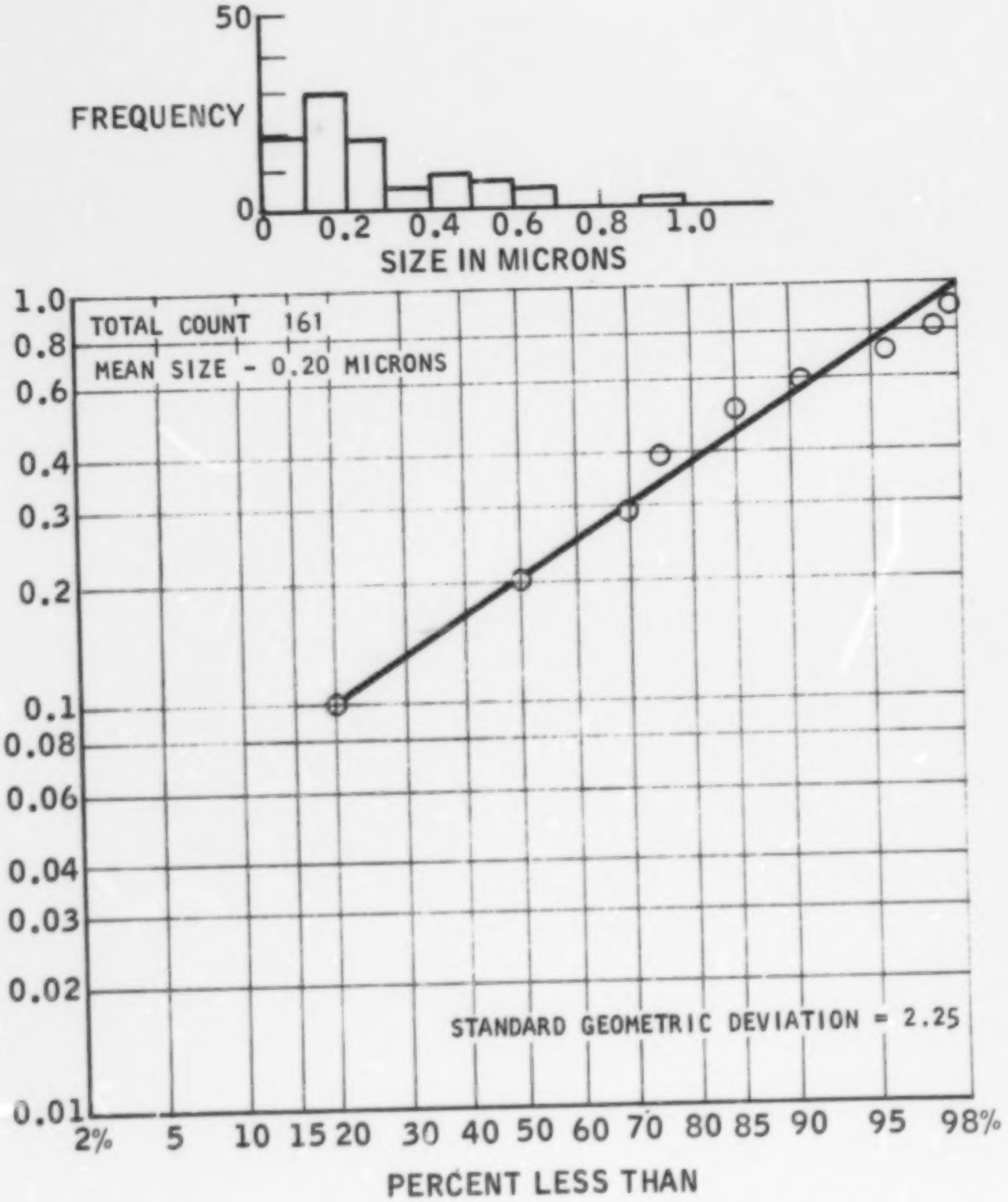

Figure 41

PARTICULATE SAMPLE — INTERNAL COMBUSTION ENGINE

SAMPLE K-2
1968 PLYMOUTH
DOWNTOWN - LOW SPEED

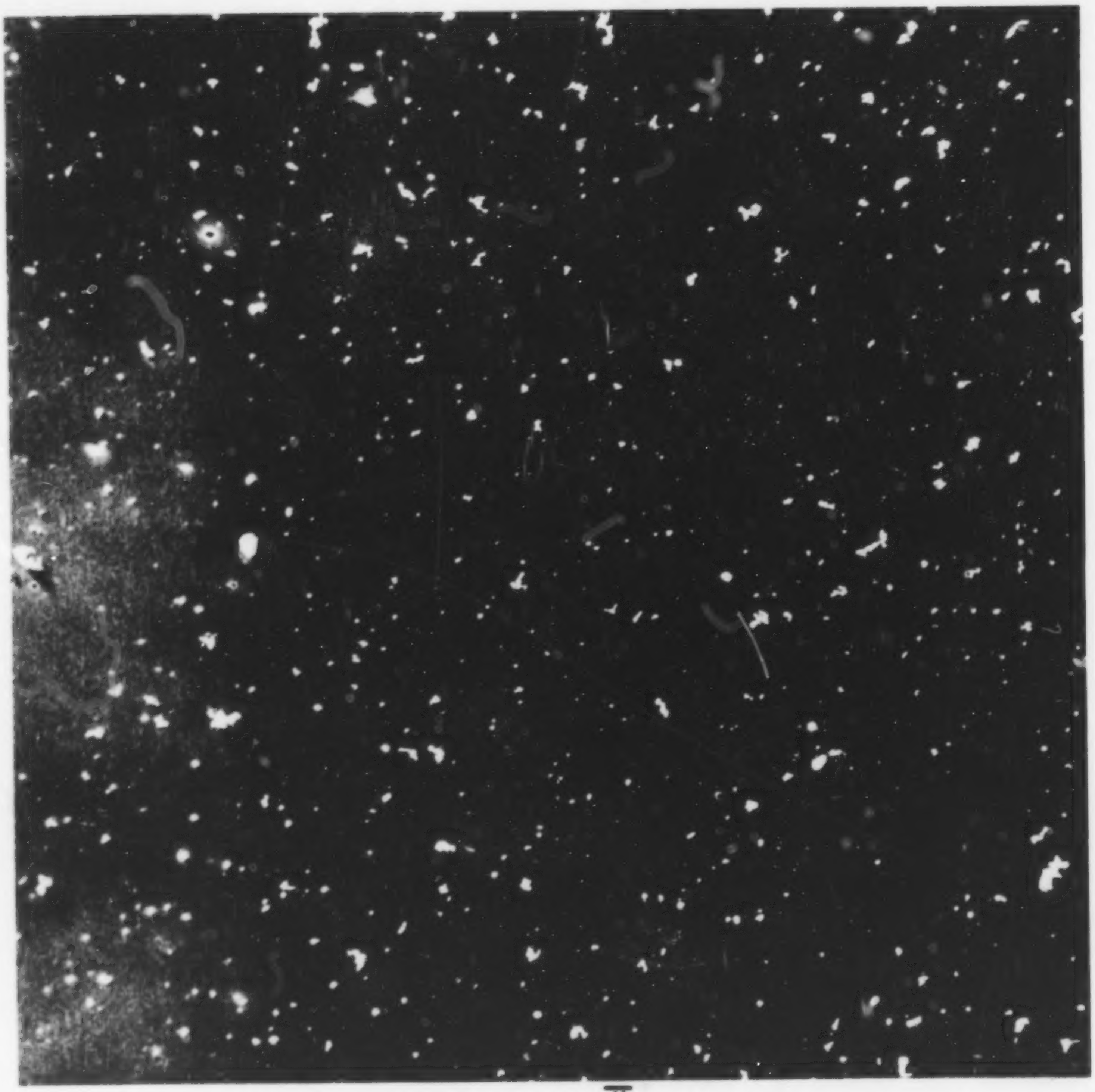

MAGNIFICATION = X5400 Figure 42

PARTICULATE SAMPLE - INTERNAL COMBUSTION ENGINE

SAMPLE K-2

1968 PLYMOUTH

DOWNTOWN - LOW SPEED

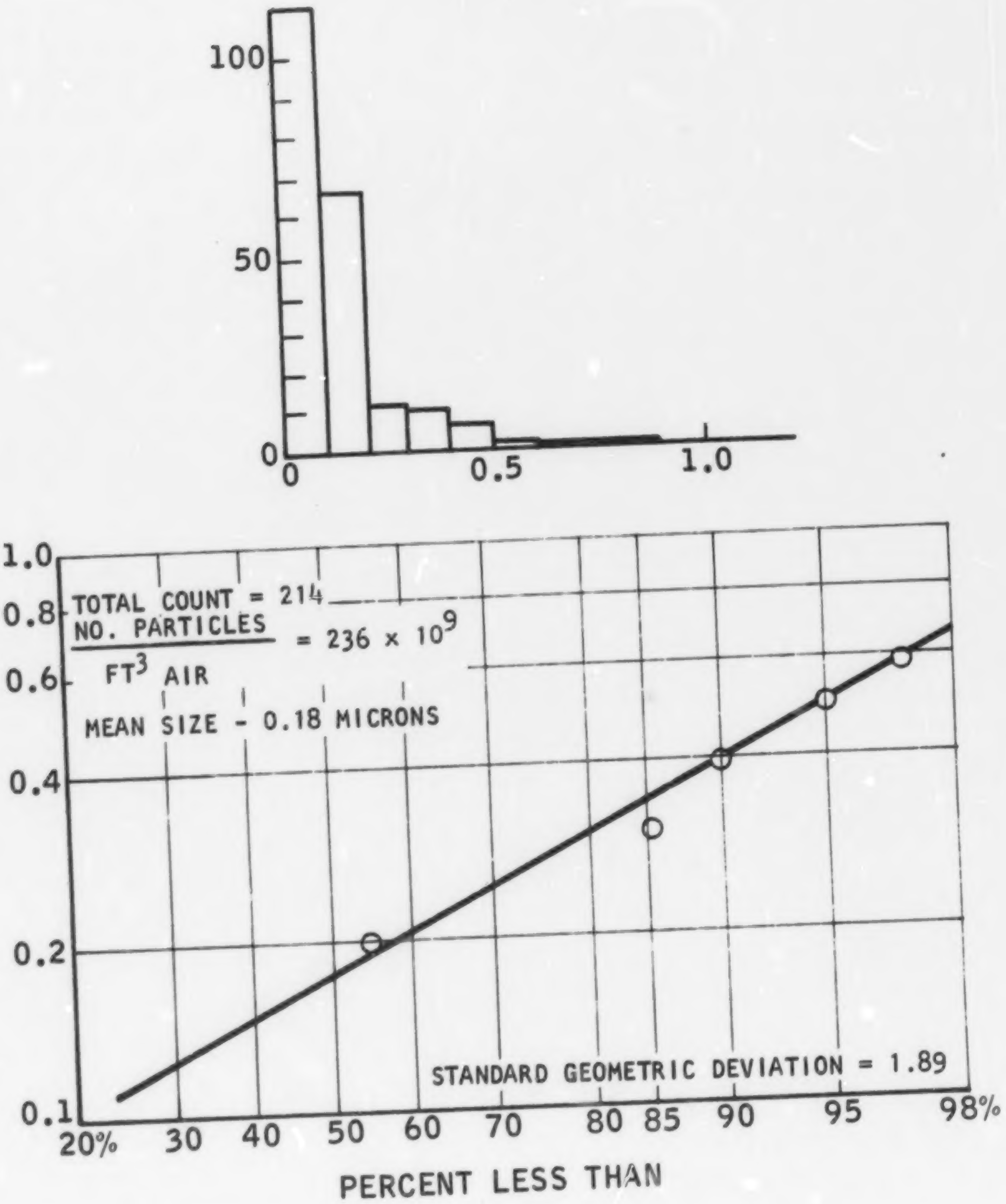

Figure 43

TYPICAL GAS TEMPERATURE DATA

VAPORIZED TMH, 3/4 FUEL FLOW

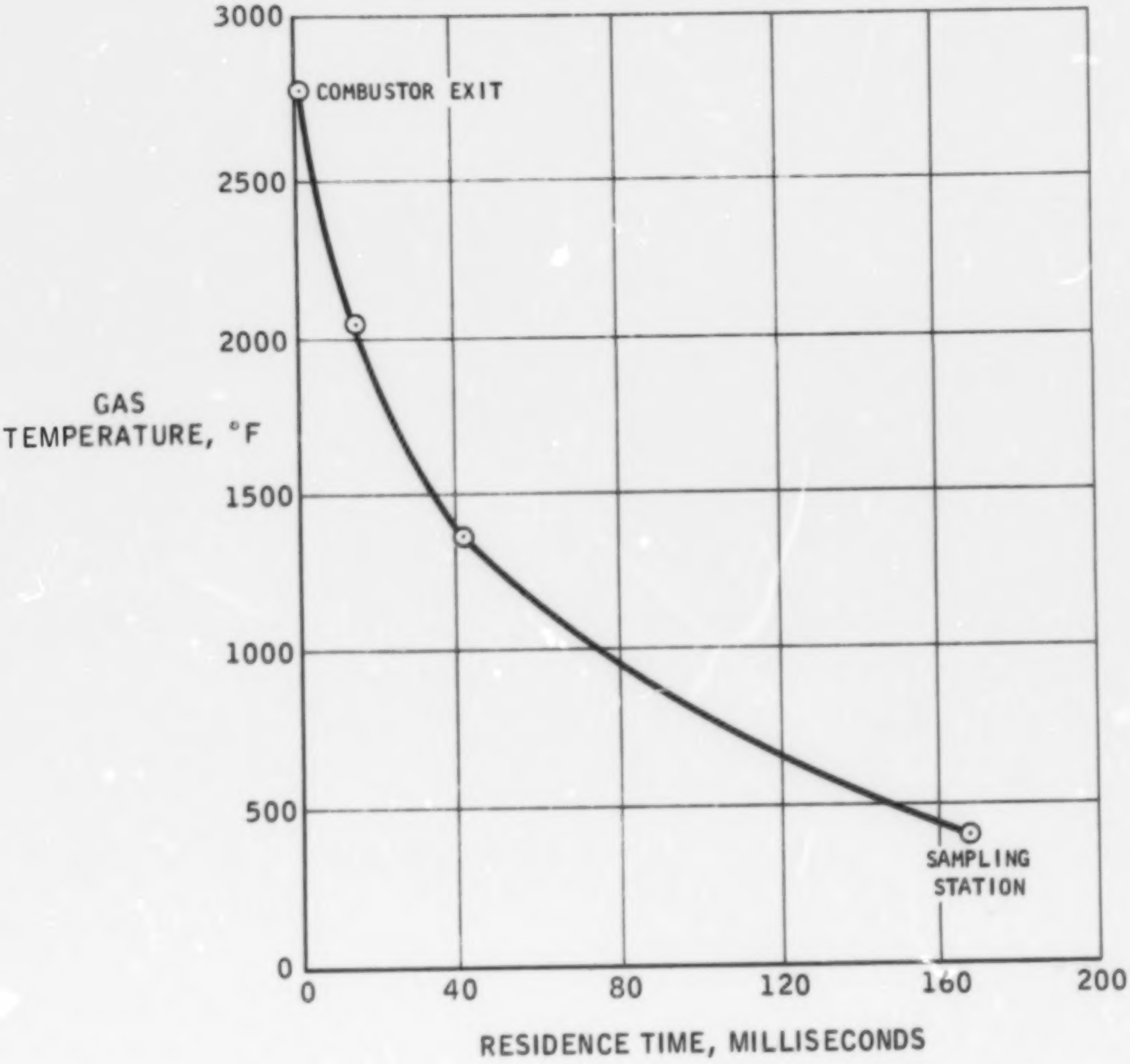

Figure 44

MEASURED FUEL INJECTOR FLOW CHARACTERISTICS

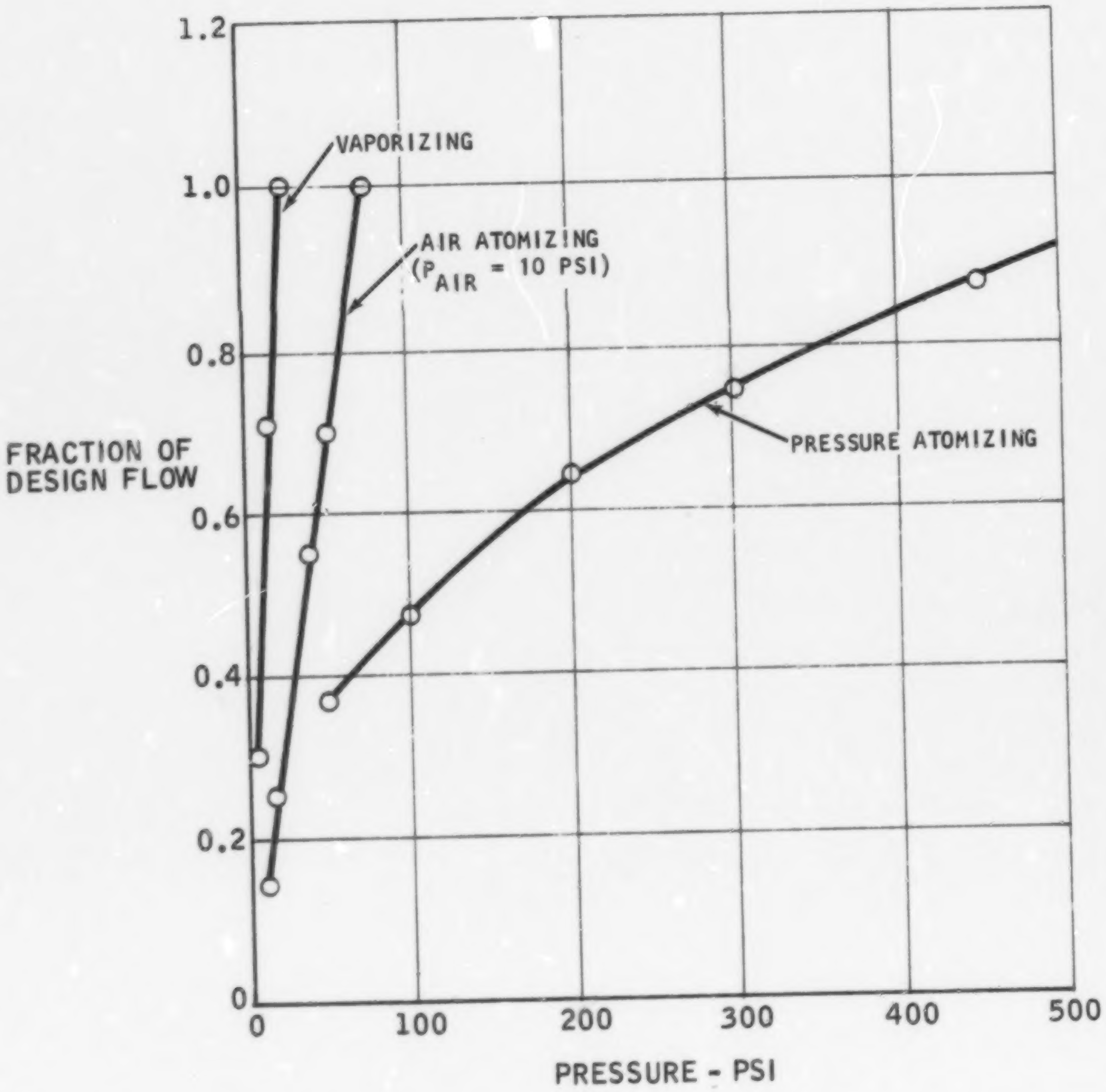

Figure 45

APPENDIX A

COMBUSTION GENERATED AIR POLLUTANTS

The various pollutants which may arise in combustion of kerosene-type fuel fall into three general classes: unburned fuel, particulate carbon, and dissociation species. The unburned fuel may, at one limiting condition, pass through the combustor essentially unchanged, and at the other limit it may be very substantially degraded, just short of conversion into particulate carbon. Regardless of the degree of degradation, the basic cause and means of alleviation are concerned with the fuel/air mixing process, as discussed below. Formation of particulate carbon is attributable to inadequate mixing at the microscopic level, and this is discussed in turn. Under most conceivable combustion conditions, the most prominent dissociation species which might endure at quench temperatures are CO and NO (aside from H_2, which is of course of no consequence in the present context).

Hydrocarbons

The problem of traces of unburned hydrocarbons from a hydrocarbon/air combustor is one of mixing and not directly of reactivity. If mixing were complete with sufficient air available, one would not expect unburned material. Thus, if a reasonable flame strength is achieved associated with high temperature, conditions are extremely conducive to reaction (pyrolysis and combustion) of the last traces of fuel. This premise of the significance of mixing is important to understanding of the relative amounts of unburned hydrocarbons which may be expected from different hydrocarbon/air combustion systems.

The fuel distribution correlation devised by Longwell[12] has been employed with success in combustion design. This correlation approximates an error function. In Reference 13, Builder and Bahn demonstrated that the dispersion of fuel in a turbulent air stream reflects a statistical distribution due to the vagaries of the turbulent flow, consistent with an error function. If there is a statistical distribution of fuel over the airflow, one can envision an overall distribution which is generally quite satisfactory, with local pockets of adverse distribution scattered throughout the flow. The local fuel/air ratio in some of these adverse pockets may very likely be so far removed from stoichiometric as to preclude flames spreading into them from surrounding, more favorable regions. This barrier to combustion can be adjacent to the next most adverse regions, with the least flame-spreading capability. Then one can only hope for local radiative auto-ignition brought about by exposure to some surrounding high temperature region without the microscopic turbulence required by flame-spreading.

Analysis has shown that if 0.01% of the airflow had fuel equivalence ratios (ϕ) as adverse as either 0.1 or 10, then about 80% of the airflow would contain fuel of concentration between $\phi = 0.5$ and $\phi = 2$, which are grossly the flammability limits of hydrocarbon fuel in cold air. The very lean 10% of the air and the very rich 10% would then react with the fuel present only with difficulty. However, the summary conclusion of this analysis is that trace unburned hydrocarbons are not inherent to so-called "off-stoichiometric" design in the overall sense, but are attributable to locally very adverse mixtures, and as such are a problem which can be resolved by proper injector designs.

Particulate Matter

The problem of particulate emission in the external combustion process is related first to the formation of "smoke" particles, and second, to the emission of submicron particles formed by nonvolatile compounds in the combustion process.

Smoke evidently arises by catastrophic pyrolysis of fuel vapors when these have insufficient air to support combustion as the favored process. Gaseous fuels or vaporized liquid fuels are the easiest to burn without smoke formation because good mixing with air down to the microscopic level is most readily accomplished; burning of liquid fuels of good quality in a smoke-free process is not difficult to achieve if the fuel particle size can be made small and strong mixing and turbulence created. However, the composition of the liquid fuel is important in assuming smoke-free combustion. For example, the presence of substantial concentrations of unsaturated hydrocarbons such as olefins and diolefins can produce sooty flames as compared to cleaner burning paraffins and naphthenes.

The second problem relating to submicron particles is a more difficult one to attack. The knowledge of the history of a single fuel droplet as it undergoes fractional batch distillation and liquid-phase reactions in passing through the combustor from one temperature zone to another is necessary in order to speculate on how such particles may be formed. It has been reported[14] that gasoline, diesel, and turbine engines all may emit submicron glassy spheres. Under an electron microscope these appear as chains and rings. Individual fuel droplets are known to burn to an outside hard crust if heated rapidly, then to a vitreous mass that coalesces above 1000°C to nearly colorless glassy spheres.

Carbon Monoxide

Carbon monoxide is the requisite intermediate in the creation of CO_2 as an end product in combustion. It also can itself be an end product to a degree in the incidence of high-temperature equilibrium dissociation, such as with fuel-rich operation. The latter situation can be overcome by designing and operating so as to forestall dissociation, but the former situation is inevitable. Thus, it is necessary to ensure that CO is indeed oxidized to CO_2, as called for by the proper end point of overall reaction. The oxidation of CO in flame is primarily achieved by progress of the reaction $OH + CO = H + CO_2$, which is exothermic by 25 kcal/mole. In the flame zone there is ready mobility among the various H-O species, so that while the flame endures, a sufficiency of OH can be consistent with the rate of creation of CO. However, if the flame is quenched by abrupt admixture of excessive cold air, then recombination reactions will tend to destroy the O-H dissociation species (especially OH) in the form of O_2, H_2, and H_2O, thus leaving the CO inert at low temperature. Therefore, the fuel injection and mixing process is the deciding factor in minimizing air pollution by CO.

Nitric Oxide

The various deleterious oxides of nitrogen in air pollution derive from nitric oxide. To reduce NO concentrations, some mechanism must be used that either (a) affects the formation of NO; or (b) accelerates the decomposition of NO. Experience has shown that NO in the exhaust from hydrocarbon-air combustion processes is affected by[15]:

(1) Peak temperature and duration
(2) Availability of oxygen
(3) Rate of cooling of gases

The peak temperature and duration, availability of oxygen, and the kinetics during mixing and cooling are all strongly affected by burner design.

Although equilibrium calculations are revealing in certain aspects, the formation and fixation of nitric oxide in a combustion process is dictated by chemical kinetic considerations. This has also been pointed out by Peters[16] and was demonstrated by experiments reported by R. F. Sawyer[17 & 18]. The concentrations of nitric oxid found in experiments with both gas turbine engines and combustion rigs are appreciably less than frozen equilibrium values from the combustion zone, but often more than final equilibrium values for the situation after admixture of dilution air.

The essential reaction for formation of NO is $O + N_2 = N + NO$, with an activation energy of 75 kcal/mole, corresponding to the heat of reaction. The atomic nitrogen thus formed either may itself react to form more NO, $N + O_2 = O + NO$, or it may recombine to N_2, $N + N + M = N_2 + M$, depending upon relative concentrations. All three obvious reactions for the consumption of N, i.e., the reverse of the first, plus the second and the third, are essentially on the frequencies of the respective collisions. There is a substantial activation energy involved in the destruction of NO by the reverse of the second reaction, and until the concentration of NO has built up to its equilibrium value, the combination of adverse activation energy and adverse reactant concentrations tends to suppress this reverse reaction of destruction.

In general terms, then, NO is formed at a low rate insufficient to achieve complete equilibrium concentration and is destroyed at a rate so low as to be negligible. In order to reduce the net amount of NO formed, therefore, two approaches may be envisioned: (1) combustor operation under conditions very adverse to kinetic formation of NO, and (2) utilization of chemical scavengers to remove the NO formed.

For real understanding of the kinetically-controlled formation of NO within a flame, it is essential to base the calculation of NO formation on the concentration of atomic oxygen and atomic nitrogen in the flame. The concentration of atomic oxygen is certain to be appreciably different than the final equilibrium value as calculations have shown. As soon as the flame has done its work and consumption of fuel has been effected, rapid dilution and cooling of the flame by addition of excess air is desired, so as to quench the formation of NO. In Reference 19, Grumer, Harris, Rowe, and Cook have concluded that NO formation may be reduced "by starting to cool the combustion gases as soon as possible to about 2300°F, at which temperature concentrations of nitrogen oxides do not increase within the residence time in most gas appliances." If one accepts this as an operating principle, the inclusion of the limited NO reaction kinetics within the much more extensive pyrolysis and combustion kinetics is obviously required.

Furthermore, practical experience in combustor research and development lends assurance that a design can be made to operate well when the component steps are all specified to inhibit the formation of NO by suitable combinations of temperature, oxygen, concentration, and time. For example, the tendency toward NO formation is greatly inhibited in the fuel-rich regime where all available oxygen is needed for carbon oxidation, as calculations have clearly demonstrated. Thus, first-stage, fuel-rich combustion to a very combustible mixture of CO and H_2 at high temperature, followed by some admixture of air and rapid second-stage reaction (too rapid for much NO to form), and then be followed by further cooling to reduce the temperature, is indicated by theoretical considerations (and confirmed by experimental results obtained in this program).

APPENDIX B

FUEL SELECTION

On Table B-1 are shown those fuel characteristics which are essentially constant (within 25%) for liquid hydrocarbon fuels of conceivable interest. Table B-2 lists variable characteristics and points up the significance of these characteristics. Table B-3 shows how each significant caracteristic varies as one moves from a fuel represented by gasoline toward a more volatile fuel such as propane or methane. The tendency would be to vary in the other direction in moving from gasoline toward, for example, diesel oil.

Discussion of Fuel Characteristics

Droplets of fuel burn with diffusion flames, if they have not been already evaporated upstream of the flame region. Clearly, vapor pressure indicates the feasibility of achieving complete vaporization prior to combustion. In the diffusion flame around a burning droplet, cracking of the evolved fuel vapor, to less suitable products, may occur before it is able to mix with air and burn to the desired final products of CO_2 and H_2O. Were it not for this cracking, the size of the droplet would be important only as this determines the burning time and thus the requisite combustor length. As it is, the depth of the diffusion flame around a droplet, in which adverse pyrolysis can occur, is proportional to the droplet size. Thus, large droplets are more likely to result in some deleterious pyrolysis of evolved vapors than are small ones. This consideration argues for use of lighter hydrocarbon fractions as fuels, since these atomize more easily to small droplets, as influenced by both viscosity and surface tension.

A burning droplet has as its surface temperature very nearly the boiling temperature of the liquid. For a given droplet size, and thus a given depth of diffusion flame, the high temperature exposure of fuel vapors to the liklihood of pyrolysis will be somewhat lessened by evolution of the vapor at a lower temperature, even if the maximum temperature of the diffusion flame is the same (as it is at about the stoichiometric value for all burning droplets). More important than this, however, is the temperature exposure of the droplet before vaporization occurs. Thermal degradation may occur in the liquid phase, accelerating with temperature as liquids of different boiling points are examined. These considerations relate principally to the possible employment of fuels less volatile than gasoline, such as fuel oils.

In tables B-2 and B-3, fuel characteristics dealing with combustion reactions are summarized as ignition energy, burning rate, and smoking tendency/coking tendency. In gross terms, ignition energy is greater, or ignition is more difficult, with smaller hydrocarbon molecules (i.e., more volatile fractions), and contrariwise, the tendency toward production of smoke or coke is greater with larger, less volatile molecules. Volatility aside, as it affects the creation of a combustible mixture of fuel vapor and air, there cannot be said to be good basic data on comparative burning rates of various fuels under constant-pressure conditions. To be sure, there are data on flame speeds through flammable mixtures, but this represents propagation, not burning to completion, and is not really germane to defining the details of a continuous-flow system.

Analysis

In a continuous-flow combustion system, there is an anchored flame source, rather than a continuous sparking action or the equivalent. The design of the system is such that fresh combustible mixture is continuously fed into the flame source region, and burning material is continuously bled off to ignite the bulk of the combustible flow which bypasses the flame source region. By some mixing pattern, combining burning and fresh materials, flame is spread into the whole flow. Finite-chemical-kinetics calculations have been performed which have connotation for selection of fuel type for least emission of objectionable effluent substances. A large hydrocarbon molecule distributed in air in reasonable proportions for ensuing combustion evidently must be converted to small fragments before significant reactions providing heat release can occur. Two calculations were performed with comparable starting conditions (using very hot air to dictate prompt auto-ignition) to compare the combustibility of nonane (C_9H_{20}) and highly pyrolyzed nonane. In the latter case, combustion was essentially completed in about one-tenth of the time required by the former case. Considering the available time at high temperature to produce NO, the pyrolyzed fuel is surely preferable in being quicker to burn, and thus an argument is presented for the use of a more volatile fuel of smaller molecular size, corresponding to pyrolyzed fuel. The argument can also be made that if the fuel is burned more rapidly to CO_2 and H_2O, there is less chance of its being pyrolyzed to free carbon as an objectionable product.

In summary, there is no firm direction for selection of one "most appropriate" fuel. The benefits of the system may be such that a less refined fuel than gasoline may be wholly suitable, or a fuel the equivalent of unleaded gasoline may be called for, or even the benefits of lighter hydrocarbon fractions may be utilized later to fully realize minimization of pollutants. The influence of fuel type is one of degree, not of "go/no go" significance, but it is important that the system can readily utilize lighter hydrocarbons than gasoline if this should prove to be logistically favorable. The distillation curves for some common hydrocarbon fuels are presented in Figure B-1.

TABLE B-1

FACTORS ESSENTIALLY CONSTANT REGARDLESS OF FUEL

Heating Value
Density
Stoichiometric Fuel/Air Ratio
Identity and Properties of Theoretical Combustion Products
Storage Stability (Fuel Inert Internally and with Materials)
Toxicity
Heat of Vaporization

TABLE B-2

VARIABLE FACTORS EXAMINED AS TO SIGNIFICANCE

Melting Point	Not a problem
Boiling Point and Vapor Pressure	Evaporative losses; influence on combustibility
Viscosity	Ease of atomization
Surface Tension	Ease of atomization
Flammability Limits	Not a problem
Ignition Energy	Ease of ignition
Burning Rate	Completion of reaction relative to formation of $(NO)_x$
Smoking Tendency and Coking Tendency	Liklihood of objectionable effluent

TABLE B-3

TRENDS OF VARIABLE FACTORS MOVING FROM GASOLINE TOWARD MORE VOLATILE FRACTIONS

Vapor Pressure	Increases
Boiling Point	Decreases
Viscosity	Decreases
Surface Tension	Decreases
Ignition Energy	Increases
Burning Rate	Increases
Smoking Tendency/Coking Tendency	Decreases

DISTILLATION CURVES
HYDROCARBON FUELS

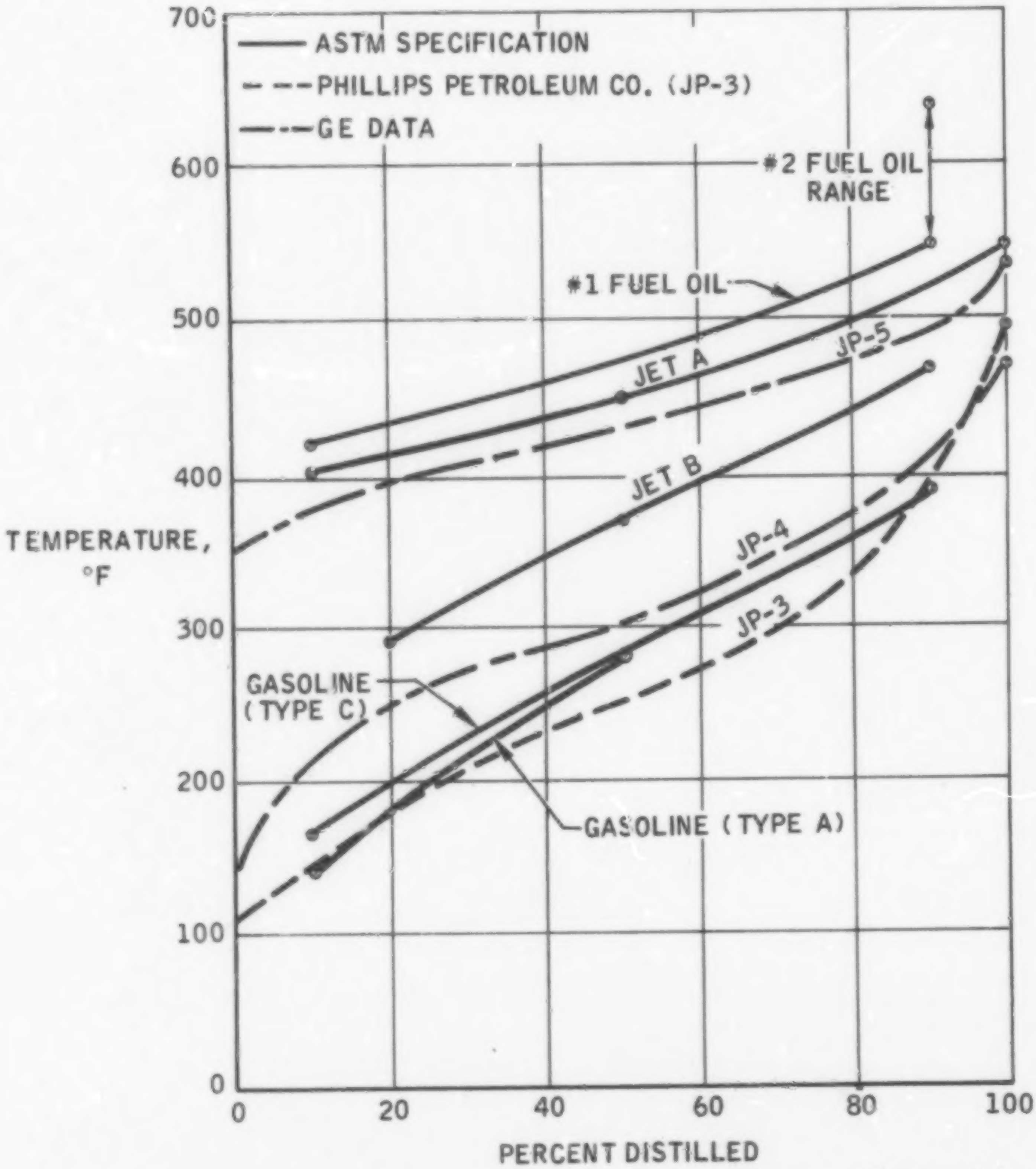

Figure B-1

APPENDIX C

TEST FUELS SPECIFICATIONS

FUEL SPECIFICATIONS

AEROSHELL TURBINE FUEL 640
(JET A OR KEROSENE)

PROPERTIES

Gravity, °API	39.8 (0.826)
Color, Saybolt	30+
Flash, Tag c.c., °F	136
Pour Point, °F	B-60
Viscosity, cs at 30°F	10.24
Copper Strip at 122°F	1
Copper Strip at 212°F	1
Corrosion, Silver Strip	0
Mercaptan Sulfur, % wt	0.0001
Odor	ok
Smoke Point, mm	20
Aromatics, % vol	14.1
Freezing Point, ASTM °F	B-58
Water Reaction, Inc. or Dec., ml	0.5
Interface Rating	1
ASTM Distillation, °F - I.B.P.	344
10% Evaporated	365
50% Evaporated	419
90% Evaporated	478
95% Evaporated	491
End Point	504
Recovery, % vol	98
Residue, % vol	1.0
Loss, % vol	1.0
Aniline Gravity Constant	5532
BTU/lb (Calc)	18,500
Gum, Existent, Steam Jet Mgs.	1
Gum, Potential, Steam Jet, Mgs.	1
TAN-C	Neutral
SAN-C	Nil
Olefine, % vol	0.7
Naphthalenes, (Diaromatics)	0.31
Water Separometer Index Mod	98
Luminometer Number	47.3

Thermal Stability, ACTM-CFR Coker

Pressure Drop, In. Hg	.05
Preheater Deposit Rating	0

FUEL SPECIFICATIONS

2,2,5-TRIMETHYLHEXANE - TECHNICAL GRADE

95 MOL PERCENT MINIMUM PURITY

Typical Properties	Technical Grade	Test Methods
Freezing point, F	-	ASTM D1015
Boiling point, F	-	Modified Cottrell
Distillation range - Initial Boiling point, F	255.3	Modified Cottrell
Dry point, F	255.7	
Specific gravity of liquid at 60/60F	0.711	ASTM D1298
at 20/4C	-	Westphal balance
API gravity at 60F	67.5	ASTM D287
Density of liquid at 60F, lb/gal	5.92	ASTM D1250
Vapor pressure at 70F, psia	0.3	Calculated
at 100F, psia	0.7	ASTM D323
at 130F, psia	1.4	Calculated
Refractive index at 20C	1.399	ASTM D1218
Flash point, approximate, F	55	ASTM D1310
Color, Saybolt	+30	ASTM D156
Sulfur content, weight percent	<0.01	ASTM D1266
Acidity, distillation residue	Neutral	ASTM D235
Nonvolatile matter, grams/100 ml	<0.0005	ASTM D1353

FUEL SPECIFICATION

METHANE

SPECIFICATIONS COMPONENT	TECHNICAL GRADE GUARANTEED
Methane	97.0 mol. %
Oxygen/Argon	< 0.025 mol. %
Nitrogen	< 0.80 mol. %
Carbon Dioxide	< 0.01 mol. %
Ethane	< 2.50 mol. %
Propane and Higher Hydrocarbons	< 0.60 mol. %
Water	< 0.0126 mol. %
Water (Dew Point)	< -40°F

PHYSICAL PROPERTIES:

Chemical Formula	CH_4
Molecular Weight	16.04
Specific Volume at 60°F, 1 atm.	23.61 cu. ft/lb
Boiling Point at 1 atm.	-258.7°F
Freezing Point at saturation pressure	-296.5°F
Specific Gravity (Air = 1)	0.555
Critical Pressure	673.1 psia
Critical Temperature	-115.78°F
Critical Volume	0.0991 cu. ft/lb
Flammable Limits in air, by volume	
Lower Explosive Limit	5.3%
Upper Explosive Limit	14.0%
Autoignition Temperature	1000°F
Latent Heat of Vaporization at boiling point, 1 atm.	219.22 Btu/lb
Latent Heat of Fusion	0.05562 Btu/lb
Heat of Combustion at 25°C	978 Btu/cu.ft.
Gross Heat of Combustion at 60°F, 1 atm.	1011.6 Btu/cu.ft.

APPENDIX D

DATA SUMMARY

This section presents the pertinent data for each test. The tabular presentation is in two recurring data formats. The legend for this table is as follows:

ϕ_P	Primary equivalence ratio, calculated from flow rates
ϕ_T'	Overall equivalence ratio, calculated from flow rates
W_A	Primary air flow
W_B	Secondary air flow
W_T	Total air flow
W_f	Fuel flow
T_F	Fuel temperature at heat exchange outlet
P_f	Fuel pressure at nozzle inlet
P_{T_O}	Primary air gage pressure
$(P_{T_O}-P_{T_I})$	Differential pressure, primary vs. secondary air
$(P_{T_O}-P_{S_L})$	Differential pressure, primary air vs. combustor exit
T_c	Uncorrected reading of combustor thermocouple
CO	Concentration of carbon monoxide in exhaust
NO	Concentration of nitric oxide in exhaust
H.C.	Concentration of unburned hydrocarbons in exhaust, expressed as ppm carbon
CO_2	Volume percent carbon dioxide in exhaust
ϕ_T	Overall equivalence ratio computed from CO_2 concentration
$T_{H.E.1}$	First head exchanger thermocouple, 6½ ft. of heat exchanger length
$T_{H.E.2}$	Second heat exchanger thermocouple, 15 ft. of heat exchanger length
$T_{H.E.3}$	Third (exit) heat exchanger thermocouple, 34 ft. of heat exchanger length
T_{W_1}	Combustor wall thermocouple 1, Station 1
T_{W_2}	Combustor wall thermocouple 2, Station 2
T_{W_3}	Combustor wall thermocouple 3, Station 5
T_{W_4}	Combustor wall thermocouple 4, Station 8

NOTATIONS FOR FUEL CONDITIONS

Fuel

F_1	2, 2, 5-trimethylhexane
F_2	Kerosene
F_3	Methane

Fuel Condition Suffix

F-1	Superheated vapor
F-2	Ambient gas
F-3	Ambient liquid

Fuel Injector

I_{V_1}	0.10" converging vapor injector
I_{V_2}	"SUE" vapor injector
I_{L_1}	Higher pressure liquid atomizing injector
I_{L_2}	Lower pressure liquid atomizing injector

SUMMARY OF DATA

COND.	FUEL SCALE (NOM.)	ϕ_P	ϕ_T	W_A LB/SEC	W_B LB/SEC	W_T LB/SEC	W_f LB/HR	T_F °F	P_f PSIG	P_{T_O} IN Hg	$\frac{(P_{T_O}-P_{T_1})}{\text{IN } H_2O}$	$\frac{(P_{T_O}-P_{S_L})}{\text{IN } H_2O}$	T_c °F
			RUN 1			FUEL: F_1-1			INJECTOR: I_{V_1}				
1	1/2	0.59	0.59	0.0880	0.0	0.0880	12.5	361	8	1.2	1.0	1.8	2440
2	↓	0.71	0.71	0.0751	0.0	0.0751	12.8	359	↓	0.95	0.6	1.5	2620
3	↓	0.80	0.59	0.0665	0.0234	0.0899	12.7	357	↓	1.15	-0.15	1.1	2455
4	↓	0.99	0.58	0.0534	0.0376	0.0910	12.7	361	↓	1.2	-1.4	1.4	2561
5	↓	1.00	0.70	0.0526	0.0218	0.0744	12.6	366	↓	0.95	-0.55	1.5	2620
6	↓	1.24	0.59	0.0422	0.0473	0.0895	12.6	366	↓	1.1	-2.8	1.2	2290
7	↓	1.23	0.71	0.0425	0.0307	0.0732	12.5	367	↓	0.9	-1.6	1.3	2515
8	↓	0.79	0.58	0.0661	0.0234	0.0895	12.5	366	↓	1.2	-0.16	1.2	2455
9	↓	0.76	0.76	0.0678	0.0	0.0678	12.4	370	↓	0.85	0.55	1.6	2670
10	↓	0.76	0.76	0.0678	0.0	0.0678	12.9	370		0.85	0.55	1.4-1.7	2650
			RUN 2			FUEL: F_1-1			INJECTOR: I_{V_1}				
1	1/4	0.80	0.60	0.0351	0.0111	0.0462	6.7	374	4	0.35-0.4	0.24	0.5-0.7	2365
1a	1/4	0.77	0.77	0.0350	0.0	0.0350	6.5	386	4	0.3	0.40	0.5-0.7	2425
2	1/2	0.85	0.63	0.0661	0.0233	0.0894	13.5	371	8	1.2	0.40	1.2-1.3	2530
3	3/4	0.84	0.63	0.0980	0.0341	0.132	19.9	357	14	2.8	0.71	2.8-2.9	2730
3a	3/4	0.81	0.70	0.1027	0.0157	0.118	20.0	357	14-15	2.2-2.3	1.8	2.6-2.9	2790
			RUN 3			FUEL: F_3-2			INJECTOR: I_{V_1}				
1	1/4	—	—	—	—	—	1.1×10^{-3} lb/sec	amb	2	0.3	-0.55	0.5	1565
1a	1/4	—	—	—	0.0152	—	1.7×10^{-3}	"	5	0.4	-0.49	0.6	2185
2	1/2	0.93	0.60	0.0658	0.0244	0.0902	3.2×10^{-3}	"	18	1.4	-0.17	1.1	2455

SUMMARY OF DATA

CONDITION	CO PPM	NO PPM	H.C. PPM_C	CO_2 %	ϕ_T	$T_{H.E._1}$ °F	$T_{H.E._2}$ °F	$T_{H.E._3}$ °F	T_{W_1} °F	T_{W_2} °F	T_{W_3} °F	T_{W_4} °F
				RUN	1							
1	130	83	4	8.8	0.62	1660	1072	266	360	—	799	573
2	85	103	3.8	10.7	0.75	1820	1185	302	862	—	1065	1247
3	90	85	3.8	8.8	0.62	1725	1174	312	—	320	674	693
4	80	79	4	8.7	0.62	1760	1167	318	405	550	802	1185
5	90-105	95	4	10.9	0.76	1915	1202	305	976	1192	1150	1271
6	120-210	67	4-8	9.2	0.65	1790	1185	312	855	1033	1271	1404
7	70-440	71-88	8-30	11.2	0.78	1850	1220	307	917	1195	1357	1367
8	80	90	5	9.1	0.64	1790	1171	316	111	360	616	616
9	90-105	105	4	11.2	0.78	1915	1220	302	903	1160	1087	895
10	95-125	105	4	10.9	0.76	1930	1213	305	917	1160	1083	899
				RUN	2							
1	88-95	75	4-10	8.3-9.6	0.54-0.67	1400	806	132	380	646	765	577
1a	105	90	4	11.3	0.78	1550	829	175	814	780	880	616
2	80	88	3.5	9.3-9.6	0.65-0.67	1850	1160	307	75	270	596	616
3	88	92	3.5	9.5	0.67	2005	1330	402	160	490	731	757
3a	85	107	3.4	10.8	0.75	2035	1360	409	292	835	917	854
				RUN	3							
1	65	30	5	4.9	0.445	1020	393	154	269	517	655	490
1a	85	44	3	8.0	0.705	1400	517	194	1062	1312	1374	1115
2	70	62	3.5	7.9	0.70	1615	1019	305	780	712	1240	847

SUMMARY OF DATA

COND.	FUEL SCALE (NOM.)	ϕ_P	ϕ_T	W_A LB/SEC	W_B LB/SEC	W_T LB/SEC	W_f LB/HR	T_F °F	P_f PSIG	P_{T_O} IN Hg	$(P_{T_O}-P_{T_1})$ IN H_2O	$(P_{T_O}-P_{S_L})$ IN H_2O	T_c °F
3	1/2	0.83	0.68	0.0671	0.0145	0.0816	3.0×10^{-3} lb/sec	amb.	19	1.0	-0.3	1.0	2635
			RUN 4			FUEL:	F_1 -	3	INJECTOR:		I_{L1}		
1	1/2	0.85	0.63	0.0654	0.0234	0.0843	13.5	amb	180	1.2	0.0	2.8	2455
2	1/2	0.85	—	0.0654	—	—	13.4	↓	175	1.0	0.8	2.8	2515
3	1/4	0.43	—	0.0656	—	—	6.8		40	0.7	0.3	0.8-1.2	1790
4	1/4	—	—	—	—	—	6.8		40	0.35	-0.2	0.7-1.0	2260
5	1/4	—	—	—	—	—	6.8		40	0.3	-0.08	0.7	2425
6	3/4	0.84	0.63	0.0955	0.0320	0.1275	19.2		370	2.4	0.5	2.2-2.5	2670
7	3/4	0.81	—	0.0990	—	—	19.1		370	1.9	1.5	2.0-2.3	2670
8	1/2	0.55	—	0.102	—	—	13.6		180	1.8	1.6	2.5	2275
9	1/2	0.85	0.63	0.0654	0.0234	0.0843	13.5		180	1.25	0.0	2.7	2500
10	3/4	0.85	0.67	0.0990	0.0258	0.125	20.2		420	2.35	0.9	2.6	2730
			RUN 5			FUEL:	F_2 -	3	INJECTOR:		I_{L1}		
1	1/2	0.94	0.69	0.0650	0.0235	0.0885	15.0	amb	130	1.25	-0.08	3.1	2455
2	↓	0.92	0.77	0.0661	0.0132	0.0793	15.0	↓	130	1.2	0.8	2.9	2440
3		0.95	0.95(?)	0.0643	0.0	0.0643	15.0		130	0.9	1.2	2.2-2.5	2440
4		0.94	0.60	0.0653	0.0362	0.1015	15.0		130	1.7	-1.2	3.1	2400
5		1.05	0.68	0.0582	0.0319	0.0901	14.9		130	1.4	-0.45	2.8	2400
6		1.12	0.665	0.0531	0.0365	0.0899	14.6		150	1.3	-1.7	3.0	2365
7		0.93	0.69	0.0655	0.0233	0.0888	15.0		130	1.3	-0.08	3.0	2515
8		1.04	0.80	0.0589	0.0176	0.0765	14.9		130	1.1	0.2	2.7	2560
9		0.775	0.775	0.0664	0.0	0.0664	12.6		90	0.85	0.94	1.8	2365

SUMMARY OF DATA

CONDITION	CO PPM	NO PPM	H.C. PPM_C	CO_2 %	ϕ_T	$T_{H.E._1}$ °F	$T_{H.E._2}$ °F	$T_{H.E._3}$ °F	T_{W_1} °F	T_{W_2} °F	T_{W_3} °F	T_{W_4} °F
3	75	73	3.5	9.0	0.78	1695	1080	310	280	873	1340	943
			Run 4									
1	75	84	2.8	10.0	0.70	1805	1118	300	NOT OPERATING		1259	917
2	400-500	88-94	6-18	11.6	0.80	1975	1209	316			1333	994
3	1800	16	1650	5.0	0.38	1143	784	236			1662	447
4	70	80	11	9.8	0.69	1450	825	178			1330	655
5	110-140	100-105	7.5	12.6	0.87	1550	806	155			1357	712
6	400-850	80	30-70	10.0	0.70	2005	1340	406			1397	976
7	3000-3300	90-94	240-400	—	—	2065	1405	410			1605	946
8	1000-1100	38	280-370	7.4	0.53	1615	1108	357			1484	674
9	80	91	9	10.0	0.70	1820	1167	345			1131	708
10	350-1200	92	30-220	11.0	0.815	PRINT CHART MALFUNCTIONED						
			Run 5									
1	70-80	88	3.5	10.6	0.715	1850	1199	332	513	1302	1444	866
2	250-615	98-102	6	11.8	0.80	1960	1240	347	761	1300	1480	873
3	>5000	80	400-600	13.0	0.87	2035	1323	350	658	1125	1143	899
4	80	78	5.5	9.3	0.65	1805	1266	411	354	930	1234	806
5	95-160	81	4-6	10.0	0.68	1885	1230	403	460	1110	1367	843
6	165-365	83	6-20	10.2	0.70	1850	1220	391	435	1180	1460	917
7	70-85	94	3.5	10.9	0.74	1915	1209	397	497	1195	1278	825
8	260-465	102	5-15	12.0	0.81	2005	1244	385	393	1300	1387	877
9	155-365	83	4-6	11.6	0.78	1885	1146	323	651	985	1065	769

SUMMARY OF DATA

COND.	FUEL SCALE (NOM.)	ϕ_P	$\phi_{T'}$	W_A LB/SEC	W_B LB/SEC	W_T LB/SEC	W_f LB/HR	T_F °F	P_f PSIG	P_{T_O} IN Hg	$(P_{T_O} - P_{T_1})$ IN H_2O	$(P_{T_O} - P_{S_L})$ IN H_2O	T_c °F
10	1/2	0.61	0.54	0.0999	0.0132	0.113	15.0	amb	130	1.8	1.4	2.7	2305
11	1/2	0.91	0.76	0.0662	0.0132	0.0794	14.8	255	140	1.1	0.4	1.7	2530
			RUN 6			FUEL:	F_2-3		INJECTOR:		I_{L_1}		
1a	1/2	0.93	0.655	0.0656	0.0235	0.0841	15.0	amb	125	1.3	0.7	2.4-3.0	FAILED
1b	1/2	0.93	0.69	0.0656	0.0234	0.0890	14.9	↓	125	1.3	0.7	2.3-2.8	DURING
2	3/4	0.90	0.67	0.0995	0.0356	0.135	22.0		315	2.7	1.7	2.6-3.5	TEST
1C	1/2	0.94	0.69	0.0654	0.0233	0.0887	14.9		125	1.3	0.8	2.7-3.2	
4	3/4	1.025	0.66	0.0879	0.0480	0.136	22.0		315	2.8	0.8	2.9-3.3	
5	3/4	1.025	0.58	0.0878	0.0671	0.155	22.0		315	3.25	-0.94	2.3-3.2	
			RUN 7			FUEL:	F_3-2		INJECTOR:		Iv2		
4	1/4	0.56	0.37	0.0457	0.0227	0.0684	1.49×10^{-3} lb/sec	amb	25	0.65	-0.24	0.4	1800
5	1/4	0.56	0.56	0.0457	0.0	0.0457	1.45×10^{-3}	↓	25	0.45	0.63	0.6	2060
6	1/4	0.37	0.37	0.0687	0.0	0.0457	1.44×10^{-3}		24 1/2	1.3-1.8	-0.46-32	-0.3	1340
8	1/2	0.765	0.57	0.0691	0.0230	0.0921	3.08×10^{-3}		60	1.3	1.6	1.7	2525
1	1/4	0.72	0.36	0.0346	0.0344	0.0690	1.45×10^{-3}		19	0.6	-0.7	0.1	1560
2	1/4	0.75	0.56	0.0345	0.115	0.0460	1.50×10^{-3}		20 1/2	0.4	0.47	0.4	2105
3	1/4	0.75	0.75	0.0345	0.0	0.0345	1.52×10^{-3}		21 1/2	0.4	0.63	0.5	2225
			RUN 8			FUEL:	F_1-2		INJECTOR:		Ive		
2	1/4	0.80	0.60	0.0343	0.0114	0.0457	6.6	323	3	0.35	-0.68	0.2	1950
1	↓	0.80	0.40	0.0344	0.0344	0.0688	↓	298	2	0.55	-1.03	-0.1	1605
3		0.80	0.80	0.0344	0.0	0.0344		314	2	0.25	0.24	0.3	2420

SUMMARY OF DATA

CONDITION	CO PPM	NO PPM	H.C. PPM_C	CO_2 %	ϕ_T	$T_{H.E._1}$ °F	$T_{H.E._2}$ °F	$T_{H.E._3}$ °F	T_{W_1} °F	T_{W_2} °F	T_{W_3} °F	T_{W_4} °F
10	1250-1730	54	200-400	5.4	0.58	1740	1188	410	1004	1435	1289	731
11	205-295	94	5	11.6	0.78	1975	1254	407	557	961	1083	769
			RUN 6									
1a	70	91	5	10.7	0.73	1930	1244	338	497	954	1350	791
1b	70	89	5	10.8	0.73	1840	1202	353	480	943	1360	776
2	2770-3550	89	200-500	10.6	0.72	2005	1441	468	925	1306	1316	840
1c	70	90	19	10.6	0.72	1850	1216	390	480	899	1330	821
4	1680-3730	92	210	10.5	0.715	2005	1474	464	880	1237	750	899
5	550-2200	79	120	9.2	0.63	1880	1357	468	678	1199	1058	825
			RUN 7									
4	75	21	1-6	4.4	0.40	1100	744	184	280	416	767	416
5	65	29	1	6.5	0.58	1255	744	170	626	695	974	491
6	700	8	~9000	1.4	—	1025	416	116	606	437	503	325
8	70	62	1.5	7.5	0.665	1613	1081	305	1409	637	1021	602
1	65	32	0.7	4.1	0.37	1046	676	174	974	672	919	437
2	65	57	0.5	7.0	0.62	1256	527	163	1134	1329	1145	507
3	65	67	0.4	8.6	0.75	1314	740	166	1273	1442	1239	539
			RUN 8									
2	65	76	4	9.4	0.66	1305	754	160	577	776	954	537
1	70	38	5	5.7	0.41	1130	716	193	282	476	799	505
3	60	97	5	11.2	0.78	1355	769	168	769	968	1062	577

SUMMARY OF DATA

COND.	FUEL SCALE (NOM.)	ϕ_P	ϕ_T	W_A LB/SEC	W_B LB/SEC	W_T LB/SEC	W_f LB/HR	T_F °F	P_f PSIG	P_{T_O} IN Hg	$(P_{T_O}-P_{T_1})$ IN H_2O	$(P_{T_O}-P_{S_L})$ IN H_2O	T_c °F
4	1/4	0.60	0.40	0.0459	0.0230	0.0689	6.6	314	2	0.60	-0.8	-0.1	1935
5	↓	0.60	0.60	0.0460	0.0	0.0460	↓	315	2	0.40	0.08	0.1 to 0.4	2310
6		0.47	0.47	0.0584	0.0	0.0584		314	2	0.3 to 2.0	-2.4 to -0.6	0.2 to 2.3	1600-2020
8	1/2	0.80	0.60	0.0681	0.0229	0.0910	13.1	314	19	1.2	0.0	0.5	2780
9		0.80	0.80	0.0683	0.0	0.0683		314	19	1.0	0.6	0.8	2885
7		0.80	0.40	0.0681	0.0680	0.136		314	18	2.1	-4.1	-0.5	2070
10		0.60	0.40	0.0907	0.0457	0.136		314	18	2.2	-1.3	0.3 to 0.6	2100
11		0.60	0.60	0.0910	0.0	0.0910		310	18	1.4	1.3	1.1 to 1.5	2490
12	↓	0.53	0.53	0.103	0.0	0.103	↓	311	18	1.5 to 2.0	-1.0 to 1.4	0.5 to 0.8	2310
			RUN	9		FUEL:	F_1-1		INJECTOR:	I_{V_1}			
2	1/2	0.80	0.60	0.0686	0.0228	0.0914	13.2	300	1	1.2	-0.79	0.4	2610
4	1/2	0.80	0.80	0.0686	0.0	0.0686	13.2	296	1	0.9	-0.40	0.1	2750
5	3/4	0.795	0.60	0.1033	0.0338	0.137	19.7	325	9	2.7	-2.1 to -2.4	-0.5	2460-2640
6	3/4	0.80	0.70	0.1028	0.0141	0.117	19.7	332	9	2.2	-0.5 to -1.3	-0.5 to 0.5	25[illegible]; 2420
7	3/4	0.80	0.80	0.1028	0.0	0.1028	19.7	324	9	1.9	0.63	0.6	2850
			RUN	10		FUEL:	F_1-1		INJECTOR:	I_{V_1}			
1	1	0.85	0.73	0.1288	0.0204	0.149	26.2	305	12	4.1	-1.0	0.5	2825
			RUN	11		FUEL:	F_1-1		INJECTOR:	I_{V_1}			
1	1/10	0.80	0.60	0.0137	0.0046	0.0183	2.6	450-490	~0	0.25	-0.3	-0.5	1540-2130
2	1/10	0.51	0.51	0.0136	0.0	0.0136	2.6	430-440		0.15	-0.16	-0.1	1600-2100
3	1/30	0.80	0.60	0.0046	0.0015	0.0061	0.88	530-550	↓	—	—	—	750-1600

SUMMARY OF DATA

CONDITION	CO PPM	NO PPM	H.C. PPM$_C$	$\overline{CO_2}$ %	ϕ_T	$T_{H.E._1}$ °F	$T_{H.E._2}$ °F	$T_{H.E._3}$ °F	T_{W_1} °F	T_{W_2} °F	T_{W_3} °F	T_{W_4} °F
4	70	41	8	5.9	0.425	1185	776	218	216	447	624	414
5	50	63	5	8.5	0.60	1340	814	209	521	727	895	480
6	1700-2150	15-22	3000-5000	4.2-6.2	—	1235	635	186	569	670	756	414
8	60	120	8	9.5	0.67	1685	1115	314	443	670	1271	866
9	60	146	6	11.1	0.77	1780	1153	310	573	851	1340	720
7	75	68	5	6.0	0.435	1390	997	324	133	328	925	585
10	70-120	45	10-50	5.8	0.42	1370	1015	341	144	328	658	472
11	50	66	5	8.7	0.615	1650	1101	331	517	585	1040	639
12	300-730	50	400-700	7.5	0.535	1520	1069	323	513	727	910	569
			RUN	9								
2	70	133	2.7	9.2	0.65	1640	1150	312	amb.	191	456	427
4	88-103	148	2-3	11.7	0.81	1750	1185	307	264	541	914	639
5	80	102-127	2-5	9.3	0.655	1780	1309	406	139	350	523	616
6	90-320	148	2.5-15	11.2	0.78	1920	1380	408	259	435	806	727
7	250-630	161	2.5-10	11.4	0.82	1970	1404	408	367	628	961	772
			RUN	10								
1	52 to >1000	105	25-150	11.3	0.785	2040	1540	519	211	415	658	727
			RUN	11								
1	220-370	52-59	25-100	7.9-11.6	—	802	513	108	259	456	761	371
2	650 to >2000	50-75	50-6000	10.3-12.5	—	584	414	102	447	674	802	350
3	1000 to 75000	19-56	10,000-15,000	3.5-8.2	—	497	191	—	557	537	401	160

SUMMARY OF DATA

COND.	FUEL SCALE (NOM.)	ϕ_P	ϕ_T	W_A LB/SEC	W_B LB/SEC	W_T LB/SEC	W_f LB/HR	T_F °F	P_f PSIG	P_{T_O} IN Hg	$(P_{T_O} - P_{T_1})$ IN H_2O	$(P_{T_O} - P_{S_L})$ IN H_2O	T_c °F
			RUN 12			FUEL:	F_1-1		INJECTOR:	I_{V2}			
1	1/30		UNABLE TO OBTAIN IGNITION. POST RUN INSPECTION SHOWED THAT HIGH-										
2	1/40		VOLTAGE SPARK WAS ARCING TO WALL RATHER THAN AT ELECTRODE TIPS										
			RUN 13			FUEL:	F_1-1		INJECTOR:	I_{V2}			
1	1/2	0.80	0.60	0.0686	0.0229	0.0915	13.2	411	22	1.2	0.24 to 0.47	1.1	2550
2	↓	0.80	0.80	0.0685	0.0	0.0685	↓	377	23	0.9	1.2	1.3	2760
3	↓	1.00	0.60	0.0550	0.0361	0.0911	↓	381	23	1.25	-0.8	1.1	2250
4	↓	1.00	0.80	0.0550	0.0138	0.0688	↓	356	23	0.85	0.7	1.5	2670
5	↓	1.22	0.60	0.0459	0.0450	0.0909	↓	386	23	1.2	-1.7	0.6	2220
6	↓	1.22	0.80	0.0458	0.0225	0.0683	↓	356	23	0.8	-0.23	0.7 to 1.1	2610
			RUN 14			FUEL:	F_1-1		INJECTOR:	I_{V2}			
1	1/2	1.20	0.60	0.0458	0.0455	0.0913	13.2	366	23	1.4	-1.6	0.9	2235
2	↓	1.20	0.80	0.0459	0.0229	0.0688	↓	368	↓	0.9	0.0	1.1	2625
3	↓	1.00	0.60	0.0549	0.0366	0.0915	↓	366	↓	1.3	-0.7	1.4	2265
4	↓	1.00	0.80	0.0544	0.0140	0.0689	↓	359	↓	0.9	0.5	1.8	2565
5	3/4	1.21	0.80	0.0681	0.0342	0.1023	19.7	396	34	2.0	-0.4 to -0.8	2.0	2535-2700
6	↓	1.00	0.80	0.0820	0.0205	0.1025	↓	401	35	2.0	1.2 to 1.6	3.0 to 3.5	2790
7	↓	1.20	0.60	0.0682	0.0688	0.137	↓	358	↓	2.9	-5.5 to -7.9	1.2	2255
8	↓	1.00	0.60	0.0820	0.0552	0.137	↓	396	↓	2.8	-0.7	1.6	2715
9	1/4	1.20	0.60	0.0229	0.0228	0.0457	6.6	378	5	0.4	-0.47	0.2	1965
10	↓	1.01	0.61	0.0271	0.0182	0.0453	↓	396	5	0.4	-0.16	0.2	1995
11	↓	1.22	0.81	0.0225	0.0115	0.0340	↓	352	5	0.3	0.0	0.3	2325

SUMMARY OF DATA

CONDITION	CO PPM	NO PPM	H.C. PPM$_C$	CO$_2$ %	ϕ_T	$T_{H.E._1}$ °F	$T_{H.E._2}$ °F	$T_{H.E._3}$ °F	T_{W_1} °F	T_{W_2} °F	T_{W_3} °F	T_{W_4} °F
		RUN 12										
1		UNABLE	TO	OBTAIN	IGNITION	POST	RUN	INSPECTION	SHOWED	THAT		
2		HIGH	VOLTAGE	SPARK	WAS	ARCING	TO WALL,	RATHER	THAN	AT	ELECTRODE	TIPS
		RUN 13										
1	70	79	5	8.7	0.615	1543	1475	330	226	577	844	604
2	75	106	3.5	11.1	0.77	1635	1150	312	208	906	1047	712
3	70	56	3.6	8.6	0.61	1507	1097	327	414	608	986	670
4	75	87	3.5	11.8	0.82	1650	1140	298	658	844	1083	750
5	75	54	3.5	8.7	0.615	1505	1111	326	336	497	1037	689
6	95-220	75	3.5	11.7	0.81	1685	1168	305	541	697	1146	723
		RUN 14										
1	70	54	3.7	8.2	0.58	1505	1097	325	310	497	1037	685
2	80	79	3	11.7	0.81	1685	1168	301	501	768	1132	723
3	70	62	3	8.7	0.615	1540	1097	323	460	701	849	655
4	85	86	3	12.0	0.83	1685	1140	300	862	928	1037	731
5	280	52	10-15	11.6 to 10.7	0.75-0.80	1855	1390	410	255	635	791	802
6	85	105	5	11.7	0.81	1840	1340	401	380	769	939	844
7	1800-2400	55	100-200	8.4	0.60	1670	1278	417	282	655	632	616
8	70	73	3.7	8.8	0.62	1670	1289	421	259	628	704	537
9	95	53	7	7.9	0.56	1146	731	165	468	682	1055	545
10	7[illegible]	75	42	8.2	0.55	1132	731	165	551	750	1012	513
11	95	71	22	11.3	0.755	1254	735	105	549	799	983	557

SUMMARY OF DATA

COND.	FUEL SCALE (NOM.)	ϕ_P	ϕ_T'	W_A LB/SEC	W_B LB/SEC	W_T LB/SEC	W_f LB/HR	T_F °F	P_f PSIG	P_{T_O} IN Hg	$(P_{T_O} - P_{T_1})$ IN H_2O	$(P_{T_O} - P_{S_L})$ IN H_2O	T_c °F
12	1/4	1.02	0.81	0.0269	0.0069	0.0338	6.6	366	5	0.3	0.16	0.3	2505
			RUN	15			FUEL:	F_1-1		INJECTOR:	I_{V2}		
1	1/10	0.80	0.60	0.0137	0.0046	0.0183	2.6	437	~10	0.05	0.04	0.05	2085
2	↓	0.80	0.80	0.0137	0.0	0.0137	↓	436	↓	0.05	0.08	0.0	2220
3	↓	1.00	0.60	0.01095	0.0073	0.0182	↓	441	↓	0.1	0.0	↓	2010
4	↓	1.00	0.80	0.01095	0.0027	0.0136	↓	480	↓	0.05	0.04	↓	2100
5	↓	1.20	0.60	0.00913	0.0042	0.0153	↓	430	↓	0.1	-0.16	↓	1840
6	↓	1.20	0.80	0.00915	0.0046	0.0137	↓	428	↓	0.05	0.0	↓	2025
			RUN	16			FUEL:	F_1-1		INJECTOR:	I_{V2}		
1	1/30	0.81	0.60	4.57×10^{-3}	1.53×10^{-3}	6.10×10^{-3}	0.99		~0	~0	-3.5	~0	
2	↓	0.81	0.81	4.58×10^{-3}	0.0	4.58×10^{-3}	↓		↓	↓	0	↓	
3	↓	1.00	0.63	3.67×10^{-3}	2.21×10^{-3}	5.88×10^{-3}	↓		↓	↓	-7.1	↓	
4	↓	1.00	0.81	3.68×10^{-3}	3.7×10^{-4}	4.55×10^{-3}	↓		↓	↓	-2.4	↓	
5	↓	1.21	0.61	3.06×10^{-3}	3.02×10^{-3}	6.08×10^{-3}	↓		↓	↓	-13.4	↓	
6	↓	1.21	0.83	3.06×10^{-3}	1.38×10^{-3}	4.44×10^{-3}	↓		↓	↓	-3.1	↓	
			RUN	17			FUEL:	F_1-1		INJECTOR:	I_{V2}		
1	1/2	1.20	0.60	0.0459	0.0456	0.0915	13.2	416	22	1.1	-2.2	-0.2	2100
2	↓	1.39	0.60	0.0393	0.0525	0.0918	↓	421	↓	1.1	-3.1 to -7.1	-0.5 to 0.5	2100
3	↓	1.36	0.60	0.0422	0.0488	0.0916	↓	422	↓	1.1	-2.4 to -3.1	-0.5 to 0.5	2130
4	↓	1.59	0.60	0.0345	0.0571	0.0916	↓	422	↓	0.5 to 1.5	-4 to -7.1	1.0	2070

SUMMARY OF DATA

CONDITION	CO PPM	NO PPM	H.C. PPM_C	CO_2 %	ϕ_T	$T_{H.E._1}$ °F	$T_{H.E._2}$ °F	$T_{H.E._3}$ °F	T_{W_1} °F	T_{W_2} °F	T_{W_3} °F	T_{W_4} °F
12	80	110	9	11.1	0.77	1209	735	105	1122	917	1206	537
			RUN	15								
1	65	84	5.8	8.7-9.6	0.61-0.68	847	460	~amb	493	655	1058	384
2	75	108	5	10.7-11.6	0.75-0.80	862	447	↓	658	829	1097	414
3	90-115	50	5	8.7-9.6	0.61-0.68	844	460	↓	674	731	1062	410
4	250-1100	54	5	11.8-12.5	0.82-0.86	844	435	↓	769	880	1104	431
5	115-175	33-39	4.5	9.1-9.9	0.64-0.69	847	468	↓	647	735	788	476
6	550-1050	4-6	6.5-8	11.8-12.8	0.82-0.88	825	435	↓	712	806	814	456
			RUN	16								
1	NEVER ACHIEVED STEADY STATE COMBUSTION AT THIS LOW FUEL RATE.											
2	COMBUSTION WAS OF AN INTERMITTENT NATURE. NO MEANINGFUL											
3	GAS ANALYSIS OR TEMPERATURE DATA											
4												
5												
6												
			RUN	17								
1	80	55	14	7.7	0.55	1589	1044	316	376	497	880	704
2	90	58	8.5	7.3-7.4	0.52-0.56	1405	1126	301	231	435	697	655
3	85	68	7.5	7.7	0.55	1455	1556	311	476	537	895	693
4	840 to 2500	54	100 to 750	7.2-7.7	0.51-0.55	1490	1008	316	166	350	553	612

SUMMARY OF DATA

COND.	FUEL SCALE (NOM.)	ϕ_P	$\phi_{T'}$	W_A LB/SEC	W_B LB/SEC	W_T LB/SEC	W_f LB/HR	T_F °F	P_f PSIG	P_{T_O} IN Hg	$(P_{T_O}-P_{T_1})$ IN H_2O	$(P_{T_O}-P_{S_L})$ IN H_2O	T_c °F
			RUN 18				FUEL: F_1-1			INJECTORS: IV			
1	1/2	1.20	0.60	0.0459	0.0456	0.0915	13.2	378	1	1.1	-3.1	0.2	2145
2	↓	1.20	0.80	0.0458	0.0227	0.0685	↓	386	↓	0.8	-1.2	0.4	2460
3	↓	1.00	0.60	0.0549	0.0365	0.0914	↓	386	↓	1.2	-2.4	~-1	2130
4	↓	1.00	0.80	0.0547	0.0137	0.0684	↓	356	↓	0.8	-0.3	0.3	2460
5	3/4	1.20	0.80	0.0681	0.0340	0.1021	19.7	417	8	1.6	-2.0	~-1	2520
6	↓	1.00	0.80	0.0820	0.0203	0.1023	↓	427	↓	1.7	-1.3	~-0.5	2625
7	↓	1.20	0.60	0.0684	0.0690	0.1374	↓	410	↓	2.5	-6.1	-71	2145
8	↓	1.00	0.60	0.0916	0.0555	0.1371	↓	403	↓	2.65	-5.1	-71	2220
9	1	1.20	0.80	0.0911	0.0462	0.1373	26.3	368	13	3.0	-4.7	0.1	2425
10	1	1.00	0.80	0.1098	0.0277	0.1375	26.3	359	13	3.3	-2.4	~-1	2595
11	1/4	1.22	0.61	0.0224	0.0229	0.0453	6.6	355	~0	0.3	-0.44	~-0.5	1950
12	↓	1.03	0.61	0.0267	0.0181	0.0448	↓	364	↓	0.35	-0.8	~-0.5	2085
13	↓	1.23	0.81	0.0223	0.0115	0.0338	↓	354	↓	0.25	-0.4	~-0.5	2265
14	↓	1.02	0.815	0.0268	0.0069	0.0337	↓	364	↓	0.3	-0.4	~-0.5	2400
			RUN 19				FUEL: F_2-3			INJECTOR: IL2			
1	1/2	0.81	0.60	0.0690	0.0224	0.0919	13.6	amb.	63	1.3	-0.8	0.7	2460
2	↓	0.81	0.81	0.0691	0.0	0.0691	↓	↓	63	1.0	-0.3	0.6	2310
3	↓	0.61	0.61	0.0912	0.0	0.0912	↓	↓	63	1.7	-0.8	0 to 0.5	2450
4	↓	1.01	0.60	0.0550	0.0368	0.0918	↓	↓	65	1.45	-2.8	0	2400
5	↓	1.01	0.90	0.0550	0.0140	0.0690	↓	↓	70	1.0	-0.3	0.9	2540
6	↓	1.20	0.80	0.0462	0.0230	0.0692	↓	↓	75	1.0	-1.2	0.9	2415
7	3/4	0.90	0.60	0.1031	0.0345	0.1376	20.1	↓	145	3.1	-1.6 to -4	0 to -1	2490

SUMMARY OF DATA

CONDITION	CO PPM	NO PPM	H.C. PPM$_C$	CO_2 %	ϕ_T	$T_{H.E._1}$ °F	$T_{H.E._2}$ °F	$T_{H.E._3}$ °F	T_{W_1} °F	T_{W_2} °F	T_{W_3} °F	T_{W_4} °F
			RUN	18								
1	100	34	5	7.6	0.54	1440	1018	300	259	435	651	581
2	85	54	3.7	10.5	0.735	1585	1080	283	418	712	858	655
3	90	48	3.8	7.6	0.54	1455	1058	309	—	236	447	397
4	85	52	3.6	10.5	0.735	1605	1090	286	505	746	884	610
5	75	78	3.7	10.3	0.72	1810	1278	371	—	240	460	480
6	75	72	3.5	10.2	0.715	1777	1275	379	166	336	608	620
7	315-460	30	5-6.5	2.6	0.54	1570	1185	327	144	305	525	497
8	105-195	28	8-15	2.2	0.515	1570	1174	386	206	328	533	529
9	75000	34	1850	10.3	0.72	1890	1474	498	384	525	788	712
10	4200 to 75000	48	100-200	10.5	0.74	1980	1527	571	529	624	895	769
11	90	67	8.5	8.4	0.595	1285	806	160	—	231	414	384
12	90	71	5	8.2-8.6	0.59-0.61	1285	825	161	—	221	414	371
13	120-460	78	5-10	11.0-11.6	0.76-0.81	1405	818	143	186	393	643	464
14	90-560	94	4	11.2-11.6	0.78-0.80	1405	825	143	186	371	674	456
			RUN	19								
1	85	86	10	10.1	0.69	1685	1195	342	414	679	917	735
2	4400-4700	61	170-220	11.8	0.80	1780	1333	409	639	954	1097	772
3	550-1100	63	50-210	8.6	0.59	1665	1240	439	545	844	1340	731
4	105-200	86	8	9.9	0.675	1655	1254	399	371	635	595	788
5	840-1700	102	25-100	13.0	0.87	1843	1289	351	592	903	1062	510
6	4200 to 75000	75	250-400	12.5	0.54	1810	1323	349	517	850	1234	510
7	3200 to 25000	71	500-1000	9.1	0.62	1780	1370	497	226	674	1299	761

SUMMARY OF DATA

COND	FUEL SCALE (NOM.)	ϕ_P	ϕ_T	W_A LB/SEC	W_B LB/SEC	W_T LB/SEC	W_f LB/HR	T_F °F	P_f PSIG	P_{T_0} IN Hg	$(P_{T_0} - P_{T_1})$ IN H_2O	$(P_{T_0} - P_{S_L})$ IN H_2O	T_c °F
8	3/4	0.74	0.74	0.1037	0.0	0.1037	20.1	amb	198	2.5	-0.8 to -1.6	0 to 0.5	2550
9	↓	0.64	0.64	0.128	0.0	0.128	↓	↓	193	3.6	-0.8 to -3.1	-0.5 to 0.5	2400
10	↓	0.49	0.60	0.0824	0.0555	0.138	↓	↓	193	3.1	-3.1 to -6.3	-21	2490
11	1	1.03	0.81	0.1078	0.0281	0.136	27.1	↓	280	3.0 to 3.6	-0.8 to -4.7	-0.5 to 0.5	2690
12	1	0.86	0.86	0.128	0.0	0.128	27.0	↓	270	3.8	0 to -1.6	0.5 to 1.5	2660
13	1/4	0.81	0.60	0.0345	0.0116	0.0461	6.9	↓	~10	0.4	-0.9	-0.2	2160
14	↓	0.81	0.81	0.0345	0.0	0.0345	↓	↓	↓	0.3	-0.24	0.2	2205
15	↓	0.60	0.60	0.0461	0.0	0.0461	↓	↓	↓	0.5	-0.24	-0.2 to 0.2	1980
16	↓	1.02	0.61	0.0276	0.0183	0.0459	↓	↓	↓	0.4	-0.8	-0.3 to 0.3	2175
17	↓	1.02	0.81	0.0276	0.0068	0.0344	↓	↓	↓	0.25	-0.24	-0.3 to 0.3	2295

SUMMARY OF DATA

CONDITION	CO PPM	NO PPM	H.C. PPM_C	CO_2 %	ϕ_T	$T_{H.E._1}$ °F	$T_{H.E._2}$ °F	$T_{H.E._3}$ °F	T_{W_1} °F	T_{W_2} °F	T_{W_3} °F	T_{W_4} °F
8	75000	79	900-1500	9.9	0.675	1810	1420	532	363	899	1379	810
9	2400-3070	58	900-650	8.2	0.56	1700	1340	550	476	954	1323	731
10	2400-3500	80	200-600	9.2	0.63	1825	1405	541	133	537	784	731
11	25000	115	1500-3000	11.4	0.77	1980	1512	563	269	723	1108	844
12	75000	108	1250-1750	10.7	0.725	1950	1540	584	447	936	1306	855
13	147	80	39	10.8	0.73	1441	925	208	731	765	855	651
14	500-1450	94	50-250	13.3	0.89	1540	954	207	880	880	990	655
15	105-130	79	20	10.1	0.69	1507	990	217	674	799	946	537
16	180-890	80	20-115	10.5	0.71	1490	968	225	712	954	990	750
17	3200-9600	102	350-1000	13.5	0.90	1526	954	234	844	950	972	765

APPENDIX E

DATA ANALYSIS

Detailed Run Analysis

This section presents an expanded analysis of the data for a typical test, namely, Run No. 10, Condition 1C. This was a full scale test using 2, 2, 5-trimethylhexane superheated vapor, with the 0.10" converging vapor nozzle. The overall equivalence ratio based on CO_2 analysis was 0.785. The input data of this test are given in Appendix D, together with similar data for each test condition. Parts V through IX give calculations applying to each run.

I. Combustion Temperature

A. Calculated Flame Temperature

A generalized computational procedure was used throughout this program to calculate flame temperatures. Based on the stoichiometry of combustion for a given fuel, the composition of the exhaust gases was determined as a function of ϕ, the overall equivalence ratio. The standard state heat of combustion of the fuel was corrected for: (a) the actual fuel conditions at the fuel nozzle inlet, and (b) the heat removed from the combustor by the cooling water. This fixed the net amount of heat (per mole of fuel) available to heat up the combustion products. A graphical presentation of the mean specific heat of each component gas, between 0°C and the upper temperature 'T' was used. The working equation then became:

$$\Delta H_c = \Sigma \, Ni \left[\bar{C}_{pt} \times T - \bar{C}_{pt_1} \times T_1 \right] \qquad (1)$$

where: ΔH_c = net heat of combustion per mole of fuel

Ni = moles of component 'i' per mole of fuel

T = flame temperature, °C as measured at the station of 'T_c' thermocouple

$\bar{C}_{pt}$ = mean specific heat of component 'i' between 0°C and T

T_1 = temperature of fuel at fuel nozzle inlet, °C

$\bar{C}_{pt_1}$ = mean specific heat of component 'i' between 0°C and T_1

Equation (1) was then solved for T, the corrected theoretical flame temperature, by a combination of computation and graphical techniques.

For the case of 2, 2, 5-trimethylhexane, the relationship between Ni and ϕ is, per mole of fuel:

i	N_i
H_2O	10
CO_2	9
O_2	$14\ (\frac{1}{\phi} - 1)$
N_2	$\frac{52.8}{\phi}$

With this technique, a curve was constructed relating the corrected theoretical flame temperature to equivalence ratio. For Run 10, Condition 1C, this calculated flame temperature was 3080°F.

B. Corrected Thermocouple Temperature

The uncorrected thermocouple temperature was 2825°F. As discussed in Section V-C, a bare thermocouple, exposed to the environment of the combustor can be expected to introduce some error, primarily due to the radiation from the thermocouple junction. The situation is aggravated here in that the junction can 'see' walls which are at a much lower temperature than the surrounding gas stream whose temperature it is desired to measure.

An extimate was made of the magnitude of the errors to be expected for this particular installation, using the methods of Reference 20. The relationship for radiation correction is:

$$E_R = T_t - T_j = \frac{K_R \sigma \epsilon A_R (T_j^4 - T_w^4)}{h_c A_c} \qquad (2)$$

where:

T_t = gas total temperature, °R
T_j = thermocouple junction temperature, °R
K_R = radiation view factor (assumed equal to unity)
σ = Stefan - Boltzman constant
ϵ = emissivity of junction
A_R = area of radiant transfer from junction
h_c = coefficient of convective heat transfer, gas to junction
A_c = area of convective heat transfer, gas to junction.

Evaluation of the key factors was as follows:

(a) Reference 20, pg. 563, states that ϵ of clean Pt is 0.18 (no temperature given) and that it can go up to 0.30 or even 0.55 due to contamination by exhaust. During this program, however, the bead of a similar combustor thermocouple was examined under the microscope after Run 6, in which it had been subjected to conditions which caused a heavy carbon deposit on the combustor walls. The thermocouple bead appeared unaffected, with a shiny luster similar to that of a new junction. Based on this observation, therefore, and on the data of McAdams (Reference 21), pg. 475, ϵ was taken to be 0.18.

(b) The diameter of each thermocuople wire was 0.003"; a spherical bead of 0.01" diameter was estimated. For the existing configuration, $A_R \approx A_c$.

(c) The coefficient of convective heat transfer was estimated from the correlation of Reference 21, pg. 266, to be 170 Btu/ft^2 hr. $^\circ$F.

These quantities resulted in a computed radiation error of 210°F. The conduction error, also estimated by the method of Reference 20, was 8°F. No other errors were found to be significant. It should be noted that this radiation correction is relatively slight for a bare thermocouple at this temperature; the primary reasons for this are the fine wire used in the couple, with the resulting small bead, and the low emissivity of the noble metal surface of the bead.

The above corrections, applied to the measured junction temperature of 2825°F, gave a corrected measured flame temperature of approximately 3040°F. This is only 40°F below the computed flame temperature. This is quite close agreement, although perhaps somewhat fortuitous, since the accuracy of determining thermocouple error terms is usually not great.

II. Heat Balance

Basic to the goals of this program is the availability of a high flux of heat energy for transfer to a working fluid. Accordingly, the heat removed from the exhaust gases in the heat exchanger section was computed. This was done by the following procedure.

The composition of exhaust gases was determined from the measured CO_2 content with the assumption of complete combustion. It was assumed that the composition of this gas remained unchanged after leaving the combustor. The composition of this gas mixture was computed to be, in mole fractions:

i	Xi
H_2O	0.1109
CO_2	0.0998
O_2	0.0439
N_2	0.7453

with an average molecular weight of 28.6.

The following specific heat equation was computed for this gas mixture based on the pure component values of page 371, Reference 22.

$$C_p = 6.42 + 2.69 \times 10^{-3} T - 5.76 \times 10^{-7} T^2 \quad (3)$$

where

C_p is in cal/gmol $^{\circ}$K, and T is $^{\circ}$K.

Based on the measured total flow rate, the enthalpy change of the gas was calculated between each pair of heat exchanger thermocouples. The corrected measured value of T_c was used. Radiation correction was also made for the first heat exchanger thermocouple (uncorrected reading - 2040°F), but the correction was only 18°F. No corrections were necessary for the remaining two thermocouples in the heat exchanger.

The heat absorbed by the cooling water was also calculated. The results are shown below:

Section	Heat Removed from Exhaust Gases Btu/min	Heat Absorbed by Cooling Water Btu/min
1st Heat Exchanger T_c to $T_{H.E.\ 1}$	3010	2100
2nd Heat Exchanger $T_{H.E.\ 1}$ to $T_{H.E.\ 2}$	1520	1330
3rd Heat Exchanger $T_{H.E.\ 2}$ to $T_{H.E.\ 3}$	2750	2150
Totals	7,280 Btu/min 436,000 Btu/hr	5,580 Btu/min 335,000 Btu/hr

First, it should be noted that the calculated heat removed from the exhaust gases is in good agreement with the nominal heat release of 500,000 Btu/hr, based on fuel flow. The calculated figure of 435,000 Btu/hr does not include the heat dissipated in the double wall combustor itself, but only in the heat exchanger section.

The calculated heat absorbed by the cooling water is 77% of the heat removed, as calculated from the thermocouple measurement. This is due primarily to certain aspects of the heat exchanger layout. In the first heat exchanger section there was a significant amount of radiative heat transfer to the surroundings, because two short sections of heat exchanger fittings were not surrounded by copper cooling coils.

The third section of heat exchanger is the open water trough. The exit water temperature from this trough was 156°F, so that a significant amount of vaporization from the water surface occurred.

III. Heat Exchanger Performance

Heat exchanger performance data for Run 10, Condition 1C are summarized in Figure E-1, in which the following quantities are plotted vs. heat exchanger length.

(1) Gas temperature, °F, based on T_c and the three heat exchanger thermocouples.

(2) Cumulative heat transfer, Btu/hr, based on the heat removed from the gas, as calculated above.

(3) Cumulative residence time, milliseconds. This was determined by computing the average gas velocity, ν, at each thermocouple station, plotting $1/\nu$ vs. L, and graphically integrating.

These data show that the corrected gas temperature dropped to 2500°F within 5 milliseconds, and to 2000°F in about 13 milliseconds. Total residence time in the heat exchanger was computed to be 109 milliseconds. The graphs of these three items agree well with a similar plot of calculated quantities performed during the heat exchanger design, prior to fabrication. The main difference is that the convective heat transfer coefficient from the copper-coil wrapped sections was less than that predicted, with radiative heat transfer being significant in the first section.

The pressure drop across the heat exchanger length of 34 feet, plus the additional 4 feet of exhaust line, was 3.6 in. Hg, or 1.8 psi. The design value, based on a 33-ft. length, was 1.5 psi.

IV. Velocities in Igniter Tube

The igniter tube was 2" O.D. x 0.035" wall x 6" long. The primary air flow was 0.129 lb/sec. Therefore, the average air velocity in the igniter tube (neglecting fuel flow) was 76 ft/sec, which corresponds to a residence time of 4.4 milliseconds for the 4 inches of length between the fuel nozzle exit and the combustor inlet.

The measured fuel flow was 26.2 lb/hr = 0.0073 lb/sec. Assuming sonic flow at the fuel nozzle exit, with the measured nozzle inlet pressure of 26 psia, the calculated fuel flow (for choked nozzle flow) is 0.00735 lb/second. Thus, the fuel nozzle was operating in the choked condition, with the fuel vapor leaving the nozzle at sonic velocity. This was calculated to be 550 ft/sec at existing conditions, in good agreement with the throat velocity calculated from continuity. This relatively low sonic velocity is a consequence of the high molecular weight of 2,2,5-trimethylhexane.

V. Equivalence Ratio as Function of CO_2 Content

The method of calculation assumed complete combustion of the fuel to CO_2 and H_2O. The levels of CO, NO, and unburned hydrocarbon encountered during these tests were, in all but a very few exceptional cases, so low as to not exert a significant effect.

The equation for stoichiometric combustion was written for each fuel. Thus, for 2, 2, 5-trimethylhexane,

$$(1) \qquad C_9H_{20} + 14O_2 \longrightarrow 9CO_2 + 10\ H_2O$$

Based on the definition of equivalence ratio, ϕ, one then obtains an expression relating the moles of O_2 to N_2 (per mole of fuel). It was assumed that kerosene could be adequately represented by an average molecular formula of the type C_nH_{2n}. Hence, the equation for stoichiometric combustion for kerosene became:

$$(2) \qquad C_nH_{2n} + \frac{3n}{2} O_2 \longrightarrow nCO_2 + nH_2O$$

These results are summarized below for each fuel in the form of mole fraction of CO_2. The water vapor in the exhaust was removed by the sample gas equipment upstream of the NDIR's. Accordingly, the water formed in each combustion reaction was deleted from the following calculations.

Fuel	X_{CO_2}
2, 2, 5-trimethylhexane	$\dfrac{9}{\frac{66.8}{\emptyset} - 5}$
Kerosene	$\dfrac{1}{\frac{7.14}{\emptyset} - 0.5}$
Methane	$\dfrac{1}{\frac{9.52}{\emptyset} - 1}$

These equations for X_{CO_2} vs. $\emptyset$ are plotted in Figures E-2. The NDIR analysis of CO_2 is read directly in volume %(= mole%) CO_2.

VI. Comparison of Equivalence Ratio Calculations

Two independent methods were used to determine the overall equivalence ratio, $\emptyset_o$, defined as:

$$(1) \qquad \emptyset_o = \frac{\left(\frac{W_f}{W_t}\right)_{actual}}{\left(\frac{W_f}{W_t}\right)_{stoich}}$$

where W_f = fuel flow rate to combustor

W_t = total air flow rate to combustor.

The first method was direct substitution in Eq. (1) of the measured values of fuel and air rates. The second method was based on the CO_2 analysis of the exhaust gas, as discussed previously. This latter measurement permits the calculation of equivalence ratio independent of any of the flow rate measurements, provided that combustion is essentially complete.

In many cases the two valves agreed closely. In other cases, they did not. A detailed analysis was made of this question, and possible reasons examined for those discrepancies which occurred. The analysis is summarized in this section.

Assume that the standard relative error of the measurement of fuel flow and of the total air flow was 3%, and that this cumulative random error from all sources is normally distributed. It should be noted that, in this discussion, standard error refers to σ, the standard deviation of the class of measurements under consideration. The standard relative error is σ/μ, where μ is the population mean; i.e., the true value. It follows from this definition that, statistically, the probability is 68.3% that the error of any one measurement is included within the range ± 3%. It is then apparent that the standard relative error of ϕ_o, computed from flow rates, is $\sqrt{0.03^2 + 0.03^2}$, or 4.2%.

The standard relative error of the NDIR measurement of CO_2 content of the exhaust gases is assumed to be 2% (and hence of the equivalence ratio). It is thus seen that, consistent with these assumptions, the NDIR-derived value of equivalence ratio should be considered as the primary value. Concerning the statistically expected agreement between the two computations of ϕ, it may be shown that, based on typical values, this should be 4.7%. That is, in 68.3% of the cases the agreement should be within 4.7%.

A compilation of the differences between the two values of equivalence ratio was made. The percent difference was defined as $\frac{\phi_1 - \phi_2}{\phi_2} \times 100$, where ϕ_1 and ϕ_2 are the values based on NDIR analysis, and on flow rates, respectively. Of a total of 113 data points in which both estimates of ϕ were obtained, in 56 cases (49.6%), the difference was $\leq \pm$ 5%. In accordance with the above discussion, these cases were considered to represent good agreement. There were 12 cases (10.6%) in which the difference was in the range of ± 5-8%.

A study was made in which it was attempted to correlate each of the following factors (either alone or in conjunction with others) with those cases of discrepancy greater than 5%.

1) Fuel scale
2) Primary equivalence ratio
3) Overall equivalence ratio
4) Type of fuel
5) Physical condition of fuel (temperature and pressure at fuel nozzle inlet)
6) Type of fuel nozzle
7) Primary air venturi
8) Secondary air venturi
9) Type of gas sample probe
10) Combustion temperature
11) Presence or absence of smoke in exhaust
12) Presence or absence of high readings of unburned hydrocarbons
13) Presence or absence of high readings of CO
14) Temperature of gas at sample probe.

No correlation was observed, however, for any combination of these factors. There was no set of conditions found which was unique to those cases showing differences greater than 5%. This would indicate that the observed differences represented a random distribution of cumulative small perturbations. The trend of the data was apparently not random in certain respects, however. Thus, of those cases with differences greater than 5%, the sign of the difference was positive in every case up until Run 17, then negative in every case for Runs 17 and 18. In Runs 13 and 14, all 18 successive data points showed close agreement between the two values of equivalence ratio. Particular scrutiny was given to all the data of these runs, but again there was no set of conditions found which could be correlated with this apparent non-random behavior.

Since there was no known reason to question any of these data, the value of equivalence ratio determined from NDIR CO_2 analysis was used to represent that data point, due to its statistically-expected smaller error.

VII. Conversion of Gas Analysis Data to Include Water Vapor Content of Exhaust Gases

As previously stated, all of the gas analysis data (as measured) are on a water-free basis. It is of interest to express these results on a "water basis," that is, the actual concentrations existing in the hot exhaust gas prior to water vapor removal.

Define:

X_i = concentration of component 'i' as measured $(\frac{Ni}{N_{Tx}} \times 10^6)$

Y_i = concentration of component 'i', water basis $(\frac{Ni}{N_{Ty}} \times 10^6)$

Ni = moles component 'i' per mole of fuel

N_{Tx} = moles exhaust, water-free basis, per mole of fuel

N_{Ty} = moles exhaust, water basis, per mole of fuel

The desired conversion factor, K, is:

$$K = \frac{Y_i}{X_i} = \frac{N_{Tx}}{N_{Ty}} \qquad (3)$$

The expression for N_{Tx} had already been obtained in Part V, above. The expression for N_{Ty} was readily obtained from this by the inclusion of the stoichiometric moles of water.

Fuel	$K = Y_i/X_i$
2, 2, 5-trimethylhexane	$\dfrac{\frac{66.8}{\phi} - 5}{\frac{66.8}{\phi} + 5}$
Kerosene	$\dfrac{\frac{7.14}{\phi} - 0.5}{\frac{7.14}{\phi} + 0.5}$
Methane	$\dfrac{\frac{9.52}{\phi} - 1}{\frac{9.52}{\phi} + 1}$

The conversion factors for each fuel are plotted in Figure E-3.

VIII. Conversion of Gas Analysis Data to Basis of Mass of Pollutant per Unit Mass of Fuel

Define Li as the loading of component 'i' in milligrams (mg) per pound of fuel. It may then be seen that:

$$\text{Li} = \frac{(\text{Xi})\,(\text{M.W.}_i)\,(N_{F_x})}{\text{M.W.}_f} \times 454 \times 10^{-3} \qquad (4)$$

where, M.W._i = molecular weight of component 'i'

M.W._f = molecular weight of fuel

and, Xi and N_{F_x} have the same meanings as in Part VII, above.

What is desired is a graphical presentation of a factor which is multiplied by Xi to give Li. Accordingly, define $\beta_i = \frac{\text{Li}}{\text{Xi}}$.

It then follows that, for each fuel:

A. 2, 2, 5 - trimethylhexane

(5) $$\beta_{NO} = \frac{7.08}{\phi} - 0.530$$

(6) $$\beta_{CO} = \frac{6.60}{\phi} - 0.495$$

(7) $$\beta_{C_6} = \frac{3.39}{\phi} - 0.254$$

B. Kerosene

(8) $$\beta_{NO} = \frac{6.93}{\phi} - 0.485$$

(9) $$\beta_{CO} = \frac{6.46}{\phi} - 0.454$$

(10) $$\beta_{C_6} = \frac{3.31}{\phi} - 0.232$$

C. Methane

(11) $$\beta_{NO} = \frac{8.06}{\phi} - 0.850$$

(12) $$\beta_{CO} = \frac{7.54}{\phi} - 0.792$$

(13) $$\beta_{C_6} = \frac{3.86}{\phi} - 0.406$$

These equations are plotted in Figures E-4, E-5, and E-6. A word is necessary about the form of the results for unburned hydrocarbon. The raw data (Xi), are reported in terms of ppm carbon. It was necessary to arbitrarily select a species of hydrocarbon upon which to base the mass calculations. The species selected was n-hexane. Thus, the mass data, L, is given in terms of milligrams n-hexane per pound of fuel. In making the conversion from these graphs ($L_{C_6} = \beta_{C_6} X_C$) note that the value of X_C to use is the raw data from the hydrocarbon analyses, in ppm carbon.

IX. Evaluation of Particulate Emissions

Once the mass emissions per unit volume of exhaust products is calculated, the residual ash of fuel or mass emissions per gram of fuel can be determined. The stoichiometric combustion equation is used to give the moles of fuel from the total moles of exhaust. The molecular weight of the fuel and the temperature ($\approx 75^{\circ}F$) at thich the sample volume was measured yield the mass emissions per gm. of fuel.

The formulas for each step and example calculations are shown below:

STEPS IN CALCULATION

1. $\dfrac{\text{Particles}}{\text{cubic meter exhaust}}$

$$\frac{\text{particles}}{\text{cubic meter}} = \frac{A_1(\text{count/field})}{A_2 \times R \times T} = \frac{w \times s \times \cancel{T} \times \text{count}}{A_2 \times R \times \cancel{T}} \times \Phi$$

$$= \frac{82\text{mm} \times 4\text{mm/min} \times 10^6\mu^2 \times \text{count/field}}{30\text{cc/min} \quad 1\text{mm}^2 \times A_2(\mu)^2} \times \frac{10^6\text{cc}}{1\text{m}^2} \times \Phi$$

$$\therefore \frac{\text{particles}}{\text{cubic meter}} = 11.0 \times 10^{12} \times \frac{\text{count}}{A_2(\mu)^2} \times \Phi$$

2. $\dfrac{\text{particles}}{\text{cubic foot exhaust}}$

$$\frac{\text{particles}}{\text{cubic foot}} = \frac{\text{particles}}{\text{cubic meter}} \times \frac{1\text{m}^3}{35.2\ \text{ft}^3}$$

3. $\frac{\mu\text{gms}}{\text{cubic meter exhaust}}$

$$\frac{\mu\text{gms}}{\text{cubic meter exhaust}} = \left(\frac{\text{particles}}{\text{cubic meter}}\right)\left(\frac{4}{3}\frac{\pi}{8}\right)\left(\begin{matrix}\text{mean}\\ \text{dia.}\end{matrix}\right)^3\left(\text{Density}\right)$$

$$= \frac{\text{particles}}{\text{cubic meter}} \times 2.2\,\frac{\text{gms}}{\text{cc}} \times \frac{10^6\,\mu\text{gms}}{1\text{ gm}} \times \frac{\pi}{6} \times \left(\frac{\text{dia}}{\mu}\right)^3 \frac{1\text{cc}}{10^{12}\mu}$$

$$\therefore \frac{\mu\text{gms}}{\text{cubic meter exhaust}} = \frac{\text{particles}}{\text{cubic meter}} \times \left(\frac{\text{dia}}{\mu}\right)^3 \times 1.2 \times 10^{-6}$$

4. $\frac{\mu\text{gms}}{\text{gm fuel}}$ $C_9H_{20} + 14O_2 + 56N_2 \rightarrow 9CO_2 + 10H_2O + 56N_2$

$$\frac{\mu\text{gms}}{\text{gm fuel}} = \frac{\mu\text{gm}}{\text{cubic meter exhaust}} \times \frac{1\text{ cubic meter}}{10^3\,\ell} \times \frac{25\,\ell}{\text{mole exhaust}} \times$$

$$\frac{75\text{ moles exhaust}}{1\text{ mole fuel}} \times \frac{1\text{ mole fuel}}{128\text{ gms}}$$

$$\therefore \frac{\mu\text{gms}}{\text{gm fuel}} = \frac{\mu\text{gm}}{\text{cubic meter}} \times 14.7 \times 10^{-3}$$

EXAMPLE CALCULATION

SAMPLE 2294C

1. $$\frac{\text{particles}}{\text{cubic meter}} = 11.0 \times 10^{12} \times \frac{\text{count}}{A_2(\mu)^2} \times \Phi = 11.0 \times 10^{12} \times \frac{100}{900} \times 1.35$$

$$\frac{\text{particles}}{\text{cubic meter}} = 1.6 \times 10^{12}$$

2. $$\frac{\text{particles}}{\text{cubic foot}} = \frac{\text{particles}}{\text{cubic meter}} \times \frac{1\text{m}^3}{35\ \text{ft}^3} = 1.6 \times 10^{12} \times \frac{1}{35.2}$$

$$= 46 \times 10^9$$

3. $$\frac{\mu\text{gms}}{\text{cubic meter}} = \frac{\text{particles}}{\text{cubic meter}} \times \left(\text{dia}\right)^3 \times 1.2 \times 10^{-6}$$

$$= 1.6 \times 10^{12} \times (.47)^3 \times 1.2 \times 10^{-6}$$

$$\frac{\mu\text{gms}}{\text{cubic meter}} = 2.0 \times 10^5$$

4. $$\frac{\mu\text{gms}}{\text{gm fuel}} = \frac{\mu\text{gms}}{\text{cubic meter}} \times 14.7$$

$$= 2.0 \times 10^5 \times 14.7 \times 10^{-3}$$

$$\frac{\mu\text{gms}}{\text{gm feet}} = 2.6 \times 10^3$$

SUMMARY OF HEAT EXCHANGER PERFORMANCE

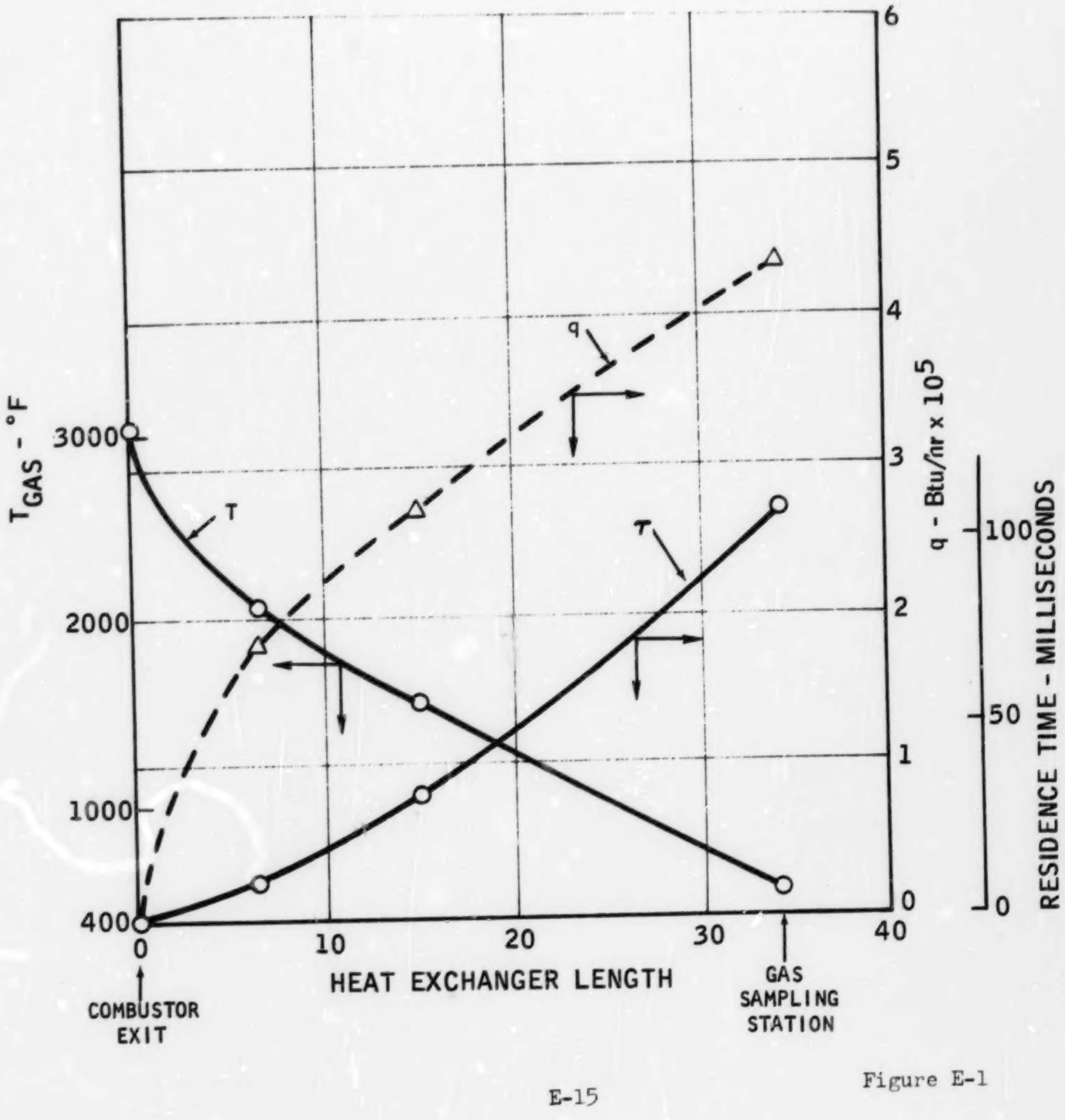

Figure E-1

EQUIVALENCE RATIO BASED ON CARBON DIOXIDE

COMPLETE COMBUSTION ASSUMED

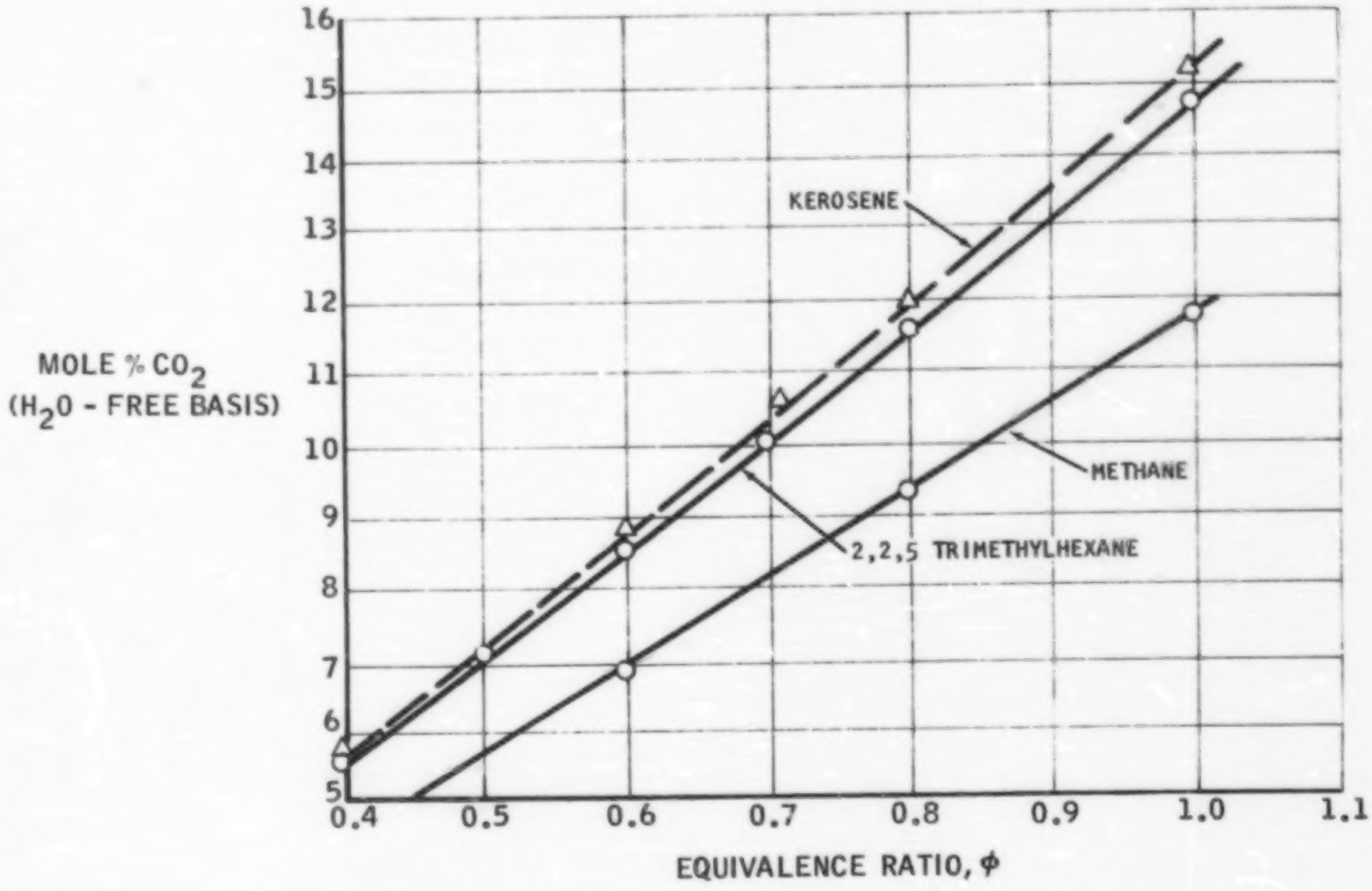

Figure E-2

CONVERSION FACTOR TO ACCOUNT FOR WATER VAPOR IN EXHAUST GASES

$$K = \frac{\text{PPM IN EXHAUST (WATER VAPOR INCLUDED)}}{\text{PPM MEASURED (WATER-FREE BASES)}}$$

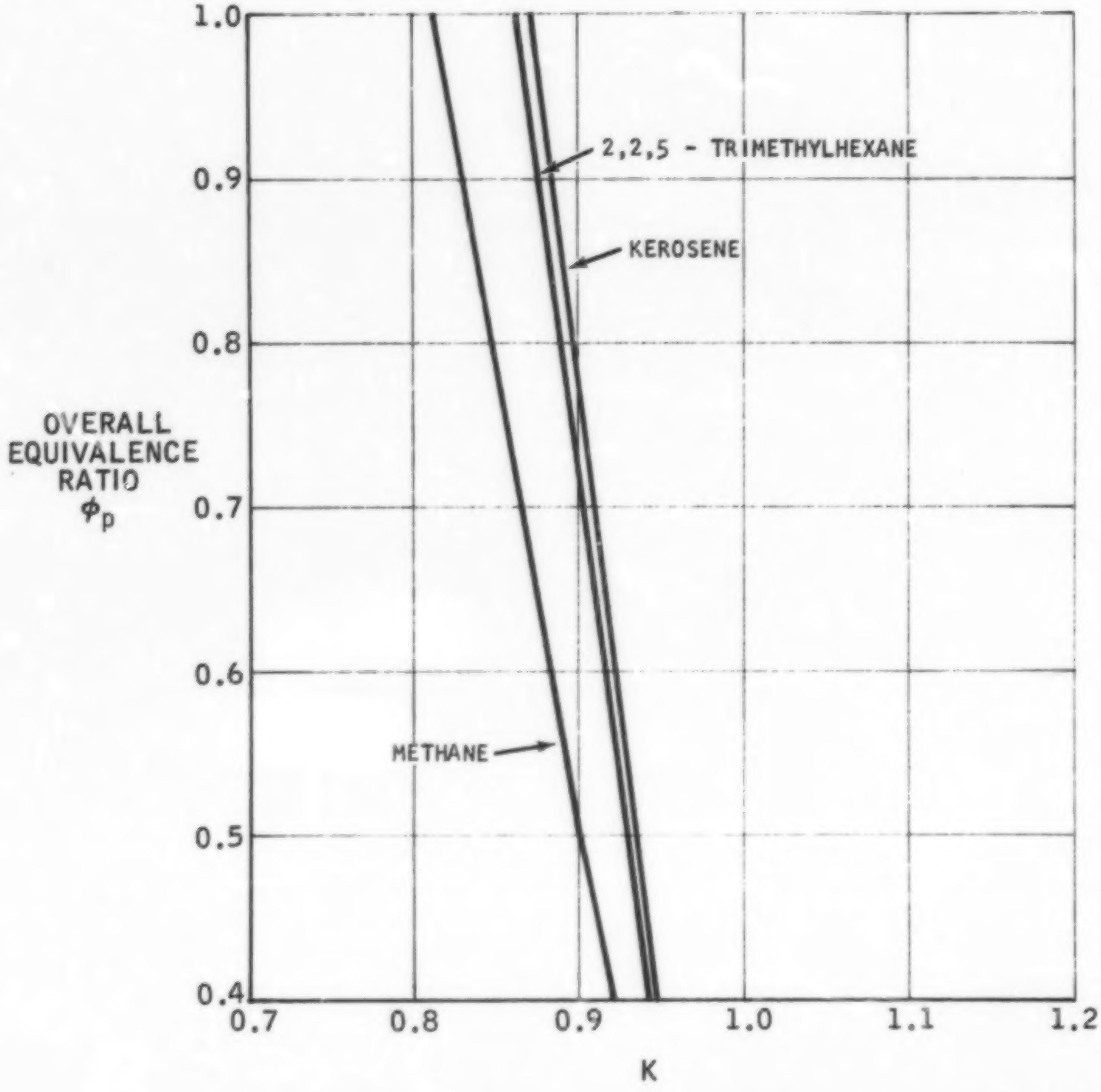

Figure E-3

CONVERSION OF GAS EMISSION DATA TO UNIT MASS OF FUEL

FUEL: 2,2,5 - TRIMETHYLHEXANE

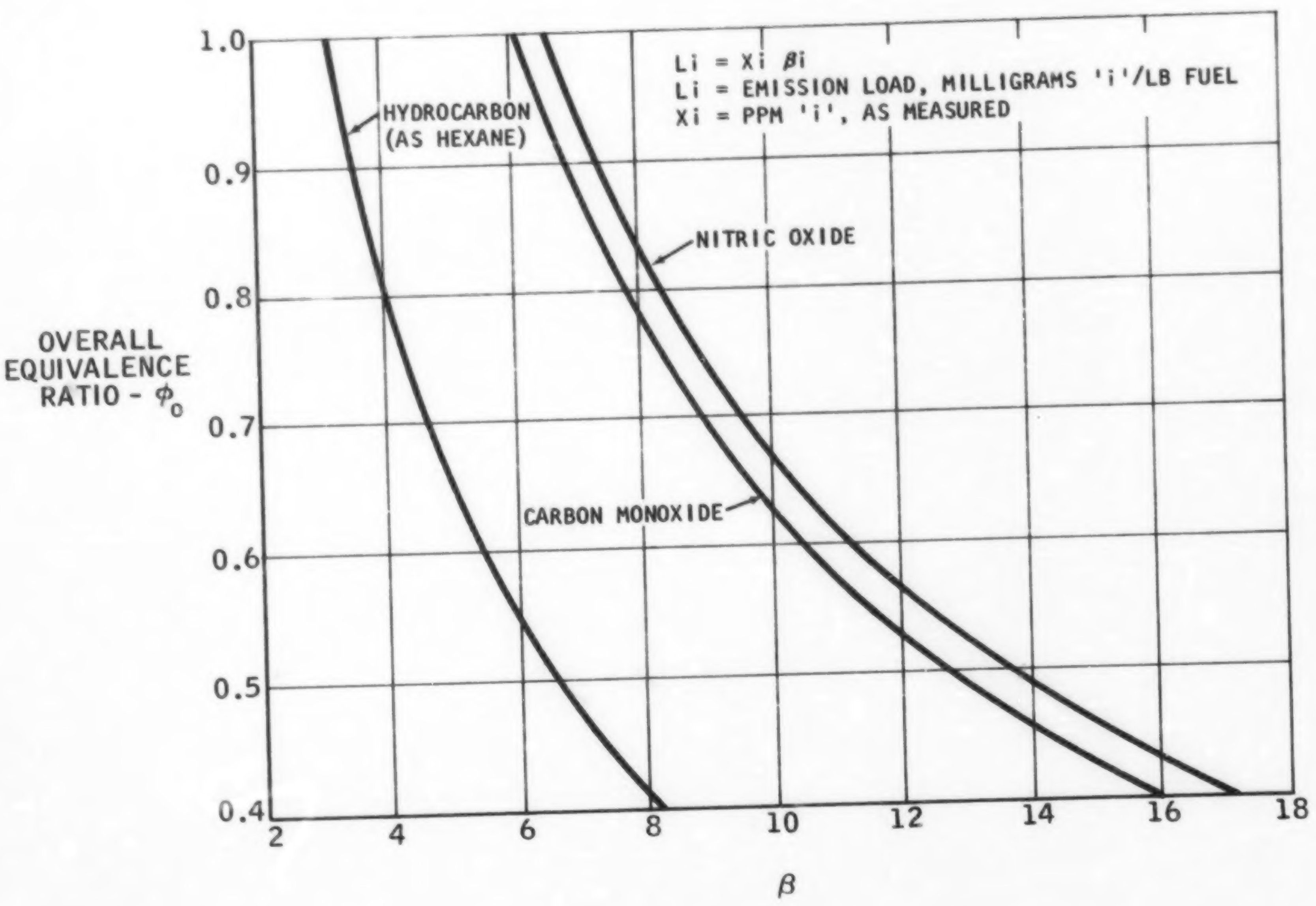

Figure E-4

CONVERSION OF GAS EMISSION DATA TO UNIT MASS OF FUEL

FUEL: KEROSENE (JET FUEL A, ASTM D1555)

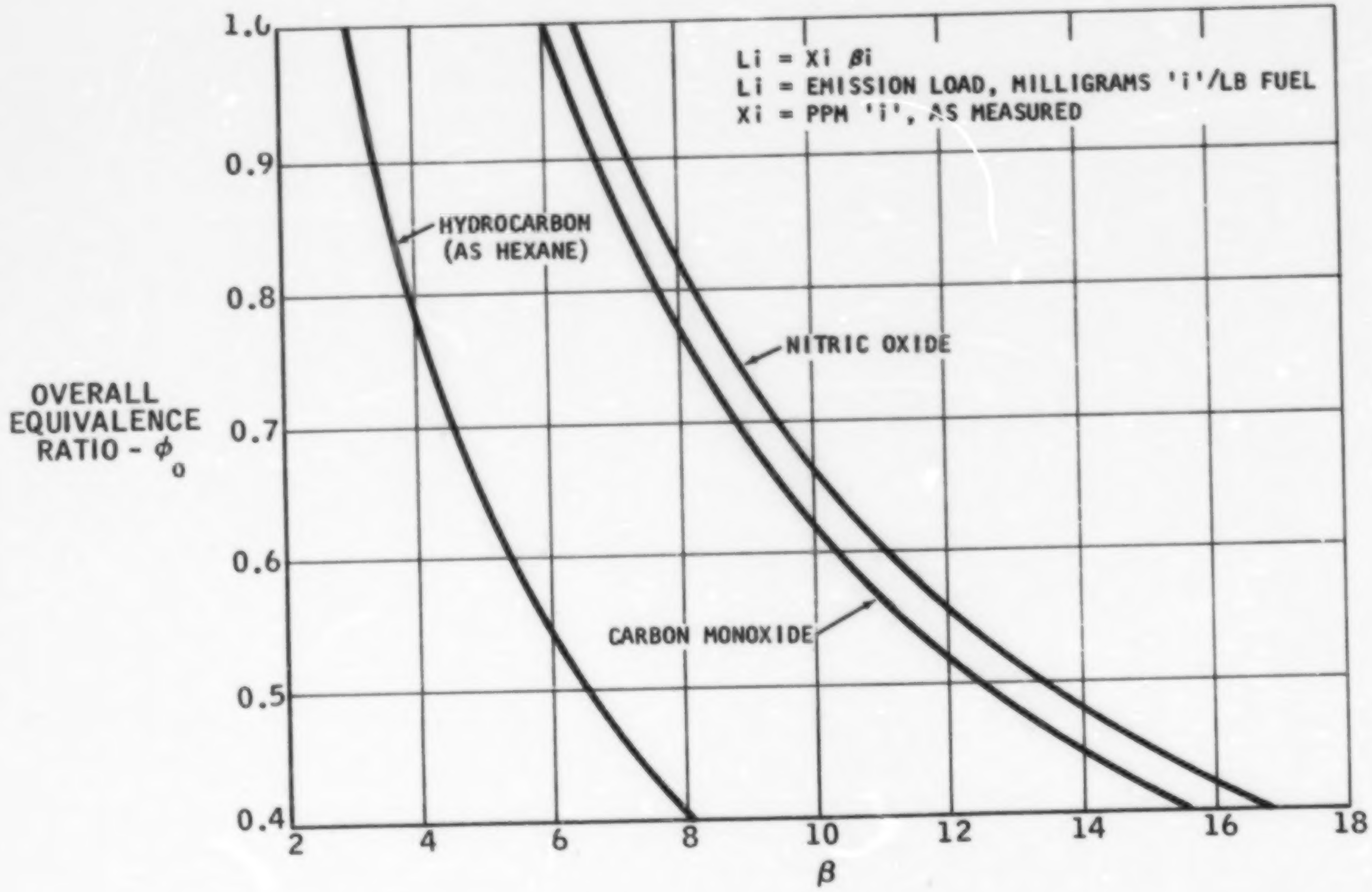

Figure E-5

V8150-19

CONVERSION OF GAS EMISSION DATA TO UNIT MASS OF FUEL

FUEL: METHANE

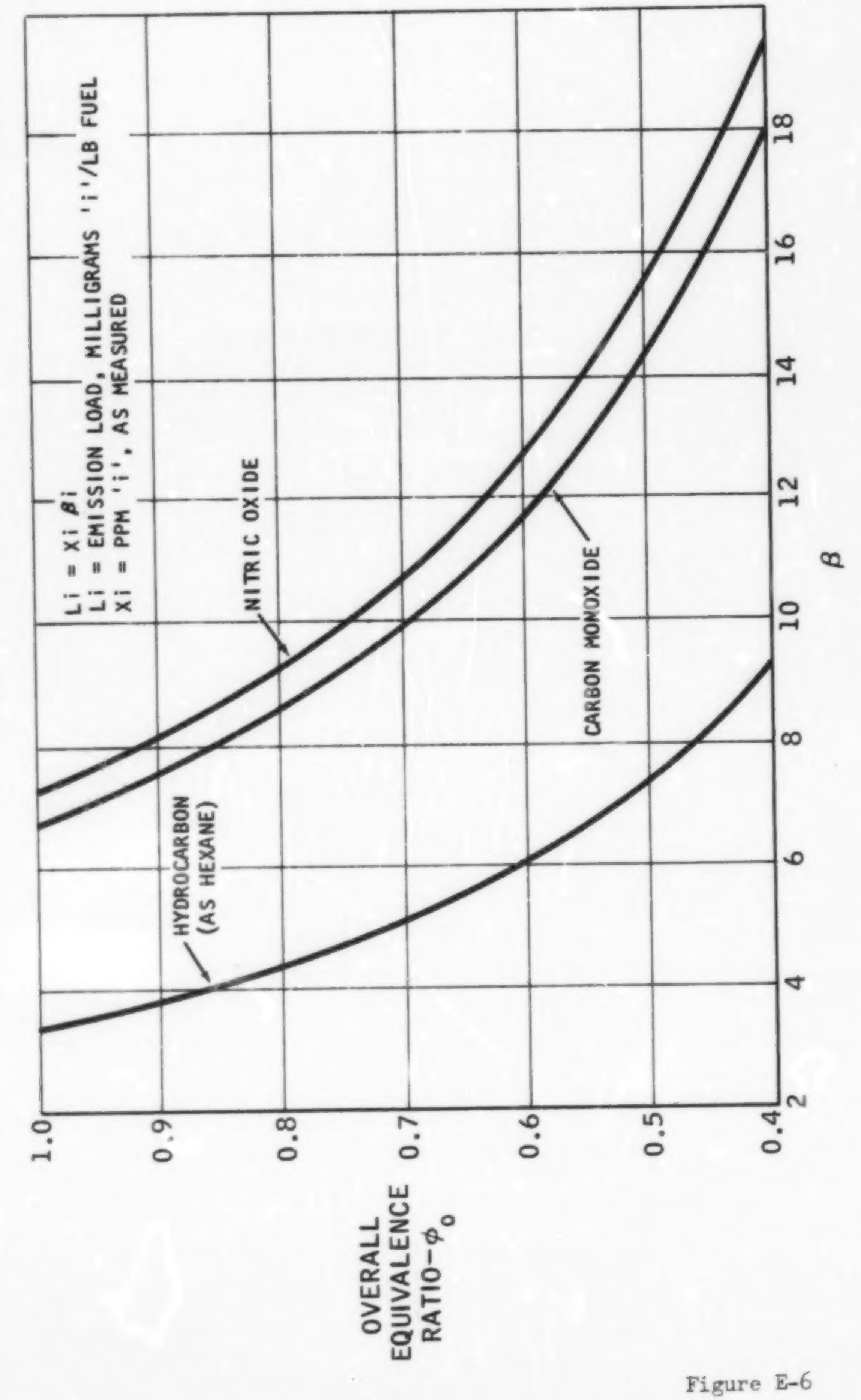

Figure E-6

STANDARD TITLE PAGE FOR TECHNICAL REPORTS

1. Report No. APTD-0574	**2. Govt. Accession No.**	**3. Recipient's Catalog No.**	

4. Title and Subtitle
Study of Continuous Flow Combustion Systems for External Combustion Vehicle Powerplants

5. Report Date

6. Performing Organization Code

7. Author(s)
C. V. Burkland, W. B. Lee, G. Bahn, & R. Carlson

8. Performing Organization Rept. No.

9. Performing Organization Name and Address
The Marquardt Company
Van Nuys, California

10. Project/Task/Work Unit No.

11. Contract/Grant No.
CPA 22-69-128

12. Sponsoring Agency Name and Address
National Air Pollution Control Administration Technical Center
411 West Chapel Hill Street
Durham, North Carolina 27701

13. Type of Report & Period Covered

14. Sponsoring Agency Code

15. Supplementary Notes

16. Abstracts
Chemical kinetic studies were employed to better understand how and at what rate air pollutants are formed in an external combustion process. With this background, an experimental combustion test rig employing a recirculating step, staged burner was built. Tests were conducted with various liquid and vaporized liquid fuel injectors using aviation turbine fuel (Jet A) and 2,2,5-trimethylhexane. A wide range of fuel-air ratios were examined by individually controlling primary and secondary air flow rates. Fuel flows were varied from a maximum corresponding to a heat release of 500,000 BTU/hr to 1/30 of this value. Two runs were also made using gaseous methane fuel. The range of test variables were: injector configurations - pressure atomizing, vaporizing, 2nd vaporizing premixed; fuel flows from 0.15 to 4.5 gallons per hour; air flows from 3.4 to 103 standard cubic feet per minute; fuel equivalence ratio - primary from 0.53 to 1.59, and overall from 0.40 to 0.84; number of test conditions - 140; and cumulative combustion time - 22 hours. The tests demonstrated that gaseous and particulate emissions less than those established as the 1980 Federal Research goals can be achieved simultaneously in a high heat release, low pressure drop, burner configuration. The emission data measured at steady state conditions is compared to current and future emission goals for automobiles.

17. Key Words and Document Analysis. (a). Descriptors

Air Pollution
External Combustion Engines
Motor Vehicle Engines
Combustion Chambers
Design Criteria
Reaction Kinetics
Jet Engine Fuels
Fuel Injectors
Hexanes
Air Flow
Flow Rate
Fuel Consumption
Heat Transfer
Methane
Kerosene
Carbon Monoxide
Hydrocarbons
Nitrogen Oxides
Aerosols
Exhaust Emissions
Temperature
Mixing
Quenching (cooling)
Surges
Experimentation

17b. Identifiers/Open-Ended Terms
Residence Time
2,2,5-trimethylhexane

17c. COSATI Field/Group 13/02, 21/11

18. Distribution Statement	**19. Security Class (This Report)** UNCLASSIFIED	**21. No. of Pages** 166
	20. Security Class. (This Page) UNCLASSIFIED	**22. Price**

FORM NBS-867(1-70)